

Supporting Information

**Rational Embedding of DMAP into Covalent Triazine
Frameworks for Efficient Heterogeneous Organocatalysis**

Xin He,^a Jingjing Ge,^a Xin Xu,^a Jiaxin Chu,^a Junjie Du,^a Zhenliang Pan,^a Yunlai Ren^a
and Wan-Kai An^{a,*}

College of Science, Henan Agricultural University, Zhengzhou, Henan 450002 (China).

E-mail: anwk@henau.edu.cn.

List of Contents

A. General Information	2
B. Synthetic Procedures	4
C. Characterization of CTFs	10
D. Catalytic Performance of DMAP-CTF	22
E. Recyclability Tests of DMAP-CTF	31
F. The possible mechanisms for the DMAP-CTF mediated reactions	33
G. References	34
H. Liquid NMR spectra of some compounds	36

A. General Information

Materials. Terephthalimidamide (TPDA), 3,5-dibromopyridin-4-amine, 3,5-dibromo-4-chloropyridine, 3,5-dibromo(pyridine-4-yl)dimethylamine, were prepared according to the literature procedures.^[1,2] Unless otherwise noted, the reagents 4-amino-pyridine, N-bromosuccinimide (NBS) *etc.* were purchased from Energy Chemical Reagent Co. Ltd and Adamas Reagent Co. Ltd and could be used without further purification. Dichloromethane (DCM) was first dried by Na and further distilled before use. Suzuki coupling reaction mediated by Pd(PPh₃)₄ was carried out under N₂ by using Schlenk line techniques.

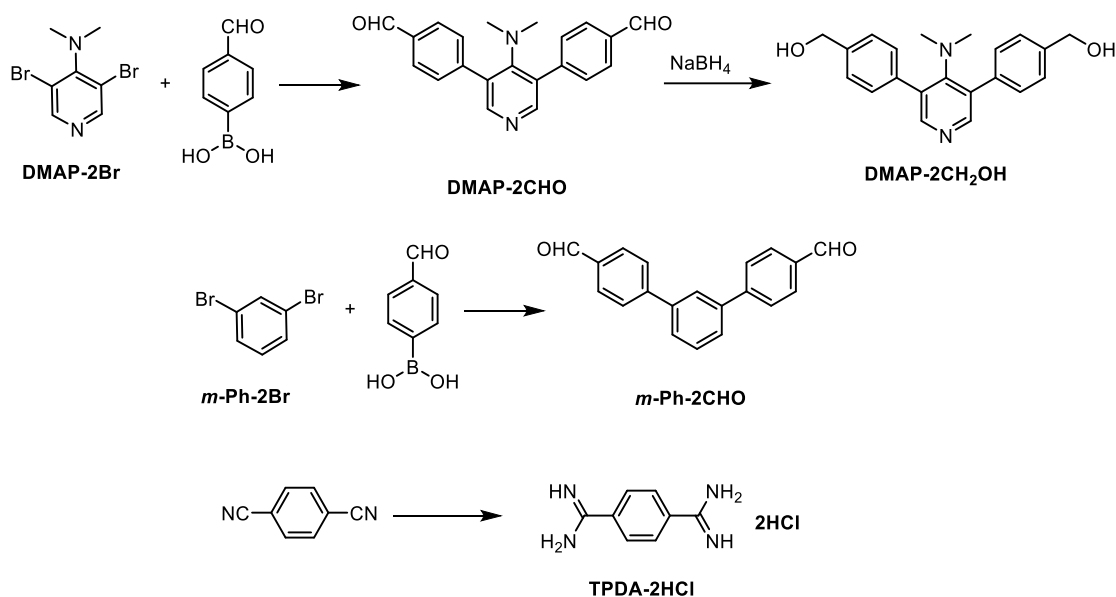
Methods. Flash column chromatography was carried out with silica gel (200-300 mesh). Liquid NMR spectra (¹H and ¹³C) were recorded on a Bruker Avance III 400 MHz NMR spectrometer (CDCl₃, *d*₆-DMSO or CF₃COOD as the solvent). The chemical shifts δ and coupling constants J are given in ppm and Hz, respectively. Solid-state NMR experiments were performed on a Bruker AvanceNEO 600 MHz NMR spectrometer (4-mm double-resonance probe). The parameters were set as following: contact time was 3 ms (ramp 100), recycle delay was 3 s and the spinning rate (ν_r) was 10.0 kHz. FT-IR spectra were obtained with a Nicolet IS 20 instrument. Nitrogen adsorption and desorption isotherms were measured at 77 K using a Quantachrome NovaWin 2200e system. The samples were outgassed at 120 °C for 8 h before analysis. Surface areas were calculated based on the adsorption data via the Brunauer-Emmett-Teller (BET) and Langmuir methods, respectively. The pore-size-distribution (PSD) curves were obtained from the adsorption branches using Quenched Solid Density Functional Theory (QSDFT) method. The micropore surface area was derived from the *t*-plot method, and the total pore volume was estimated from the amount adsorbed at P/P₀ = 0.99. Powder X-ray diffraction (PXRD) data were collected with an Ultima IV diffractometer (Rigaku Corporation) operated at 40 kV and 40 mA with Cu K α radiation at a scan rate of 4°/min.

Thermogravimetric analysis (TGA) measurements were used to study the thermal stability of the DMAP-CTF. The tests were carried out on a SDT Q600 (V20.9 Build 20) instrument from 30 to 1000 °C under a N₂ atmosphere with a heating rate of 10 °C/min. Elemental analysis was performed on a Vario EL cube instrument. Scanning electron microscope (SEM) tests were applied to analysis the surface morphologies and microstructures of the obtained materials with Zeiss Merlin compact SEM at a voltage of 10 kV. The samples used for SEM analysis were dispersed in ethanol, and then dipped and dried on a silicon wafer. Transmission electron microscopy (TEM) images were acquired by a FEI talos F200S transmission electron microscope (FEI, USA) operating

at an acceleration voltage of 200 kV. The X-ray photoelectron spectroscopy (XPS) analysis was performed on Thermo Fisher ESCALab 250Xi.

The density functional theory (DFT) calculations were employed to optimize the geometry of the model catalysts (MC, DMAP-TaZ, and *m*-Ph-TaZ) without any imaginary frequencies using the Gaussian 16 software package.^[3] The model catalysts were initially subjected to geometry optimization. Subsequently, the electrostatic potential (ESP) and the dipole moment of the structures were calculated at the B3LYP/6-31G (d,p) level. Then, the electron delocalization was presented by the Multiwfn software.^[4] The ESP map was rendered using the Visual Molecular Dynamics (VMD)^[5] software based on the files exported by the Multiwfn.

B. Synthetic Procedures



Scheme S1. Synthetic routes of monomer DMAP-2CHO, DMAP-2CH₂OH, *m*-Ph-2CHO and TPDA.

Synthesis of DMAP-2Br.^[2] To a solution of 4-amino-pyridine (2.35 g, 25 mmol) in 100 mL of CCl₄, N-bromosuccinimide (NBS, 8.9 g, 50 mmol) was added under an inert atmosphere. The resulting mixture was stirred at room temperature in the dark for 24 hours. Subsequently, the solvent was removed under reduced pressure. The crude product was purified by flash chromatography using a gradient elution with ethyl acetate/petroleum ether (4:1, v/v), yielding 3,5-dibromopyridin-4-amine as white needle-like crystals. (6.0 g, 96% yield).

Concentrated HCl (19 mL) was added to 3,5-dibromopyridin-4-amine (3.4 g, 13.55 mmol) and stirred until dissolved. Then, NaNO₂ (4.21 g, 61 mmol) was slowly added in to the above solution under 0 °C, and the reaction was stirred for 1 hour. Subsequently, the system was warmed to room temperature and reacted for 6 h. After completion, the solution was neutralized with saturated K₂CO₃ solution and extracted with ethyl acetate. The collected organic layer was dried over anhydrous Na₂SO₄, and the solvent was removed under vacuum to give 3,5-dibromo-4-chloropyridine as white solid (3.60 g, 98% yield).

The 3,5-dibromo-4-chloropyridine (2.95 g, 10.8 mmol) and dimethylamine solution (32 mL, 40%) were then placed in a 100 mL high-pressure tube. The sealed tube was heated at 118 °C for 20 hours. After cooling, the mixture was extracted three times with ethyl acetate and a saturated K₂CO₃ solution. The organic phase was dried over anhydrous Na₂SO₄, and then concentrated to yield DMAP-2Br as white solid (2.7 g,

90% yield). ^1H NMR (400 MHz, CDCl_3): δ = 8.48 (s, 2H), 2.99 (s, 6H) ppm; ^{13}C NMR (101 MHz, CDCl_3): δ = 155.3, 152.1, 119.7, 42.5 ppm.

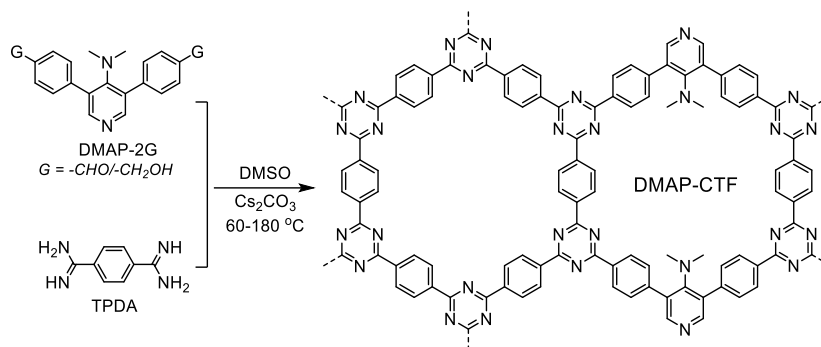
Synthesis of DMAP-2CHO. Compound DMAP-2Br (400 mg, 1.44 mmol), (4-formylphenyl)boronic acid (507 mg, 3.38 mmol), K_2CO_3 (558 mg, 4.04 mmol) and $\text{Pd}(\text{PPh}_3)_4$ (80 mg, 0.07 mmol) were added into a two-neck flask. The system was degassed and back-filled with nitrogen for three times, and then degassed 1,4-dioxane/ H_2O (24 mL, 3/1) was added. The reaction was stirred at 120°C for 48 h under N_2 atmosphere. The mixture was extracted by CH_2Cl_2 after the reaction was cooled down to room temperature. The obtained residues were purified by flash silica gel column chromatography with EtOAc/petroleum ether (1/2) as the eluent to give product DMAP-2CHO as white solid (421 mg, 82% yield). ^1H NMR (400 MHz, CDCl_3): δ = 10.08 (s, 2H), 8.34 (s, 2H), 8.00 (d, J = 8.12 Hz, 4H), 7.56 (d, J = 8.1 Hz, 4H), 2.36 (s, 6H) ppm; ^{13}C NMR (101 MHz, CDCl_3): δ = 191.7, 154.5, 151.9, 145.1, 135.3, 130.2, 130.0, 129.4, 43.4 ppm.

Synthesis of DMAP-2CH₂OH.

The compound DMAP-2CHO (250 mg, 0.75 mmol) was dissolved in 15 mL of MeOH, and then NaBH_4 (101 mg, 2.25 mmol) was slowly added. The mixture was stirred at room temperature for 1 h until the substrate was disappeared (monitor by TLC). Then the solvent was removed under pressure and recrystallized in MeOH to give DMAP-2CH₂OH as pale gray needle crystal (170 mg, 68% yield). ^1H NMR (400 MHz, d_6 -DMSO): δ = 8.16 (s, 2H), 7.42 (d, J = 8.2 Hz, 4H), 7.35 (d, J = 8.12 Hz, 4H), 4.56 (s, 4H), 3.35 (br, 2H), 3.32 (br, 2H), 2.25 (s, 6H) ppm; ^{13}C NMR (101 MHz, CDCl_3): δ = 154.4, 151.2, 141.9, 137.2, 131.4, 128.8, 127.2, 63.1, 63.0, 43.2 ppm.

Synthesis of *m*-Ph-2CHO. Compound *m*-Ph-2Br (472 mg, 2.0 mmol), (4-formylphenyl)boronic acid (660 mg, 4.40 mmol), K_2CO_3 (775 mg, 5.6 mmol) and $\text{Pd}(\text{PPh}_3)_4$ (115 mg, 0.1 mmol) were added into a two-neck flask. The system was degassed and back-filled with nitrogen for three times, and then degassed 1,4-dioxane/ H_2O (30 mL/8 mL) was added. The reaction was continuously stirred under reflux conditions for 24 hours in a nitrogen atmosphere. The mixture was then extracted by CH_2Cl_2 after the reaction was cooled down to room temperature. The obtained residues were purified by flash silica gel column chromatography with CH_2Cl_2 /petroleum ether (1/4) as the eluent to give the product as white solid (482 mg, 85% yield). ^1H NMR (400 MHz, CDCl_3): δ = 10.08 (s, 2H), 7.99 (d, J = 8.3 Hz, 4H), 7.87 (s, 1H), 7.81 (d, J = 8.2 Hz, 4H), 7.69 (d, J = 6.9 Hz, 2H), 7.64-7.57 (m, 1H) ppm. ^{13}C NMR (101 MHz, CDCl_3): δ = 192.0, 146.8, 140.8, 135.6, 130.5, 129.9, 128.0, 127.6, 126.6 ppm.

Synthesis of compound TPAD-2HCl.^[1, 6] Under a N₂ atmosphere and 0 °C, 1 M LiN(SiMe₃)₂ (40 mmol) was added dropwise into the solution of benzene-1,4-dicarbonitrile (1.28 g, 10.0 mmol) in anhydrous THF (20 mL) within 20 min. The reaction was stirred at room temperature for 3 h and then cooled to 0 °C. The mixture was quenched carefully with 6 M HCl-EtOH (40 mL) and stand overnight. The precipitate was filtered, washed with diethyl ether (3×10 mL), and then recrystallized with H₂O-EtOH (30 mL, 1/1) to give a solid. The solid was dissolved in hot *con.* HCl (5 mL), followed by removal of the volatiles under vacuum to afford terephthalamidine dihydrochloride (TPAD·2HCl) as pale-brown crystals (1.9 g, 81%). ¹H NMR (400 MHz, DMSO-*d*₆) δ 9.61 (s, 4H), 9.33 (s, 4H), 8.02 (s, 4H) ppm.



Scheme S2. Synthesis of **DMAP-CTF**.

General procedures for the preparation of DMAP-CTF:

Strategy A. The mixture of DMAP-2CHO (165 mg, 0.5 mmol), TPDA-2HCl (236 mg, 1 mmol) and Cs₂CO₃ (716 mg, 2.2 mmol) were dispersed in DMSO (20 mL). The mixture was stirred at 60 °C, 80 °C, 100 °C for 12 h in sequence, then 120 °C and 150 °C for 36 h, respectively. After the reaction cooled down to room temperature, the precipitation was collected by filtration, washed in sequence with water, DMF and MeOH. Afterward, the desired CTF was purified *via* a Soxhlet extraction for 24 h with MeOH and dried in vacuum oven for 12 h at 80 °C. The final DMAP-CTF was obtained as yellow powder (210 mg, 72% yield).

Strategy B. The mixture of DMAP-2CH₂OH (150 mg, 0.45 mmol), TPDA-2HCl (212 mg, 0.9 mmol) and Cs₂CO₃ (652 mg, 2.0 mmol) were dispersed in DMSO (15 mL). The mixture was stirred at 100 °C for 24 h, then 180 °C for 36 h, respectively. After the reaction cooled down to room temperature, the precipitation was collected by filtration, washed in sequence with water, DMF and MeOH. Afterward, the desired DMAP-CTF was purified *via* a Soxhlet extraction for 24 h with MeOH and dried in vacuum oven for 12 h at 80 °C. The material was obtained as brown powder (201 mg, 76% yield).

Strategy C. The mixture of DMAP-2CHO (165 mg, 0.5 mmol), TPDA-2HCl (236 mg, 1 mmol), NaCl (101 mg, 1.71 mmol) and Cs₂CO₃ (716 mg, 2.2 mmol) were dispersed

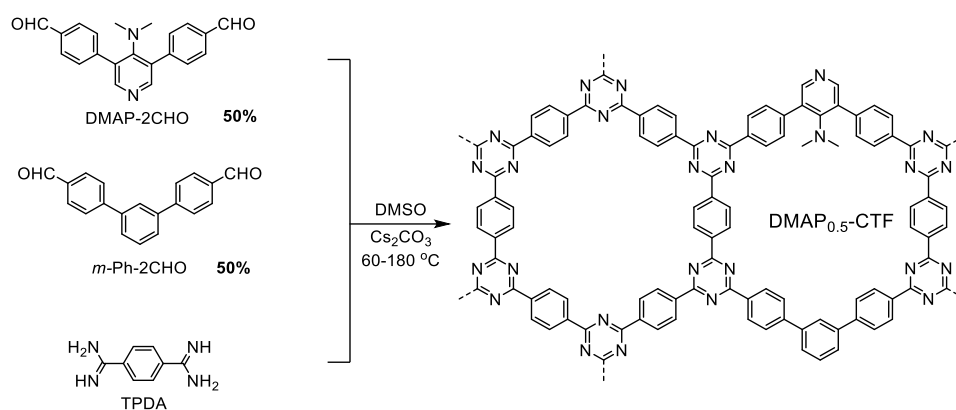
in DMSO (20 mL). The mixture was stirred at 60 °C, 80 °C, 100 °C for 12 h in sequence, then 120 °C and 150 °C for 36 h, respectively. After the reaction cooled down to room temperature, the precipitation was collected by filtration, washed in sequence with water, DMF and MeOH. Then, the desired CTF was purified *via* a Soxhlet extraction for 24 h with MeOH and dried in vacuum oven for 12 h at 80 °C. The **DMAP-CTF** was obtained as brownish-yellow powder (189 mg, 65% yield).

Strategy D. DMAP-2CHO (83 mg, 0.25 mmol) and *n*-BuNH₂ (50 μL, 0.5 mmol) were dissolved in DMSO (5 mL). The mixture was stirred at 60 °C for 2 h to afford a clear solution. Subsequently, TPDA·2HCl (118 mg, 0.5 mmol) and Cs₂CO₃ (163 mg, 0.5 mmol) were added, and the reaction mixture was heated sequentially at 100 °C for 24 h, 120 °C for 36 h, and finally 150 °C for 36 h. After cooling to room temperature, the precipitate was collected by filtration and washed successively with DMF, 1 M aqueous HCl, water, and methanol. The crude product was further purified by Soxhlet extraction with methanol for 24 h, followed by drying under vacuum at 80 °C for 12 h. The desired DMAP-CTF, was obtained as an earthy yellow powder (105 mg, 72% yield).

Strategy E. TPDA·2HCl (118 mg, 0.5 mmol) and Cs₂CO₃ (163 mg, 0.5 mmol) were added to DMSO (5 mL) and the mixture was stirred at 100 °C for 30 min. A separate solution of DMAP-2CHO (83 mg, 0.25 mmol) in DMSO (10 mL) was then added dropwise to the above mixture *via* a peristaltic pump at a rate of 0.8 mL/h while maintaining the temperature at 100 °C. The addition was completed over approximately 12.5 h, after which the reaction was continued at 100 °C for a total of 24 h. The temperature was subsequently raised to 120 °C for 36 h, and finally to 150 °C for an additional 36 h. After cooling to room temperature, the precipitate was collected by filtration and washed sequentially with DMF, 1 M aqueous HCl, water, and methanol. The crude product was further purified by Soxhlet extraction with methanol for 24 h, followed by drying under vacuum at 80 °C for 12 h. The target compound, DMAP-CTF, was obtained as a yellow powder (100 mg, 68% yield).

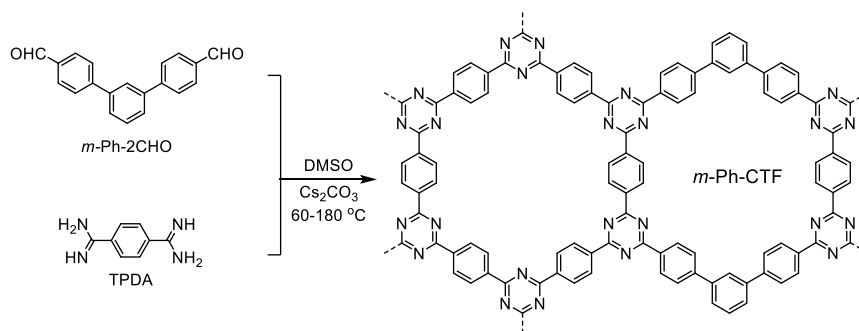
Strategy F. **DMAP-2CHO** (83 mg, 0.25 mmol) and *n*-BuNH₂ (50 μL, 0.5 mmol) were dissolved in DMSO/*o*-DCB (2.5 mL/2.5 mL). The reaction was conducted under the same procedures as the Strategy D. The desired DMAP-CTF, was obtained as dark-brown powder (107 mg, 73% yield).

General procedures for the preparation of DMAP_{0.5}-CTF and *m*-Ph-CTF:



Scheme S3. Synthesis of DMAP_{0.5}-CTF.

DMAP_{0.5}-CTF: The mixture of **DMAP-2CHO** (83 mg, 0.25 mmol), [1,1':3',1''-terphenyl]-4,4''-dicarbaldehyde (*m*-Ph-2CHO, 72 mg, 0.25 mmol), **TPDA-2HCl** (236 mg, 1 mmol) and Cs₂CO₃ (716 mg, 2.2 mmol) were dispersed in DMSO (20 mL). The mixture was stirred at 60 °C, 80 °C, 100 °C for 12 h in sequence, then 120 °C and 150 °C for 36 h, respectively. After the reaction cooled down to room temperature, the precipitation was collected by filtration, washed in sequence with water, DMF and MeOH. Afterward, the desired CTF was purified *via* a Soxhlet extraction for 24 h with MeOH and dried in vacuum oven for 12 h at 80 °C. The final **DMAP_{0.5}-CTF** was obtained as yellow powder (240 mg).

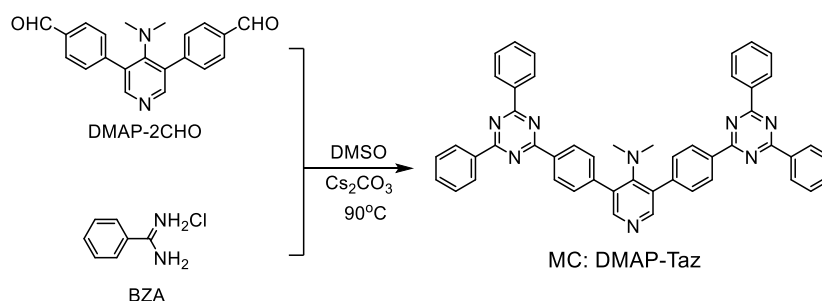


Scheme S4. Synthesis of *m*-Ph-CTF.

***m*-Ph-CTF:** *m*-Ph-2CHO (144 mg, 0.5 mmol), **TPDA-2HCl** (236 mg, 1 mmol) and Cs₂CO₃ (716 mg, 2.2 mmol) were dispersed in DMSO (20 mL). The mixture was stirred at 60 °C, 80 °C, 100 °C for 12 h in sequence, then 120 °C and 150 °C for 36 h, respectively. After the reaction cooled down to room temperature, the precipitation was collected by filtration, washed in sequence with water, DMF and MeOH. Afterward, the desired CTF was purified *via* a Soxhlet extraction for 24 h with MeOH and dried in vacuum oven for 12 h at 80 °C. The final **DMAP-CTF₀** was obtained as yellow powder (242 mg).

General procedures for the preparation of model catalysts (MC):

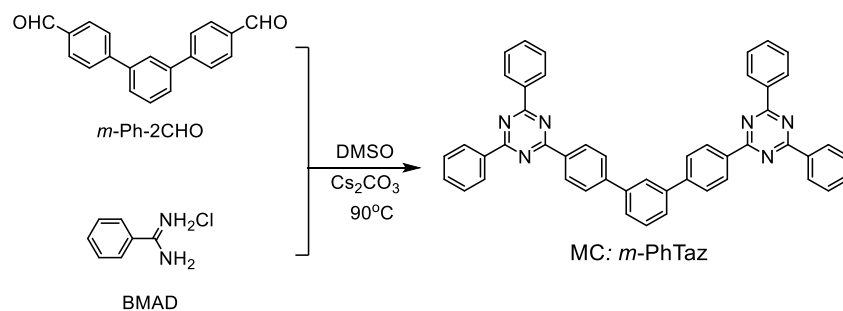
DMAP-Taz: The mixture of **DMAP-2CHO** (166 mg, 0.5 mmol), **BZA-HCl** (314 mg, 2 mmol) and Cs_2CO_3 (752 mg, 2.3 mmol) were dispersed in DMSO (2 mL). The mixture was stirred at 90 °C for 36 h. After the reaction mixture had cooled down to room temperature, it was poured into water (20 mL). Subsequently, the precipitate was collected by filtration and washed successively with a large amount of water and a small volume of EtOAc. Afterward, the desired **MC** was dried in a vacuum oven for 12 h at 80 °C. The final MC **DMAP-Taz** was obtained as pale-yellow powder (286 mg, 78% yield). ^1H NMR (400 MHz, d_6 -DMSO): δ = 8.87 (d, J = 8.1 Hz, 4H), 8.78 (d, J = 7.4 Hz, 8H), 8.39 (s, 2H), 7.39-7.66 (m, 16H), 2.41 (s, 6H) ppm. DMAP-Taz exhibits poor solubility in common deuterated solvents. Therefore, CF_3COOD was employed for NMR analysis. It should be noted that DMAP-Taz may undergo protonation under such strongly acidic conditions to generate DMAP-Taz- D^+ . The chemical shift of DMAP-Taz- D^+ showed difference with DMAP-Taz. ^1H NMR (400 MHz, CF_3COOD): δ = 9.03 (m, 4H), 8.68 (m, 8H), 8.33 (s, 2H), 7.95-7.78 (m, 16H) ppm. ^{13}C NMR (101 MHz, CF_3COOD): 170.2, 168.4, 160.3, 143.6, 140.9, 137.5, 131.9, 131.6, 130.2, 129.8, 129.6, 128.4, 44.4 ppm. DEPT 90 (101 MHz, CF_3COOD): 140.9, 137.5, 131.9, 130.2, 129.8, 129.6 ppm. DEPT 135 (101 MHz, CF_3COOD): 140.9, 137.5, 131.9, 130.2, 129.8, 129.6, 44.3 ppm.



Scheme S5. Synthesis of **DMAP-Taz**.

***m*-Ph-Taz:** The *m*-Ph-2CHO (72 mg, 0.25 mmol), BZA-HCl (157 mg, 1 mmol), and Cs_2CO_3 (326 mg, 1.0 mmol) were dispersed in DMSO (1.0 mL). The resulting mixture was stirred at 90 °C for 36 h. Once the reaction had cooled to room temperature, the reaction system was poured into water (20 mL), and the precipitate was collected by filtration. Subsequently, the precipitate was washed successively with a large amount of water and a small volume of EtOAc. Thereafter, the desired **MC** was dried in a vacuum oven at 80 °C for 12 h. The ***m*-Ph-Taz** was obtained as a white solid powder (128 mg, 74% yield). *m*-Ph-Taz also exhibits poor solubility in common deuterated solvents. Therefore, CF_3COOD was employed for NMR analysis. ^1H NMR (400 MHz,

CF₃COOD): δ = 8.74 (br, 4H), 8.58 (br, 6H), 7.80 (br, 6H), 7.84-7.68 (m, 16H) ppm. ¹³C NMR (101 MHz, CF₃COOD): 168.9, 168.6, 150.0, 139.8, 137.2, 131.1, 130.0, 129.8, 129.6, 128.9, 128.3, 128.2, 128.0, 125.9 ppm. DEPT 90 (101 MHz, CF₃COOD): 137.2, 131.1, 130.0, 129.8, 129.6, 128.1, 128.0, 125.9 ppm. DEPT 135 (101 MHz, CF₃COOD): 137.2, 131.1, 130.0, 129.8, 129.6, 128.2, 128.0, 125.9 ppm.



Scheme S6. Synthesis of *m*-Ph-Taz.

C. Characterization of CTFs.

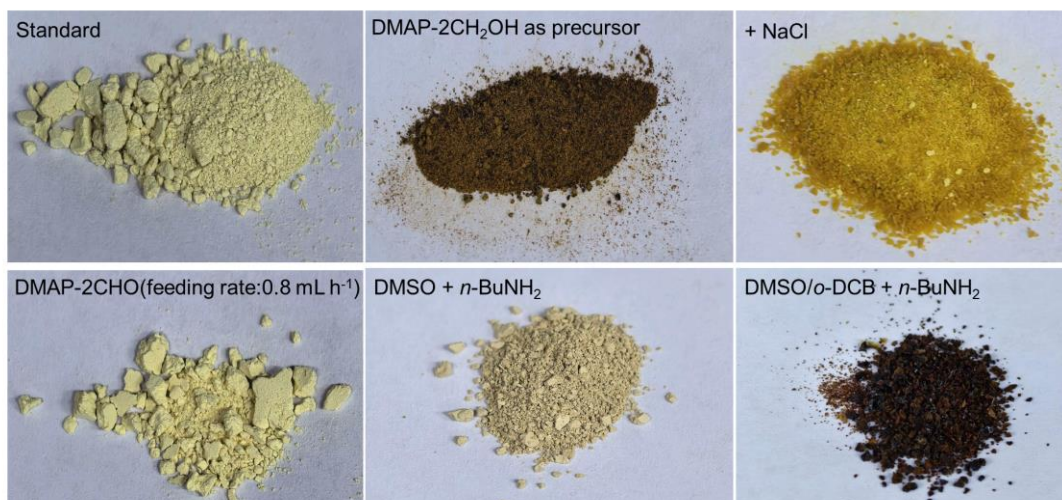


Figure S1. Images of DMAP-CTFs synthesized under different reaction conditions.

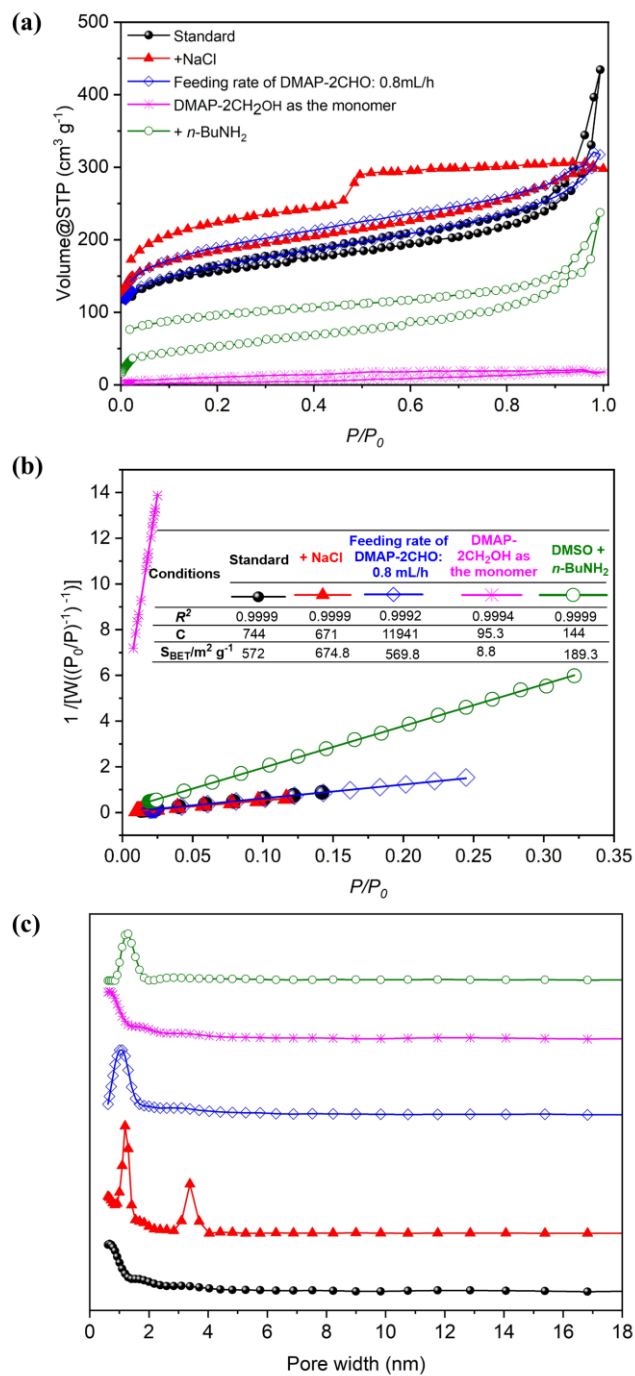


Figure S2. N₂ sorption isotherms (a), BET surface areas plots (b), and pore size distribution (c) of DMAP-CTF synthesized under different reaction conditions.

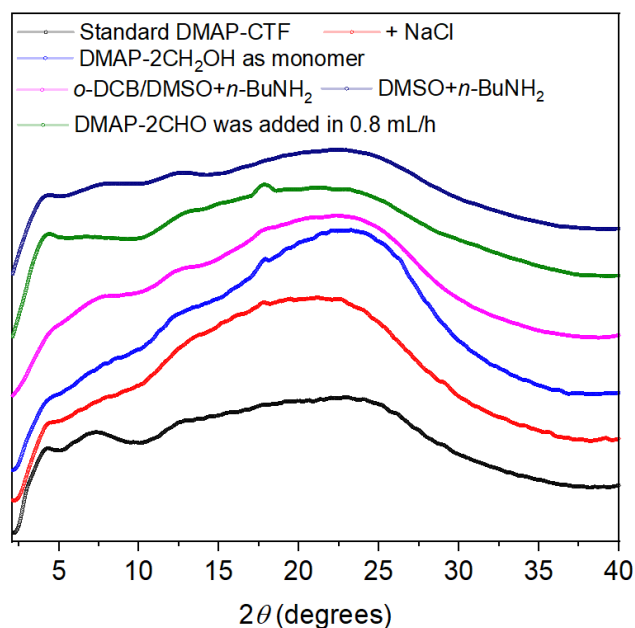


Figure S3. PXRD patterns of **DMAP-CTF** tuned under different conditions.

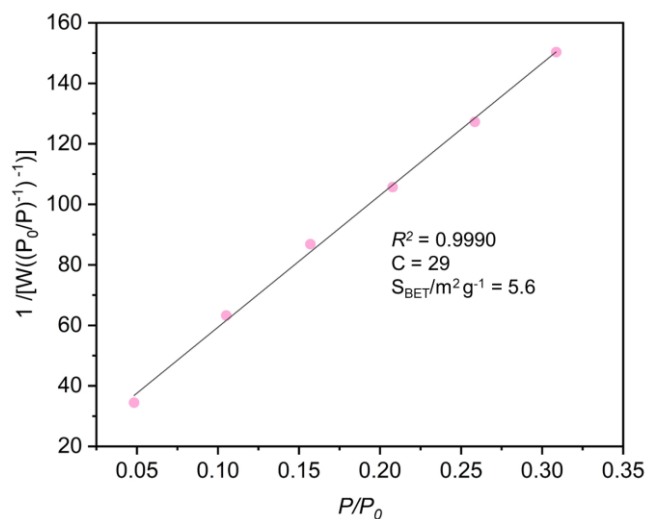


Figure S4. BET surface areas plot synthesized with DMSO/*o*-DCB (1/1) as the solvent and *n*-BuNH₂ as the modulator.

The **Strategy F** of utilizing *o*-DCB/DMSO (2.5 mL/2.5 mL) as the solvent and *n*-BuNH₂ as a modulator was employed to prepare DMAP-CTF. Nevertheless, the resultant DMAP - CTF presented as a dark - brown powder and was non - porous, and its crystallinity was not further enhanced (Figure S1, S3 and S4).

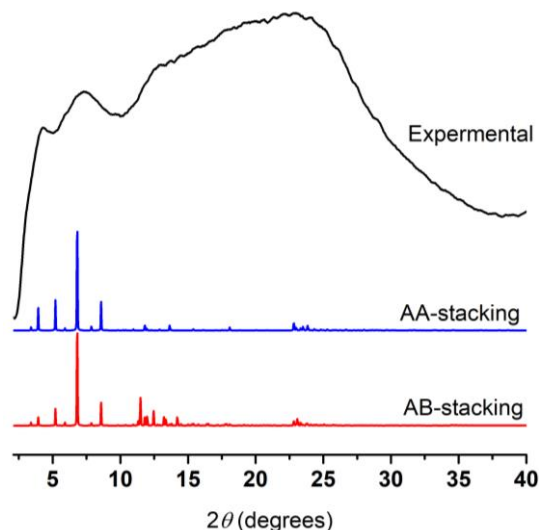


Figure S5. Powder X-ray diffraction (PXRD) pattern of the experimental (black), simulated AA stacking (blue) and simulated AB stacking (red) of standard DMAP-CTF.

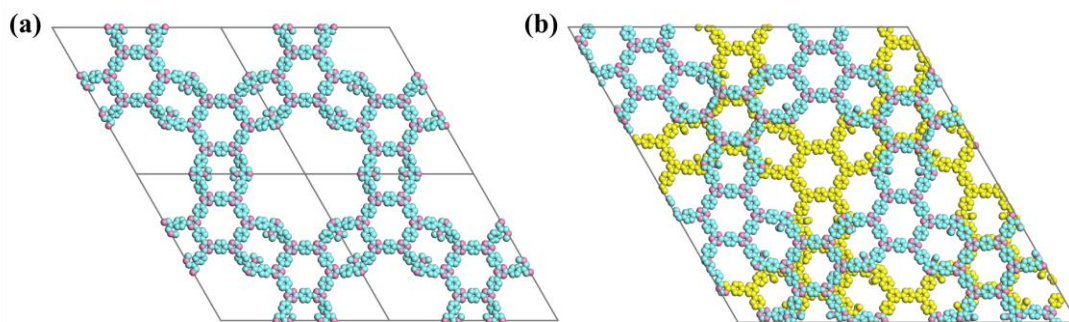


Figure S6. Graphic views of unit cell for DMAP-CTF with AA stacking (a) and AB stacking (b). C, light cyan; O, light magenta; N, green; H atoms are omitted for clarity.

Table S1. Fractional atomic coordinates for the unit cell of AA-stacking DMAP-CTF.

DMAP-CTF:							
Space group: <i>P</i> -3 2/ <i>M</i> 1 (Trigonal)							
$a = b = 51.89478 \pm 0.00017 \text{ \AA}$, $c = 3.90983 \pm 0.00015 \text{ \AA}$, $\alpha = \beta = 90^\circ$, $\gamma = 120^\circ$							
Atom	X (Å)	Y (Å)	Z (Å)	Atom	X (Å)	Y (Å)	Z (Å)
C1	0.22524	-1.5226	0.18909	C19	0.19723	-1.41484	0.40103
C2	0.25098	-1.47121	0.37515	C20	0.17028	-1.38766	0.39575
C3	0.22438	-1.49692	0.28342	C21	0.14337	-1.41488	0.40647
C4	0.06186	-1.36064	0.30805	H22	0.20514	-1.54271	0.11504
C5	0.0894	-1.35832	0.36638	H23	0.2511	-1.45108	0.451
C6	0.11494	-1.33527	0.215	H24	0.04213	-1.37743	0.42198
C7	0.11228	-1.31447	0.01131	H25	0.0908	-1.37414	0.53465
C8	0.08399	-1.31879	-0.06659	H26	0.13172	-1.29619	-0.10659
C9	0.05791	-1.3437	0.06563	H27	0.08267	-1.30387	-0.24996
C10	-0.02475	-1.43778	0.08851	H28	-0.01893	-1.44668	0.31365

C11	0.02857	-1.34991	-0.01176	H29	-0.02927	-1.45369	-0.12375
C12	0.02652	-1.32389	-0.03944	H30	-0.04626	-1.44052	0.14334
N13	0.19599	-1.33304	0.34543	H31	0.0448	-1.30128	-0.01784
C14	0.19597	-1.3072	0.29098	H32	0.21836	-1.41428	0.39505
N15	0.16967	-1.30784	0.24642	H33	0.1222	-1.4155	0.40594
C16	0.14364	-1.33406	0.26247	N34	0.0000	-1.40752	0.0000
N17	0.14405	-1.35964	0.31866	C35	0.0000	-1.37987	0.0000
C18	0.17012	-1.35938	0.35874	N36	0.0000	-1.32932	0.0000

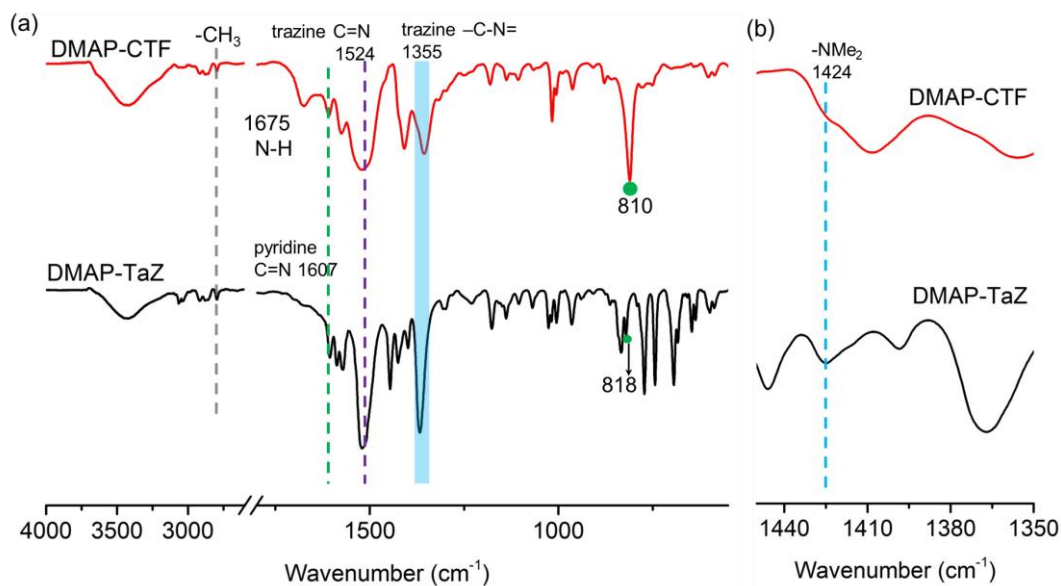


Figure S7. FT-IR spectra of standard DMAP-CTF (red) and DMAP-TaZ (black): (a) full-range spectra and (b) magnified view of the characteristic region for $-NMe_2$ groups.

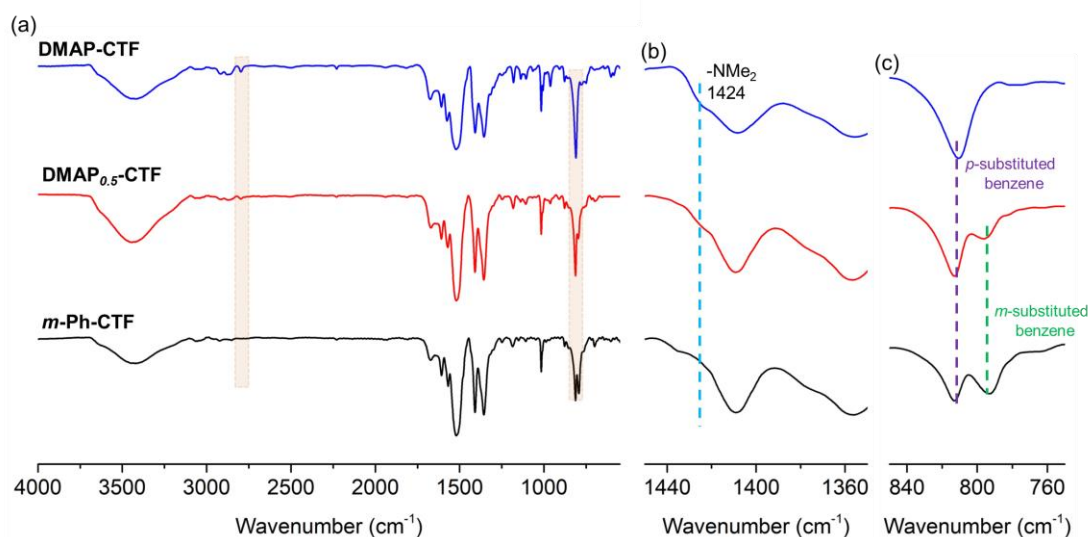


Figure S8. FT-IR spectra of m -Ph-CTF (gray), $DMAP_{0.5}$ -CTF (red) and standard DMAP-CTF (blue): (a) full-range spectra, and magnified view of the characteristic region for $-NMe_2$ groups (b) and substituted-benzene (c).

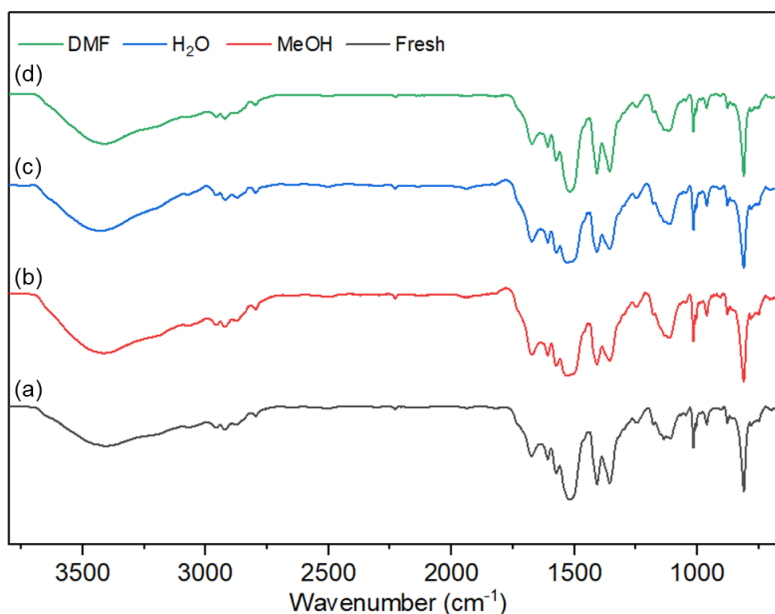


Figure S9. FT-IR spectra of standard DMAP-CTF treated with different solvents at room temperature for 48 h: (a) Fresh, (b) MeOH, (c) water, and (d) DMF.

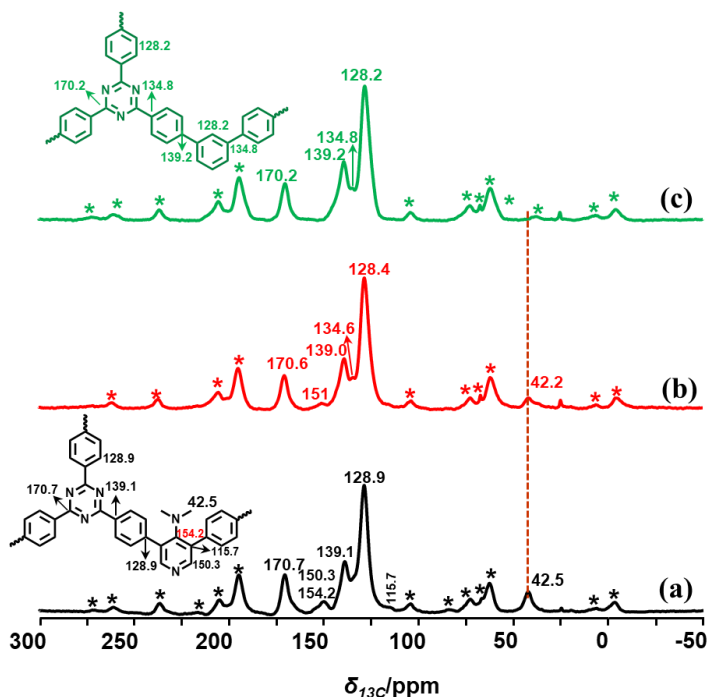


Figure S10. The solid-state ^{13}C CP/MAS NMR spectra (600 MHz) of standard DMAP-CTF (a), DMAP_{0.5}-CTF (b) and *m*-Ph-CTF (c). The asterisks denote the spinning sidebands.

To conduct a more in-depth investigation of the structural features of DMAP-CTF, three CTFs with different DMAP contents (Scheme S2-S4) were synthesized by modifying the feed ratios of DMAP-2CHO and *m*-Ph-2CHO (1/0, 1/1 and 0/1), namely DMAP-CTF, DMAP_{0.5}-CTF, and *m*-Ph-CTF. In ^{13}C CP/MAS NMR spectra of these CTFs,

characteristic signals corresponding to the triazine ring was observed at 170.7 ppm. Notably, as the DMAP content decreased, the NMR signals associated with the -N(Me)₂ carbon (*ab.* 42 ppm) and the pyridine ring (*ab.* 150 and 154 ppm) exhibited a progressively diminishing intensity. For the identification and attribution of other signals, please see Figure S10 for details.

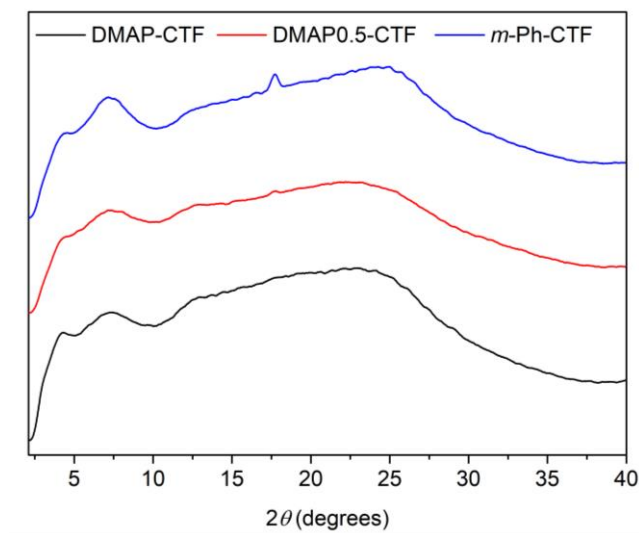


Figure S11. PXRD patterns of DMAP-CTF, DMAP_{0.5}-CTF and *m*-Ph-CTF.

As shown in Figure S11, DMAP-CTF, DMAP_{0.5}-CTF, and *m*-Ph-CTF exhibit nearly identical PXRD patterns. All the three materials show relatively low crystallinity, with *m*-Ph-CTF possessing a somewhat higher degree of structural ordering. Notably, the crystallinity decreases gradually as the amount of DMAP increases.

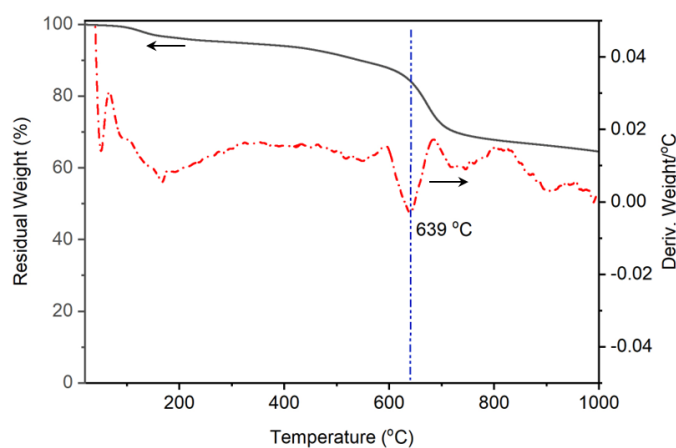


Figure S12. The TGA curve of the standard DMAP-CTF.

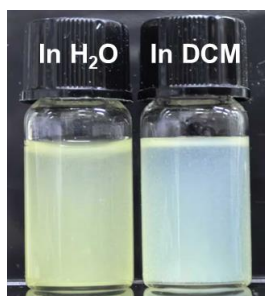


Figure S13. The dispersibility images of the standard DMAP-CTF (0.5 mg/mL) in H₂O and CH₂Cl₂.

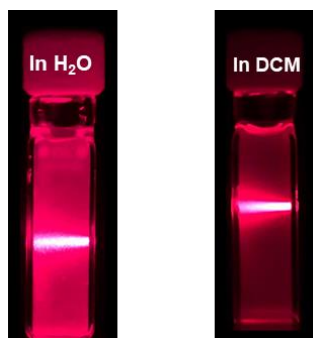


Figure S14. Tyndall effect of the standard DMAP-CTF in H₂O and CH₂Cl₂.

Table S2. Elemental analysis on the standard DMAP-CTF

Sample	C (wt%)	H (wt%)	N (wt%)
DMAP-CTF	70.10	3.734	18.87

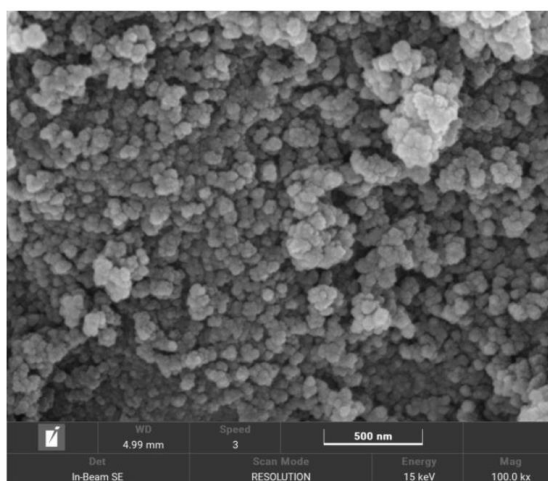
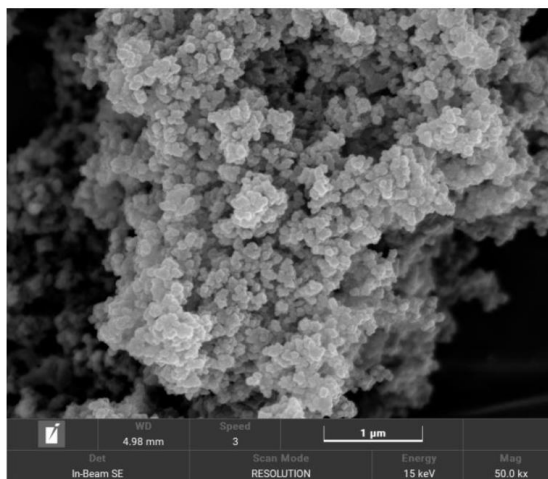


Figure S15. The SEM images of the standard DMAP-CTF.

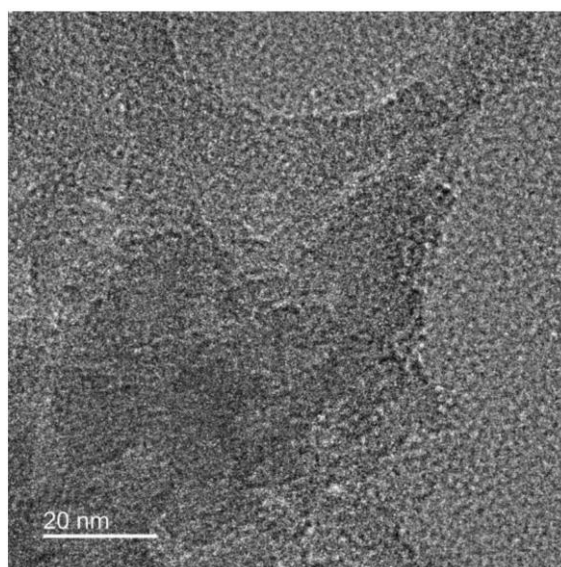
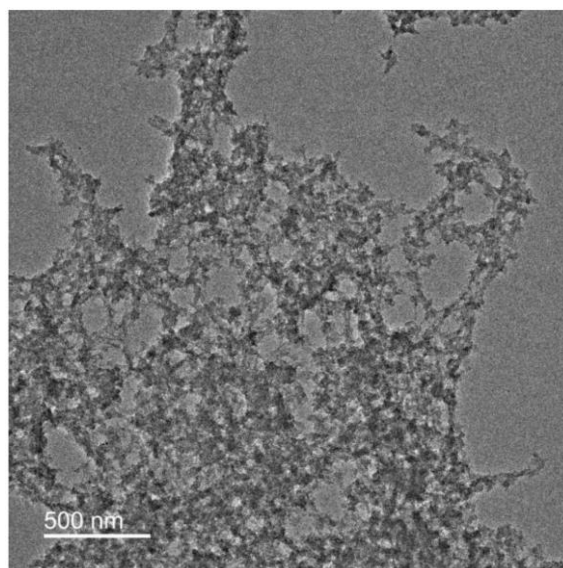


Figure S16. The TEM images the standard DMAP-CTF.

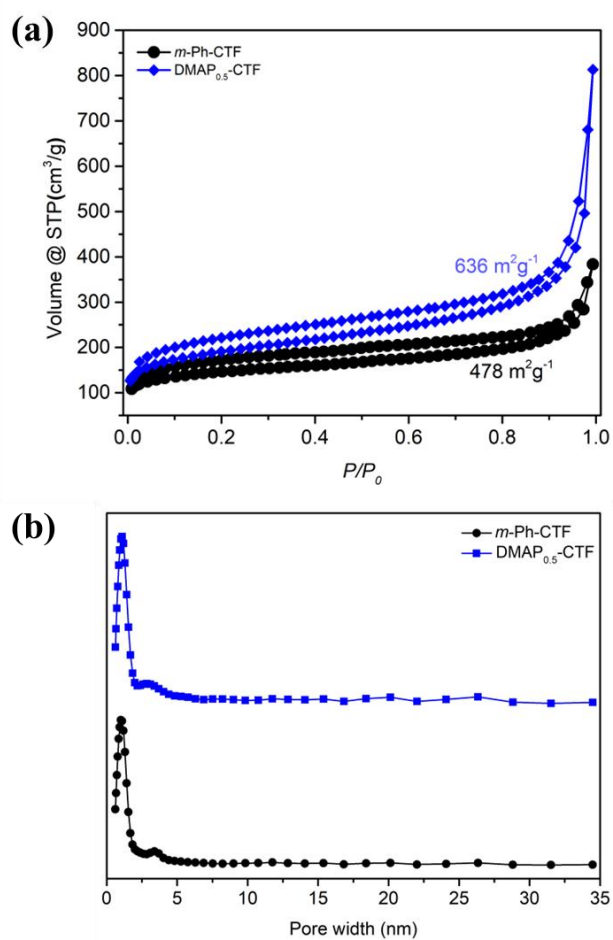


Figure S17. N₂ sorption isotherms (a) and pore size distribution (b) of DMAP_{0.5}-CTF (blue) and *m*-Ph-CTF (gray).

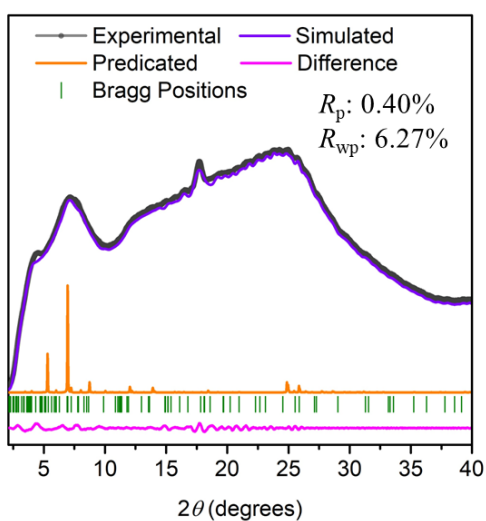


Figure S18. Experimental (gray), Pawley-refined (violet), and predicted (orange) PXRD patterns for AA stacking of *m*-Ph-CTF. The difference plot was presented in pink.

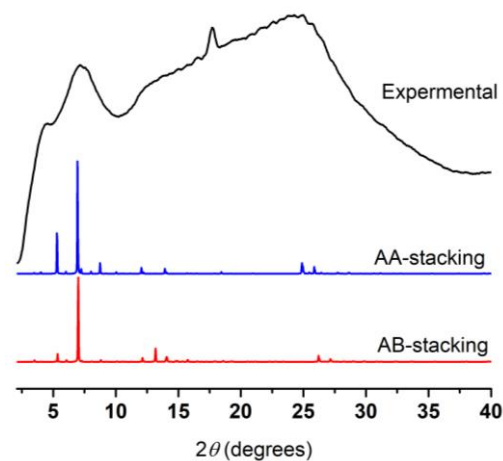


Figure S19. Powder X-ray diffraction (PXRD) pattern of the experimental (black), simulated AA stacking (blue) and simulated AB stacking (red) of *m*-Ph-CTF.

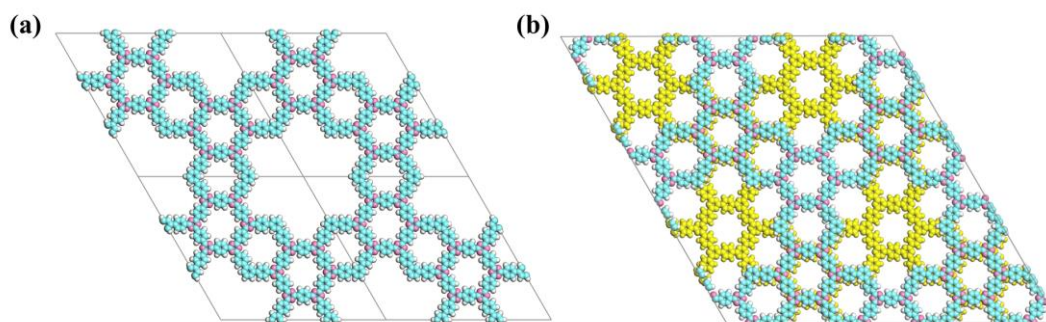


Figure S20. Graphic views of unit cell for *m*-Ph-CTF with AA stacking (a) and AB stacking (b). C, light cyan; O, light magenta; N, green; H, white.

Table S3. Fractional atomic coordinates for the unit cell of AA-stacking *m*-Ph-CTF

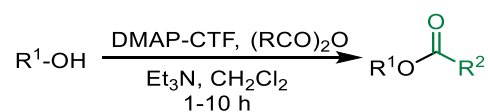
<i>m</i> -Ph-CTF:							
Space group: <i>P6/M2/M2/M</i> (Hexagonal)							
$a = b = 50.86803 \pm 0.00240 \text{ \AA}$, $c = 3.57400 \pm 0.00031 \text{ \AA}$, $\alpha = \beta = 90^\circ$, $\gamma = 120^\circ$							
Atom	X (Å)	Y (Å)	Z (Å)	Atom	X (Å)	Y (Å)	Z (Å)
C1	0.22339	-0.52576	-1.000	C18	0.19612	-0.41567	-1.000
C2	0.25085	-0.47087	-1.000	C19	0.16867	-0.38777	-1.000
C3	0.22294	-0.49831	-1.000	C20	0.14123	-0.41567	-1.000
C4	0.05854	-0.36149	-1.000	H21	0.20252	-0.54744	-1.000
C5	0.08617	-0.36108	-1.000	H22	0.25168	-0.44918	-1.000
C6	0.11383	-0.33365	-1.000	H23	0.03899	-0.38385	-1.000
C7	0.11298	-0.30654	-1.000	H24	0.08561	-0.38264	-1.000
C8	0.08538	-0.30681	-1.000	H25	0.13374	-0.28476	-1.000
C9	0.05703	-0.33432	-1.000	H26	0.08746	-0.28474	-1.000
C10	0.02849	-0.33455	-1.000	H27	0.0472	-0.28512	-1.000
C11	0.02739	-0.30732	-1.000	H28	0.21779	-0.41486	-1.000
N12	0.19512	-0.33324	-1.000	H29	0.11954	-0.41651	-1.000

C13	0.19531	-0.30643	-1.000	C30	0.000	-0.36205	-1.000
N14	0.1684	-0.3068	-1.000	C31	0.000	-0.30759	-1.000
C15	0.14161	-0.33343	-1.000	H32	0.000	-0.3828	-1.000
N16	0.14202	-0.35993	-1.000	H33	0.000	-0.28631	-1.000
C17	0.16862	-0.36013	-1.000				

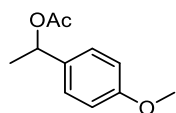
m-Ph-CTF exhibits relatively poor crystallinity, however, diffraction peaks can be observed at approximately $2\theta = 4.37^\circ$, 7.17° , 12.21° , and 24.43° . Some irregular structures or residual oligomers may exist within the framework, and the sharp signal around 17.70° is likely attributed to these impurities. Nevertheless, we remain interested in the theoretical structure of *m*-Ph-CTF and thus performed a preliminary simulation using the Material Studio software. As shown in Figure S16, the predicted diffraction pattern for AA stacking generally matches the experimental PXRD data, although the possibility of AB stacking cannot be entirely ruled out (Figure S19). Figure S20 displays the theoretically stacked structures of *m*-Ph-CTF in AA and AB configurations. For the AA structure, three small rings form a distinctive unit cell, resulting in a hexagonal structure (space group: $P6/M2/M2/M$; lattice parameters: $a = b = 50.86803 \pm 0.00240 \text{ \AA}$, $c = 3.57400 \pm 0.00031 \text{ \AA}$, $\alpha = \beta = 90^\circ$, $\gamma = 120^\circ$, Table S2). Theoretically, this would result in one large pore (ab . 29.1 \AA) and two similarly sized small pores (ab . $10.2\text{-}10.8 \text{ \AA}$) within the material. Experimentally, pore widths centered around 10.5 \AA and 33.5 \AA were obtained using the QSDFT method, showing reasonable agreement with the theoretical predictions. However, due to the synthetic challenge of achieving a highly ordered structure, the actual pore architecture in the CTF material may deviate from the ideal model, likely containing irregular or disordered pores.

D. Catalytic Performance of DMAP-CTF

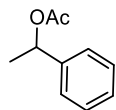
i) Typical Procedures to Acylation of Alcohols and Phenols



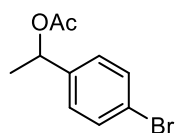
Alcohol or phenol (0.2 mmol), acid anhydride (0.4 mmol), and dry triethylamine (0.4 mmol) were sequentially added to a 10 mL reaction tube containing **DMAP-CTF** (20 mg, 17mol%) and dry CH_2Cl_2 (0.8 mL). The reaction mixture was stirred at room temperature until the substrate was disappeared, as confirmed by analytical monitoring. The solid catalyst was isolated by filtration and washed with EtOAc ($3 \times 4 \text{ mL}$). The obtained organic phase that contains the crude product was further purified by flash column chromatography (with petroleum ether/ethyl acetate = 25/1~16/1 as eluent) to provide the ester products. All the NMR data (summarized as below) are consistent with reported references.



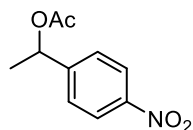
3a,^[2, 7] Colorless oil, 93% yield. ¹H NMR (400 MHz, Chloroform-*d*) δ 7.30 (d, J = 8.7 Hz, 2H), 6.88 (d, J = 8.8 Hz, 2H), 5.85 (q, J = 6.6 Hz, 1H), 3.80 (s, 3H), 2.05 (s, 3H), 1.52 (d, J = 6.6 Hz, 3H) ppm. ¹³C NMR (101 MHz, Chloroform-*d*) δ 170.5, 159.4, 133.9, 127.7, 113.9, 72.1, 55.4, 22.0, 21.5 ppm.



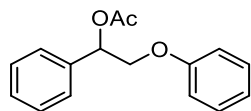
3b,^[2, 7] Colorless oil, 92% yield. ¹H NMR (400 MHz, CDCl₃): δ = 7.35-7.15 (m, 5H), 5.88 (q, J = 6.6 Hz, 1H), 2.07 (s, 3H), 1.53 (d, J = 6.6 Hz, 3H) ppm. ¹³C NMR (101 MHz, CDCl₃): δ = 170.4, 141.7, 128.5, 127.9, 126.1, 72.3, 22.2, 21.4 ppm.



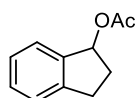
3c, Pale-yellow oil, 98% yield. ¹H NMR (400 MHz, CDCl₃): δ = 7.65 (d, J = 8.2 Hz, 2H), 7.23 (d, J = 8.2 Hz, 2H), 5.82 (q, J = 6.6 Hz, 1H), 2.07 (s, 3H), 1.51 (d, J = 6.6 Hz, 3H) ppm. ¹³C NMR (101 MHz, CDCl₃): δ = 170.2, 140.8, 131.6, 127.9, 121.8, 71.6, 22.1, 21.3 ppm.



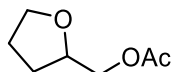
3d,^[2] Colorless oil, 99% yield. ¹H NMR (400 MHz, CDCl₃): δ = 8.19 (d, J = 8.8 Hz, 2H), 7.50 (d, J = 8.7 Hz, 2H), 5.91 (q, J = 6.6 Hz, 1H), 2.10 (s, 3H), 1.54 (d, J = 6.7 Hz, 3H) ppm. ¹³C NMR (101 MHz, CDCl₃): δ = 170.1, 149.0, 147.4, 126.8, 123.9, 71.3, 22.3, 21.2 ppm.



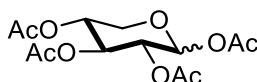
3e,^[7] Colorless oil, 84% yield. ¹H NMR (400 MHz, CDCl₃): δ = 7.42-7.32 (m, 5H), 7.28-7.24 (m, 2H), 6.94 (t, J = 7.3 Hz, 1H), 6.88 (d, J = 8.2 Hz, 2H), 6.15 (q, J = 3.8 Hz, 1H), 4.28-4.24 (m, 1H), 4.15-4.11 (m, 1H), 2.10 (s, 3H) ppm. ¹³C NMR (101 MHz, CDCl₃): δ = 170.1, 158.4, 137.0, 129.4, 128.6, 128.5, 126.7, 121.1, 114.7, 73.9, 70.3, 21.1 ppm.



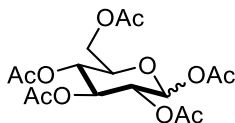
3f,^[8] Colorless oil, 90% yield. ¹H NMR (400 MHz, CDCl₃): δ = 7.41 (d, J = 7.4 Hz, 1H), 7.31-7.20 (m, 3H), 6.20 (q, J = 3.7 Hz, 1H), 3.15-3.07 (m, 1H), 2.91-2.84 (m, 1H), 2.54-2.44 (m, 1H), 2.13-2.07 (m, 1H), 2.06 (s, 3H) ppm. ¹³C NMR (101 MHz, CDCl₃): δ = 171.0, 144.4, 141.0, 128.9, 126.7, 125.5, 124.8, 78.3, 32.2, 30.1, 21.2 ppm.



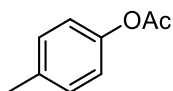
3g,^[9] Colorless oil, 94% yield. ¹H NMR (400 MHz, CDCl₃): δ = 4.16-4.07 (m, 2H), 3.98-3.93 (m, 1H), 3.90-3.85 (m, 1H), 3.81-3.76 (m, 1H), 2.08 (s, 3H), 2.03-1.85 (m, 3H), 1.62-1.55 (m, 1H) ppm. ¹³C NMR (101 MHz, CDCl₃): δ = 171.1, 76.5, 68.4, 66.6, 27.9, 25.6, 20.9 ppm.



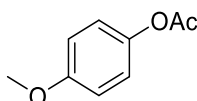
3h,^[10] White solid, 99% yield. ¹H NMR (400 MHz, CDCl₃): δ = 5.68 (d, J = 6.84 Hz, 1H), 5.16 (t, J = 8.3 Hz, 1H), 5.00-4.91 (m, 2 H), 4.11 (dd, J_1 = 12.0 Hz, J_2 = 5.0 Hz, 1H), 3.49 (dd, J_1 = 12.1 Hz, J_2 = 3.6 Hz, 1H), 2.07 (s, 3H), 2.03-2.01 (m, 9H) ppm. ¹³C NMR (101 MHz, CDCl₃): δ = 170.6, 170.1, 169.4, 169.2, 168.9, 91.7, 89.0, 72.8, 72.7, 70.2, 69.8, 69.2, 67.9, 67.7, 61.4, 20.8, 20.7, 20.6, 20.5, 20.4 ppm.



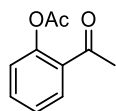
3i,^[11] White solid, 94% yield. ¹H NMR (400 MHz, CDCl₃): δ = 6.30 (d, J = 6.3 Hz, 1H, α -anomer), 5.69 (d, J = 8.3 Hz, 1H, β -anomer), 5.45 (t, J = 9.88 Hz, 1H, α -anomer), 5.26 (m, 1H, β -anomer), 5.14-5.09 (m, 4H, α - and β -anomer), 4.29-4.22 (m, 2H, α - and β -anomer), 4.11-4.06 (m, 3H, α - and β -anomer), 3.84-3.80 (m, 1H, β -anomer), 2.16-1.99 (several s, 30H, α - and β -anomer) ppm. ¹³C NMR (101 MHz, CDCl₃): δ = 169.70, 169.68, 169.2, 168.9, 91.9, 70.9, 69.4, 69.2, 68.2, 62.7, 20.7, 20.6, 20.53, 20.46 ppm.



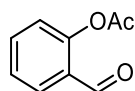
3j,^[12] Colorless oil, 92 % yield. ¹H NMR (400 MHz, Chloroform-*d*) δ 7.2 (d, J = 8.1 Hz, 2H), 7.0 (d, J = 8.4 Hz, 2H), 2.3 (s, 3H), 2.3 (s, 3H) ppm. ¹³C NMR (101 MHz, Chloroform-*d*) δ 169.9, 148.6, 135.6, 130.1, 121.4, 21.2, 21.0 ppm.



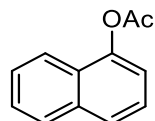
3k,^[13] Colorless oil, 94 % yield. ¹H NMR (400 MHz, Chloroform-*d*) δ 7.0 (d, J = 9.0 Hz, 2H), 6.9 (d, J = 9.1 Hz, 2H), 3.8 (s, 3H), 2.3 (s, 3H) ppm. ¹³C NMR (101 MHz, Chloroform-*d*) δ 170.0, 157.4, 144.3, 122.4, 114.6, 55.7, 21.2 ppm.



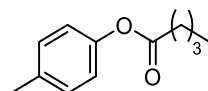
3l,^[14] Colorless oil, 96% yield. ¹H NMR (400 MHz, CDCl₃): δ = 7.81 (dd, J_1 = 7.8 Hz, J_2 = 1.4 Hz, 1H), 7.56-7.51 (m, 1H), 7.34-7.30 (m, 1H), 7.12 (d, J = 8.1 Hz, 1H), 2.56 (s, 3H), 2.34 (s, 3H) ppm. ¹³C NMR (101 MHz, CDCl₃): δ = 197.6, 169.6, 149.1, 133.5, 130.7, 130.3, 126.1, 123.9, 29.4, 21.2 ppm.



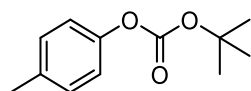
3m,^[15] Colorless oil, 98% yield. ¹H NMR (400 MHz, CDCl₃): δ = 10.11 (s, 1H), 7.88 (dd, J_1 = 7.7 Hz, J_2 = 1.5 Hz, 1H), 7.65-7.61 (m, 1H), 7.40 (t, J = 7.5 Hz, 1H), 7.18 (d, J = 8.1 Hz, 1H), 2.39 (s, 3H) ppm. ¹³C NMR (101 MHz, CDCl₃): δ = 188.8, 169.3, 151.5, 135.3, 131.3, 128.1, 126.5, 123.5, 20.9 ppm.



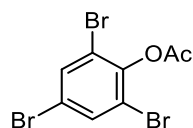
3n,^[16] Colorless oil, 98% yield. ¹H NMR (400 MHz, CDCl₃): δ = 7.87-7.84 (m, 2H), 7.73 (d, J = 8.2 Hz, 1H), 7.52-7.43 (m, 3H), 7.25-7.22 (m, 1H), 2.44 (s, 3H) ppm. ¹³C NMR (101 MHz, CDCl₃): δ = 169.5, 146.7, 134.7, 128.1, 126.8, 126.5, 126.1, 125.5, 121.2, 118.1, 21.0 ppm.



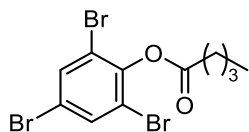
3o, Colorless oil, 91% yield. ¹H NMR (400 MHz, CDCl₃): δ = 7.17 (d, J = 8.1 Hz, 2H), 6.95 (d, J = 7.1 Hz, 2H), 2.55 (t, J = 7.5 Hz, 2H), 2.34 (s, 3H), 1.78-1.71 (m, 2H), 1.49-1.40 (m, 2H), 0.97 (t, J = 7.3 Hz, 3H) ppm. ¹³C NMR (101 MHz, CDCl₃): δ = 172.6, 148.5, 135.3, 129.9, 121.2, 34.1, 27.1, 22.3, 20.9, 13.8 ppm.



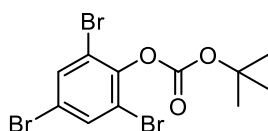
3p,^[17] Colorless oil, 96% yield. ¹H NMR (400 MHz, CDCl₃): δ = 7.16 (d, J = 8.4 Hz, 2H), 7.05 (d, J = 8.4 Hz, 2H), 2.34 (s, 3H), 1.56 (s, 9H) ppm. ¹³C NMR (101 MHz, CDCl₃): δ = 152.2, 148.9, 135.4, 129.9, 121.0, 83.3, 27.7, 20.9 ppm.



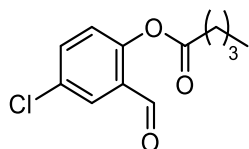
3q,^[17] White solid, 99% yield. ¹H NMR (400 MHz, CDCl₃): δ = 7.71 (s, 2H), 2.39 (s, 3H) ppm. ¹³C NMR (101 MHz, CDCl₃): δ = 167.0, 145.7, 134.8, 119.8, 118.5, 20.5 ppm.



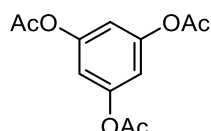
3r, White solid, 89% yield. ¹H NMR (400 MHz, CDCl₃): δ = 7.70 (s, 2H), 2.66 (t, *J* = 7.4 Hz, 2H), 1.84-1.76 (m, 2H), 1.53-1.44 (m, 2H), 0.98 (t, *J* = 7.4 Hz, 3H) ppm. ¹³C NMR (101 MHz, CDCl₃): δ = 168.6, 151.1, 112.8, 21.1 ppm.



3s,^[17] Colorless oil, 92% yield. ¹H NMR (400 MHz, CDCl₃): δ = 7.70 (s, 2H), 1.57 (s, 9H) ppm. ¹³C NMR (101 MHz, CDCl₃): δ = 149.1, 145.7, 134.8, 119.8, 118.6, 85.2, 27.6 ppm.



3t, Pale yellow solid, 91% yield. ¹H NMR (400 MHz, Chloroform-*d*) δ 10.07 (s, 1H), 7.85 (d, *J* = 2.6 Hz, 1H), 7.58 (dd, *J* = 8.7, 2.6 Hz, 1H), 7.15 (d, *J* = 8.7 Hz, 1H), 2.66 (t, *J* = 7.5 Hz, 2H), 1.77 (m, 2H), 1.46 (m, 2H), 0.98 (t, *J* = 7.4 Hz, 3H) ppm. ¹³C NMR (101 MHz, Chloroform-*d*) δ 187.3, 172.0, 150.5, 135.2, 132.3, 130.1, 129.2, 125.2, 34.0, 26.9, 22.4, 13.8 ppm.



3u,^[18] White solid, 97% yield. ¹H NMR (400 MHz, CDCl₃): δ = 6.83 (s, 1H), 2.65 (s, 3H) ppm. ¹³C NMR (101 MHz, CDCl₃): δ = 169.8, 145.8, 134.8, 119.7, 118.5, 33.6, 26.8, 22.3, 13.7 ppm.

ii) Procedure for the Continuous Flow Experiment of Acylation

The continuous flow chemical reactor was first established as the following procedures. Approximately 9.8 g of 70 mesh glass beads (*l* is about 3.5 cm) were packed as a subgrade at the bottom of a glass column (φ = 1 cm). Subsequently, the fixed glass column was filled with a mixture of glass beads (14 g, 70 mesh) and 2.1 mol% **DMAP-CTF** (100 mg) to create the catalytic section (*l* = 4.5 cm). The top of the column was sealed with 9.8 g of 70 mesh glass beads (*l* is about 3.5 cm) and absorbent cotton.

Generally, the two ends of the device were respectively connected to a peristaltic pump and two-neck flask that contained anhydrous CH_2Cl_2 solutions (50 mL) containing 8.0 mmol of substrates **1**, 12 mmol of acid anhydride, and 12 mmol of Et_3N . The flow rate through the chemical reactor was approximately 2 mL/min (Figure S21). The total time required to collect the given volume of product was recorded.

After the reaction was completed, pure CH_2Cl_2 (3×30 mL) was used to wash the reactor and collect the product adequately. The continuous flow reactor could be directly used to prepare next product. All reaction liquid was combined to recycle CH_2Cl_2 under reduced pressure. The resulted crude products were purified through flash column chromatography (with petroleum/EtOAc = 25/1~16/1 as eluent).

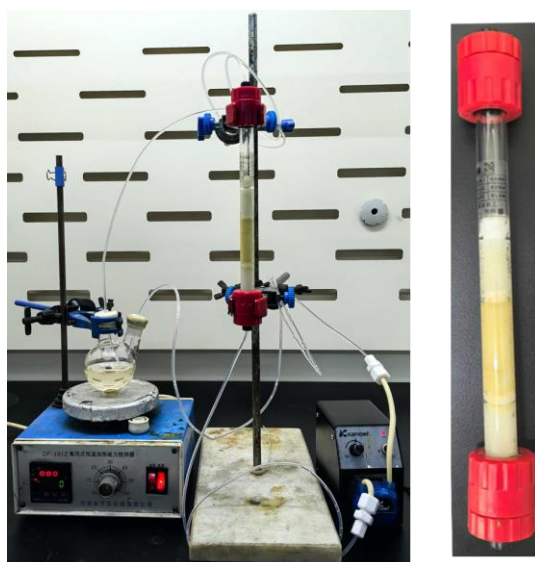
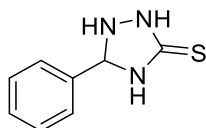


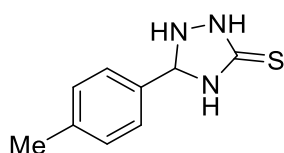
Figure S21. Continuous-flow photocatalytic reactor for acylation.

iii) Typical Procedures for DMAP-CTF mediated reaction of Aldehydes and thiocarbazon

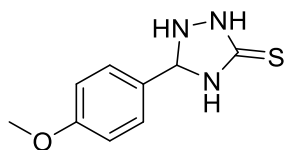
Aldehyde (0.2 mmol), thiosemicarbazide (0.22 mmol), and H_2O (0.8 mL) were sequentially added to a 10 mL reaction tube containing DMAP-CTF (20 mg, 17 mol%). The reaction mixture was stirred at room temperature for 30-60 min until the substrate was disappeared, as confirmed by TLC. The solid catalyst was isolated by filtration and washed with EtOAc (3×4 mL). The obtained organic phase that contains the crude product was further purified by flash column chromatography (with petroleum ether/ethyl acetate = 2/1 as eluent) to provide the ester products.



5a,^[11] White solid, 89% yield. ¹H NMR (400 MHz, DMSO-*d*₆): δ = 11.44 (s, 1H), 8.22 (s, 1H), 8.04 (s, 1H), 8.00 (s, 1H), 7.79 (dd, *J* = 6.8, 3.0 Hz, 2H), 7.40 (dd, *J* = 5.1, 1.9 Hz, 3H). ¹³C NMR (101 MHz, DMSO-*d*₆): δ = 178.0, 142.3, 134.2, 129.9, 128.7, 127.3.



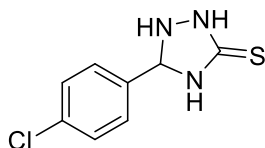
5b,^[11] White solid, 87% yield. ¹H NMR (400 MHz, DMSO-*d*₆): δ = 11.38 (s, 1H), 8.17 (s, 1H), 8.01 (s, 1H), 7.97-7.90 (m, 1H), 7.68 (d, *J* = 8.1 Hz, 2H), 7.21 (d, *J* = 7.9 Hz, 2H), 2.32 (s, 3H). ¹³C NMR (101 MHz, DMSO-*d*₆): δ = 177.8, 142.4, 139.7, 131.5, 129.3, 127.3, 21.1.



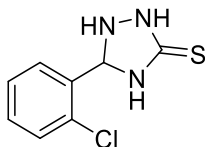
5c,^[11, 19] Pale yellow solid, 95% yield. ¹H NMR (400 MHz, DMSO-*d*₆): δ = 11.32 (s, 1H), 8.12 (s, 1H), 7.99 (s, 1H), 7.96-7.87 (m, 1H), 7.78-7.67 (m, 2H), 7.03-6.89 (m, 2H), 3.78 (s, 3H). ¹³C NMR (101 MHz, DMSO-*d*₆): δ = 177.6, 160.7, 142.3, 129.0, 126.8, 114.2, 55.3.



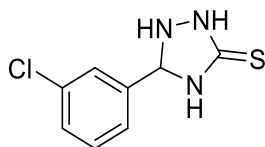
5d, White solid, 86% yield. ¹H NMR (400 MHz, DMSO-*d*₆): δ = 11.41 (s, 1H), 8.40 (s, 1H), 8.19 – 8.12 (m, 1H), 8.09 (dd, *J* = 7.8, 1.8 Hz, 1H), 7.94 (s, 1H), 7.37 (ddd, *J* = 8.7, 7.3, 1.8 Hz, 1H), 7.05 (d, *J* = 8.1 Hz, 1H), 6.95 (t, *J* = 7.5 Hz, 1H), 3.82 (s, 3H). ¹³C NMR (101 MHz, DMSO-*d*₆): δ = 177.8, 157.8, 137.9, 131.4, 126.1, 122.2, 120.6, 111.7, 55.7.



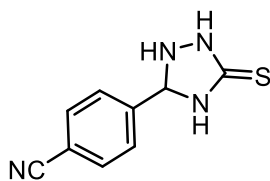
5e,^[11] White solid, 91% yield. ¹H NMR (400 MHz, DMSO-*d*₆): δ = 11.48 (s, 1H), 8.24 (s, 1H), 8.08 (s, 1H), 8.02 (s, 1H), 7.84 (d, *J* = 8.5 Hz, 2H), 7.45 (d, *J* = 8.5 Hz, 2H). ¹³C NMR (101 MHz, DMSO-*d*₆): δ = 178.1, 140.9, 134.3, 133.2, 129.0, 128.7.



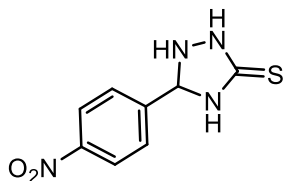
5f,^[19] Pale yellow solid, 94% yield. ¹H NMR (400 MHz, DMSO-*d*₆): δ = 11.62 (s, 1H), 8.47 (s, 1H), 8.30 (d, *J* = 5.7 Hz, 2H), 8.11 (s, 1H), 7.48 (d, *J* = 7.9 Hz, 1H), 7.43 – 7.32 (m, 2H). ¹³C NMR (101 MHz, DMSO-*d*₆): δ = 178.2, 138.2, 133.1, 131.5, 131.2, 129.8, 127.5, 127.4.



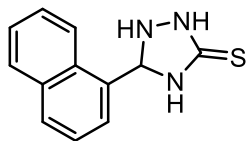
5g,^[19] White solid, 89% yield. ¹H NMR (400 MHz, DMSO-*d*₆): δ = 11.52 (s, 1H), 8.27 (s, 1H), 8.20 (s, 1H), 8.05 (d, *J* = 2.1 Hz, 1H), 8.01 (s, 1H), 7.68-7.59 (m, 1H), 7.41 (dd, *J* = 4.9, 1.8 Hz, 2H). ¹³C NMR (101 MHz, DMSO-*d*₆): δ = 178.2, 140.5, 136.5, 133.8, 130.5, 129.4, 126.7, 126.0.



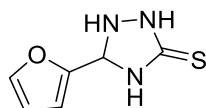
5h,^[20] white solid, 93% yield. ¹H NMR (400 MHz, DMSO-*d*₆): δ 11.65 (s, 1H), 8.36 (s, 1H), 8.22 (s, 1H), 8.06 (s, 1H), 8.01 (d, *J* = 8.5 Hz, 2H), 7.85 (d, *J* = 8.4 Hz, 2H) ppm. ¹³C NMR (101 MHz, DMSO-*d*₆): δ = 178.4, 140.1, 138.9, 132.6, 127.9, 118.8, 111.5 ppm.



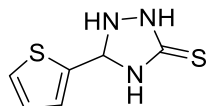
5i,^[21] pale yellow solid, 95% yield. ¹H NMR (400 MHz, DMSO-*d*₆) δ 11.72 (s, 1H), 8.41 (s, 1H), 8.27 (s, 1H), 8.22 (d, *J* = 8.9 Hz, 2H), 8.14-8.06 (m, 3H) ppm. ¹³C NMR (101 MHz, DMSO-*d*₆) δ 178.5, 147.6, 140.8, 139.6, 128.2, 123.8 ppm.



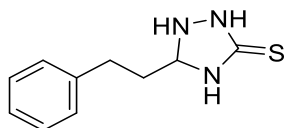
5j,^[20] white solid, 96% yield. ¹H NMR (400 MHz, DMSO-*d*₆): δ = 11.49 (s, 1H), 8.92 (s, 1H), 8.39-8.29 (m, 2H), 8.23 (d, *J* = 7.3 Hz, 1H), 8.04-7.96 (m, 3H), 7.68-7.61 (m, 1H), 7.57 (m, 2H) ppm. ¹³C NMR (101 MHz, DMSO-*d*₆) : δ = 177.9, 141.0, 133.4, 130.5, 130.3, 129.3, 128.9, 127.3, 126.2, 125.8, 125.6, 122.9 ppm.



5k,^[22] Yellow solid, 91% yield. ¹H NMR (400 MHz, DMSO-*d*₆): δ = 11.43 (s, 1H), 8.21 (s, 1H), 7.96 (s, 1H), 7.80 (t, *J* = 1.2 Hz, 1H), 7.62 (s, 1H), 6.96 (d, *J* = 3.5 Hz, 1H), 6.62 (dd, *J* = 3.5, 1.8 Hz, 1H). ¹³C NMR (101 MHz, DMSO-*d*₆): δ = 177.8, 149.4, 145.0, 132.5, 112.8, 112.3.



5l,^[11] Yellow solid, 92% yield. ¹H NMR (400 MHz, DMSO-*d*₆): δ = 11.44 (s, 1H), 8.24 (s, 1H), 8.20 (s, 1H), 7.64 (d, *J* = 5.2 Hz, 1H), 7.55 (s, 1H), 7.44 (dd, *J* = 3.7, 1.1 Hz, 1H), 7.11 (dd, *J* = 5.0, 3.6 Hz, 1H). ¹³C NMR (101 MHz,) δ 177.8, 138.9, 137.8, 130.8, 129.1, 128.2.



5m,^[11] Pale yellow solid, 94% yield. ¹H NMR (400 MHz, DMSO-*d*₆): δ = 11.09 (s, 1H), 7.98 (s, 1H), 7.46 (q, *J* = 5.0, 3.9 Hz, 2H), 7.32-7.16 (m, 5H), 2.81 (t, *J* = 7.7 Hz, 2H), 2.55-2.47 (m, 2H). ¹³C NMR (101 MHz, DMSO): δ = 177.6, 146.6, 141.1, 128.4, 128.4, 126.0, 33.4, 31.6.

E. Recyclability Tests of DMAP-CTF

Procedures for the recycling experiments: The experiments were carried out with tribromophenol (0.2 mmol) and Ac₂O (0.4 mmol), DMAP-CTF (20 mg, 17mol%), DCM (0.8 mL) and Et₃N (0.4 mmol) under the optimized reaction conditions. After the reaction was completed (monitored by TLC), the CTF was collected *via* filtration and then washed successively by EtOAc (3 mL × 4) and acetone (3 mL × 4) to remove the residual products locked in the pore channels. The organic phase was combined to remove solvent under reduced pressure. The resulted residues were purified through flash column chromatography (with petroleum/EtOAc = 20/1 as eluent). The recycled DMAP-CTF was dried and then subject to the next catalytic cycle. Moreover, the heterogeneous catalyst can be further purified to remove residual products by performing Soxhlet extraction for 12 h with MeOH and THF as solvents, respectively. Subsequently, it is dried in a vacuum oven at 80 °C for 12 hours. The purified DMAP-CTF can then be utilized for characterization.

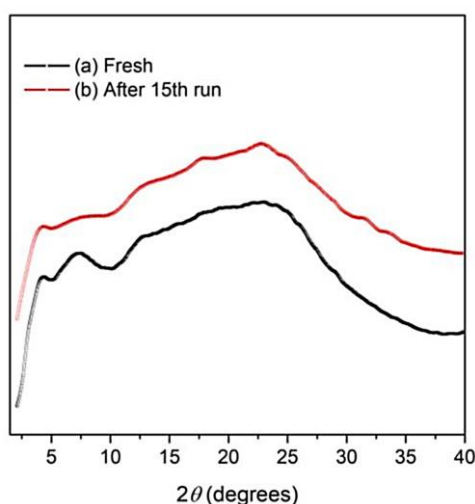


Figure S22. PXRD spectra of the fresh (a) and the recycled **DMAP-CTF** after 15th run (b).

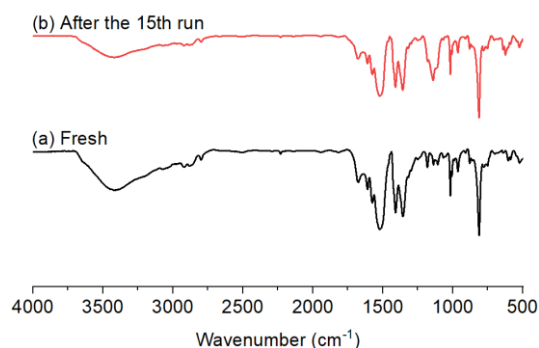


Figure S23. FT-IR spectra of the fresh (a) and the recovered (b) **DMAP-CTF**.

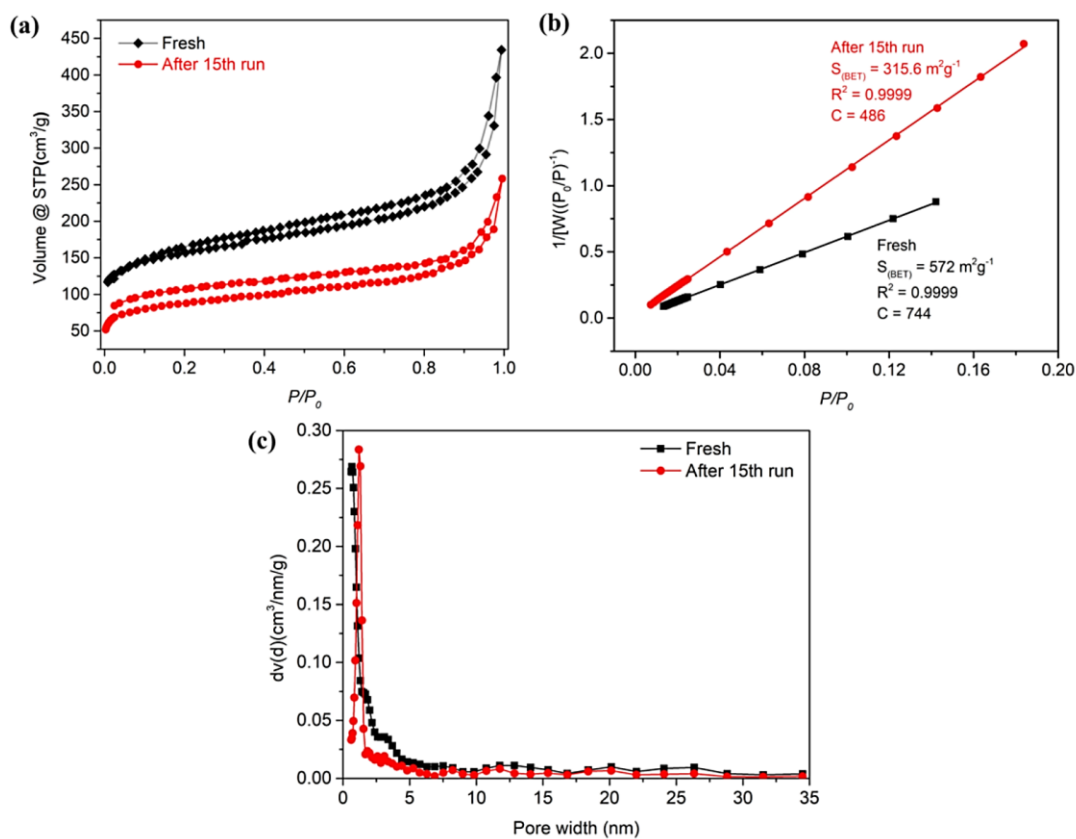


Figure S24. N₂ adsorption-desorption isotherms (a), BET surface areas plots (b) and pore size distribution (c) of DMAP-CTF: fresh (black) and after the 15th run (red). The porosity of DMAP-CTF showed a gradual downward trend. The BET surface area of the recovered DMAP-CTF after 15th run was about 316 m² g⁻¹, which was lower than the fresh catalyst (572 m² g⁻¹). STP: standard temperature and pressure.

F. The possible mechanisms for the DMAP-CTF mediated reactions

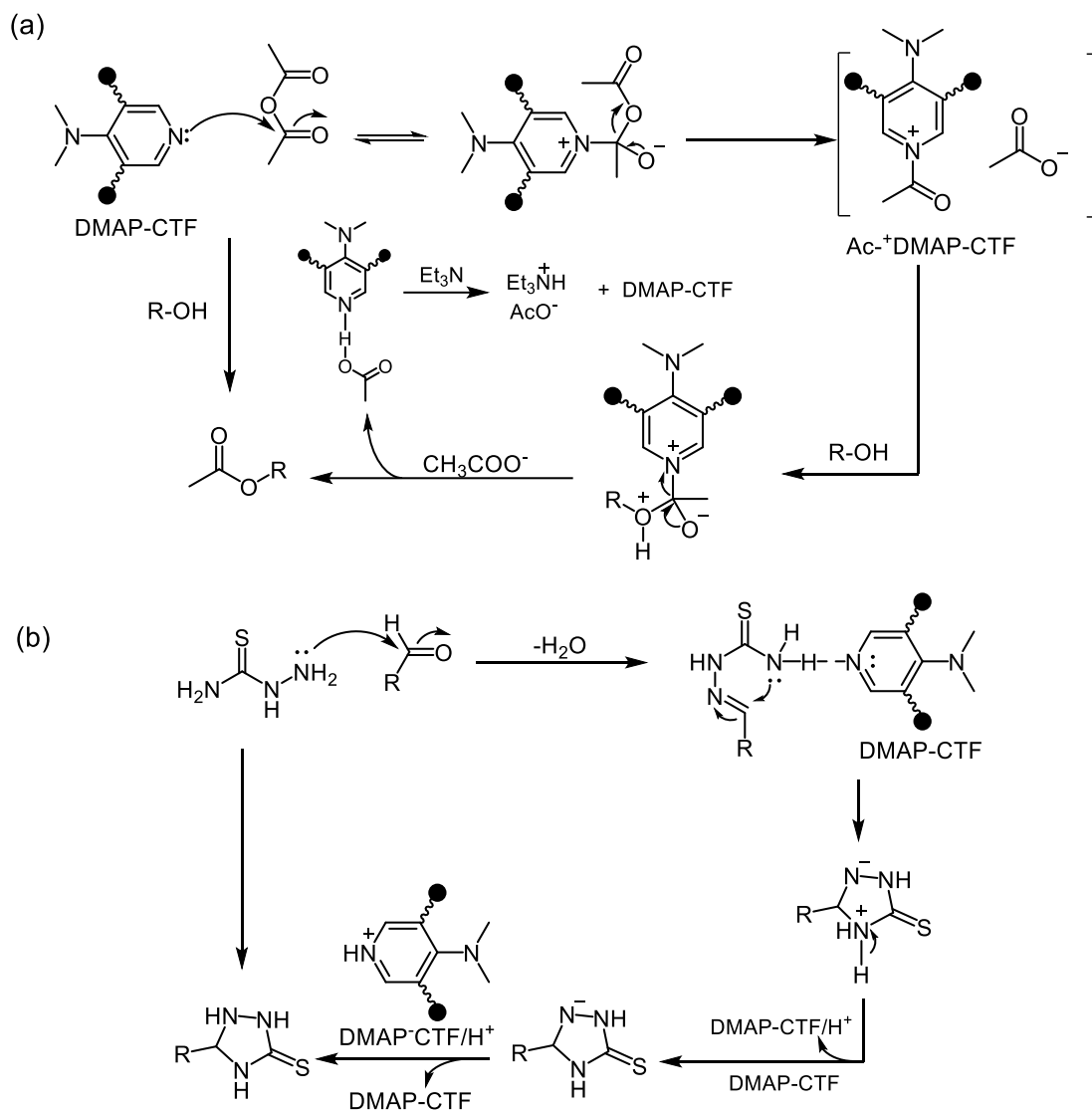


Figure S25. The proposed mechanisms for the synthesis of 1,2,4-triazolidine-3-thiones (a) and esterification reaction (b).

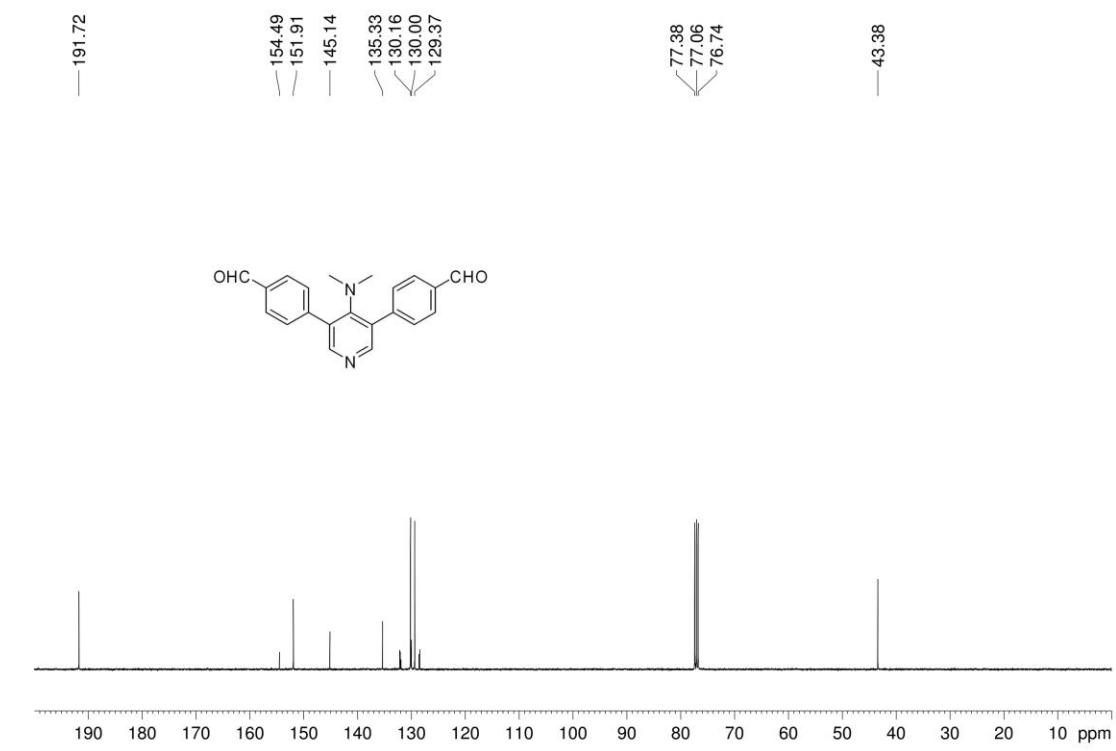
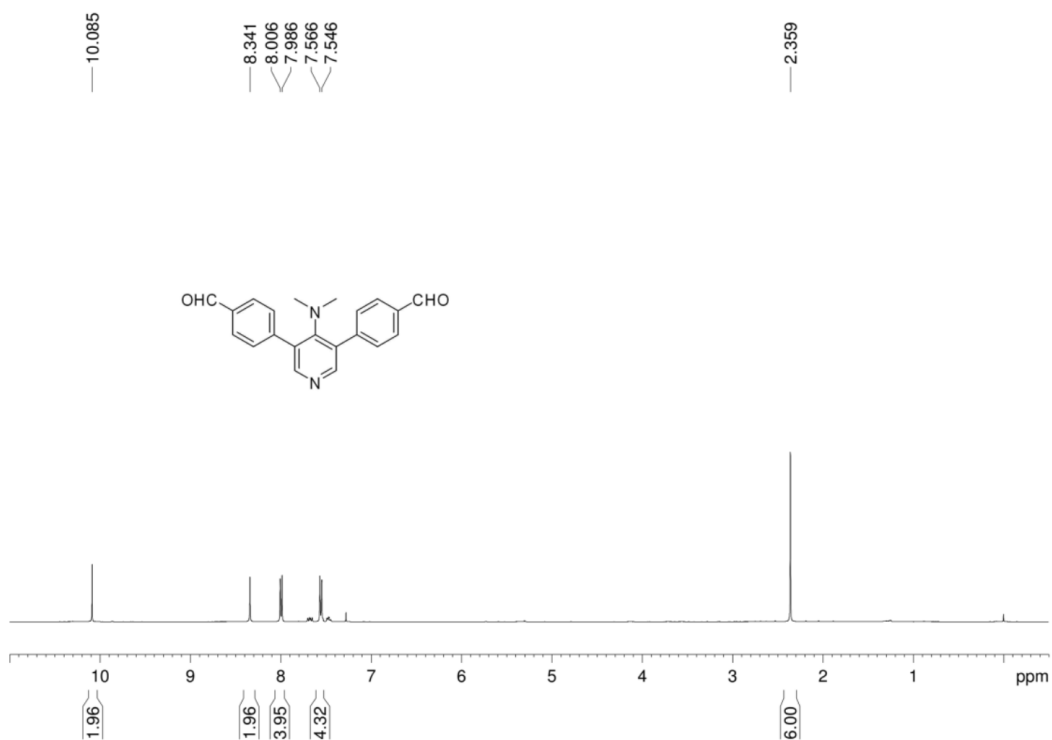
For the reaction of thiosemicarbazide with aldehydes, **DMAP-CTF** act as Lewis-base catalyst to enhance the nucleophilicity of amino through the hydrogen-bond interaction of DMAP unit with NH/NH₂. Besides, DMAP-CTF could also assisted the proton transfer to generate the triazolidine-3-thiones. For the acylation reaction, the mechanism follows the classic homogeneous DMAP-catalyzed esterification process.^[23-25] Accordingly, heterogeneous DMAP-CTF acts as a nucleophile, reacting with the anhydride and activated acyl groups. Meanwhile, the carboxylate anion mediates proton transfer, while triethylamine neutralizes the acid by-product and regenerates the carboxylate and DMAP-CTF.

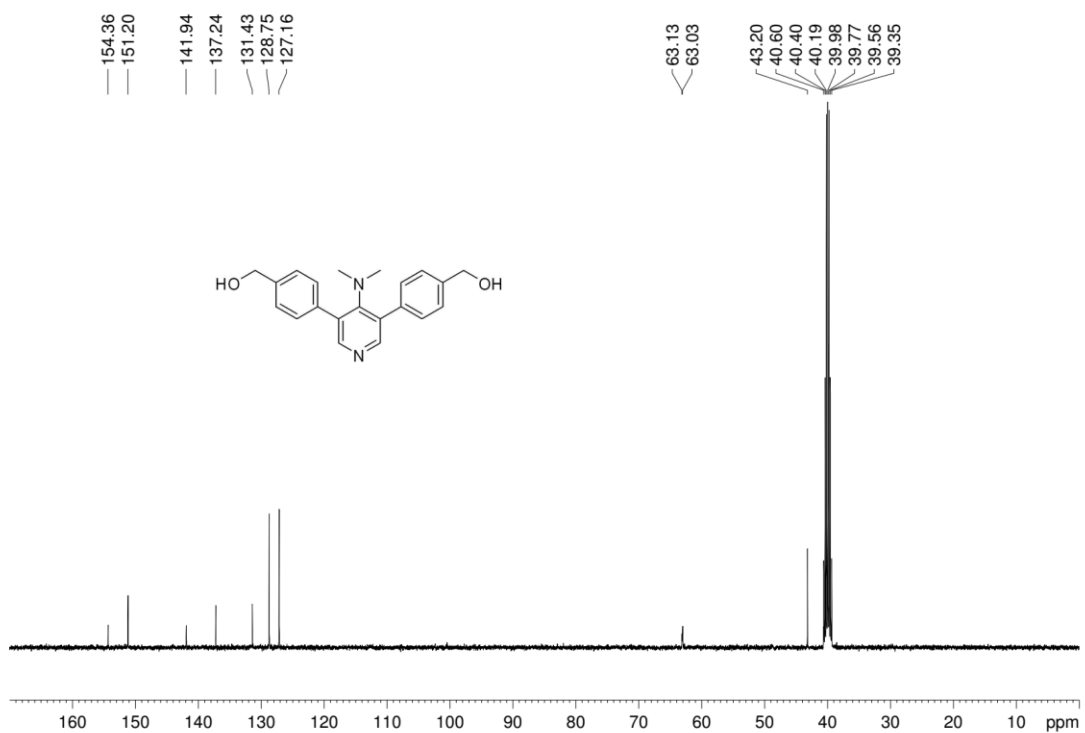
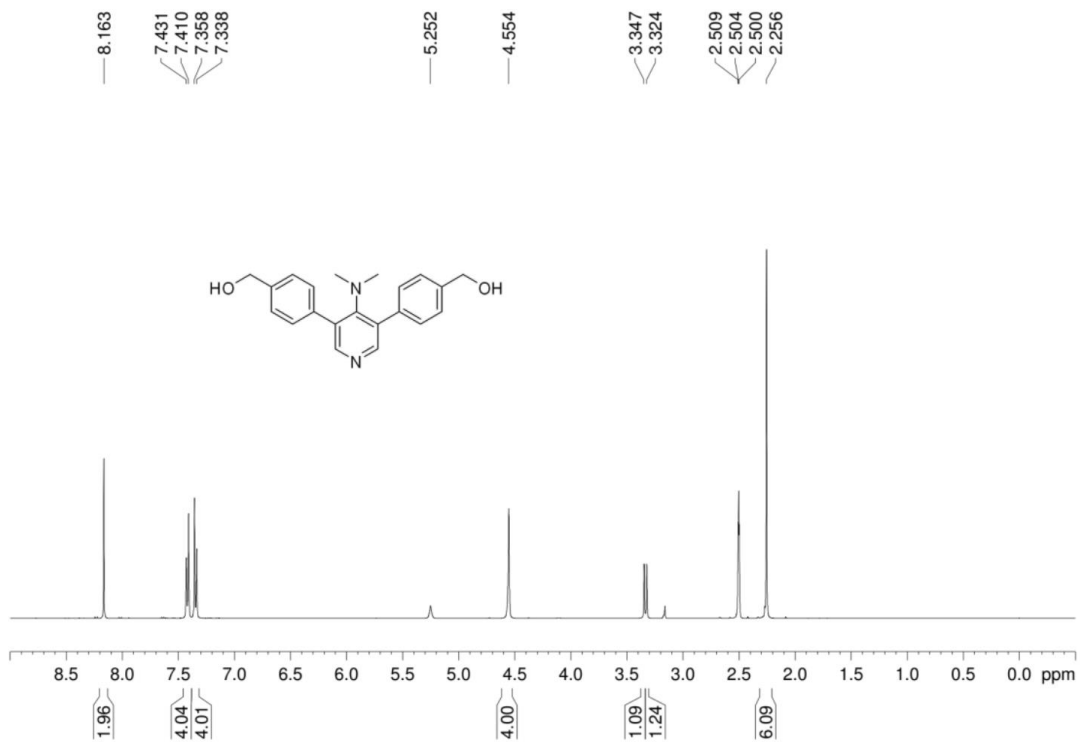
G. References

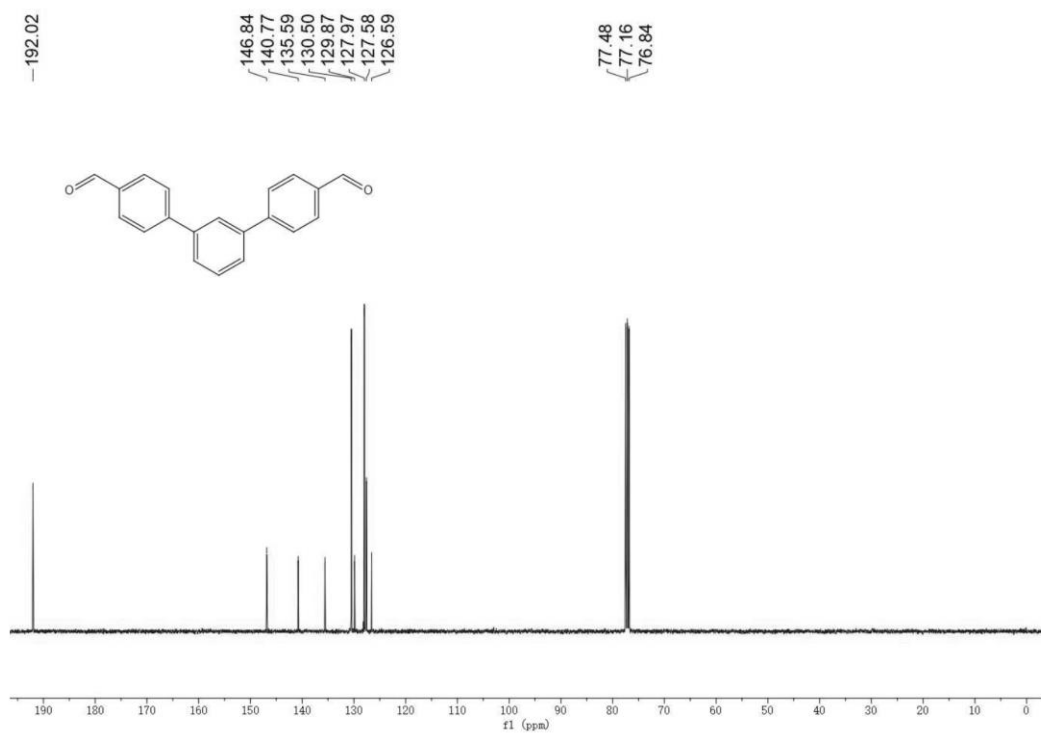
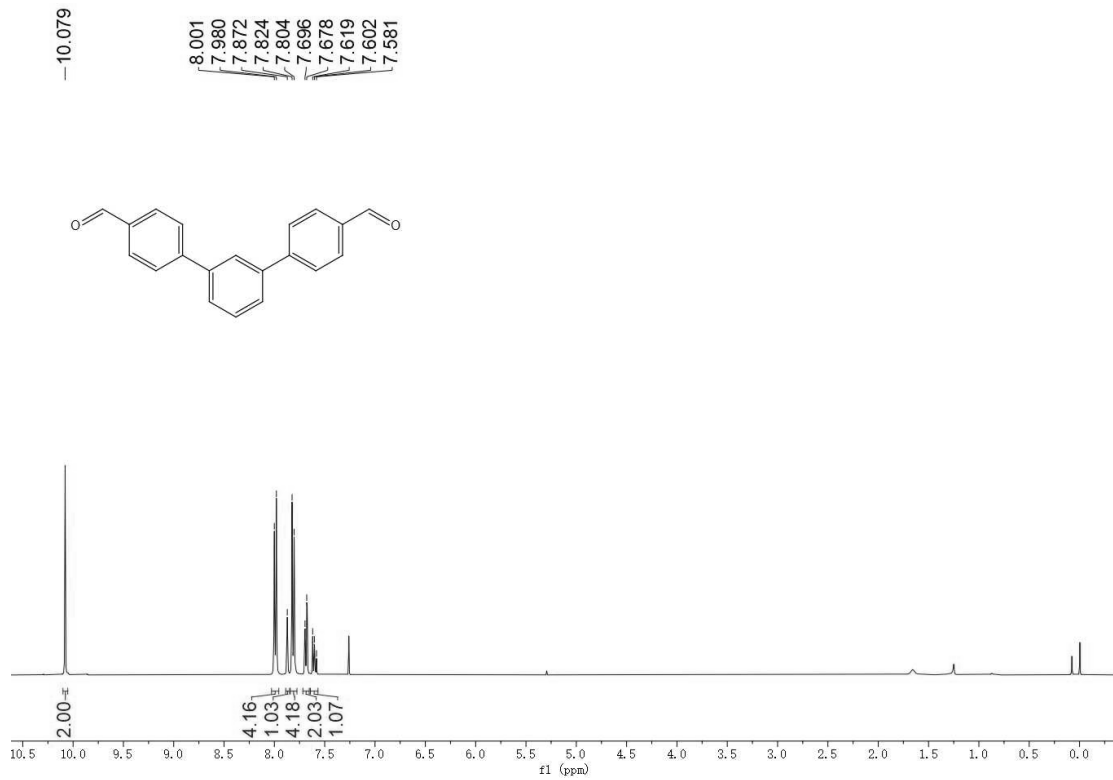
- [1] K. Wang, L.-M. Yang, X. Wang, L. Guo, G. Cheng, C. Zhang, S. Jin, B. Tan, A. Cooper, *Angew. Chem. Int. Ed.* **2017**, *56*, 14149-14153.
- [2] Y. Zhang, Y. Zhang, Y. L. Sun, X. Du, J. Y. Shi, W. D. Wang, W. Wang, *Chem. Eur. J.* **2012**, *18*, 6328-6334.
- [3] M. J. Frisch, G. W. Trucks, H. B. Schlegel, G. E. Scuseria, M. A. Robb, J. R. Cheeseman, G. Scalmani, V. Barone, G. A. Petersson, H. Nakatsuji, X. Li, M. Caricato, A. V. Marenich, J. Bloino, B. G. Janesko, R. Gomperts, B. Mennucci, H. P. Hratchian, J. V. Ortiz, A. F. Izmaylov, J. L. Sonnenberg, Williams, F. Ding, F. Lipparini, F. Egidi, J. Goings, B. Peng, A. Petrone, T. Henderson, D. Ranasinghe, V. G. Zakrzewski, J. Gao, N. Rega, G. Zheng, W. Liang, M. Hada, M. Ehara, K. Toyota, R. Fukuda, J. Hasegawa, M. Ishida, T. Nakajima, Y. Honda, O. Kitao, H. Nakai, T. Vreven, K. Throssell, J. A. Montgomery Jr., J. E. Peralta, F. Ogliaro, M. J. Bearpark, J. J. Heyd, E. N. Brothers, K. N. Kudin, V. N. Staroverov, T. A. Keith, R. Kobayashi, J. Normand, K. Raghavachari, A. P. Rendell, J. C. Burant, S. S. Iyengar, J. Tomasi, M. Cossi, J. M. Millam, M. Klene, C. Adamo, R. Cammi, J. W. Ochterski, R. L. Martin, K. Morokuma, O. Farkas, J. B. Foresman, D. J. Fox, **2016**.
- [4] T. Lu, F. Chen, *J. Comput. Chem.* **2012**, *33*, 580-592.
- [5] W. Humphrey, A. Dalke, K. Schulten, *J. Mol. Graph.* **1996**, *14*, 33-38.
- [6] W.-K. An, X. Xu, S.-J. Zheng, Y.-N. Du, J. Ouyang, L.-X. Xie, Y.-L. Ren, M. He, C.-L. Fan, Z. Pan, Y.-H. Li, *ACS Catal.* **2023**, *13*, 9845-9856.
- [7] X. Wang, H. Sun, Y. Cheng, W. Yang, X. Wang, L. Xiong, Y. Li, J. Wang, C. Gan, C. Lin, H. Xu, *RSC Adv.* **2024**, *14*, 12574-12579.
- [8] T. d. S. Fonseca, M. R. d. Silva, M. d. C. F. de Oliveira, T. L. G. d. Lemos, R. d. A. Marques, M. C. de Mattos, *Appl. Catal. A: General* **2015**, *492*, 76-82.
- [9] T. Toyao, M. Nurnobi Rashed, Y. Morita, T. Kamachi, S. M. A. Hakim Siddiki, M. A. Ali, A. S. Touchy, K. Kon, Z. Maeno, K. Yoshizawa, K.-i. Shimizu, *ChemCatChem* **2019**, *11*, 449-456.
- [10] A. M. Haydl, B. Breit, *Angew. Chem. Int. Ed.* **2015**, *54*, 15530-15534.
- [11] D. A. Mali, V. N. and Telvekar, *Synth. Commun.* **2017**, *47*, 324-329.
- [12] W. Yu, M. Zhou, T. Wang, Z. He, B. Shi, Y. Xu, K. Huang, *Org. Lett.* **2017**, *19*, 5776-5779.
- [13] F. Panahi, S. K. Dangolani, A. Khalafi-Nezhad, *ChemistrySelect* **2016**, *1*, 3541-3547.
- [14] C. Proença, H. M. T. Albuquerque, D. Ribeiro, M. Freitas, C. M. M. Santos, A. M. S. Silva, E. Fernandes, *Eur. J. Med. Chem.* **2016**, *115*, 381-392.
- [15] T. Ikawa, S. Masuda, S. Akai, *Chem. Eur. J.* **2020**, *26*, 4320-4332.
- [16] L. Shi, H. Liu, L. Huo, Y. Dang, Y. Wang, B. Yang, S. Qiu, H. Tan, *Org. Chem. Front.* **2018**, *5*, 1312-1319.
- [17] S. V. Chankeshwara, R. Chebolu, A. K. Chakraborti, *J. Org. Chem.* **2008**, *73*, 8615-8618.
- [18] R. Qiu, Y. Zhu, X. Xu, Y. Li, L. Shao, X. Ren, X. Cai, D. An, S. Yin, *Catal. Commun.* **2009**, *10*, 1889-1892.
- [19] S. N. Maddila, S. Maddila, K. K. Gangu, W. E. van Zyl, S. B. Jonnalagadda, *J. Fluorine Chem.* **2017**, *195*, 79-84.

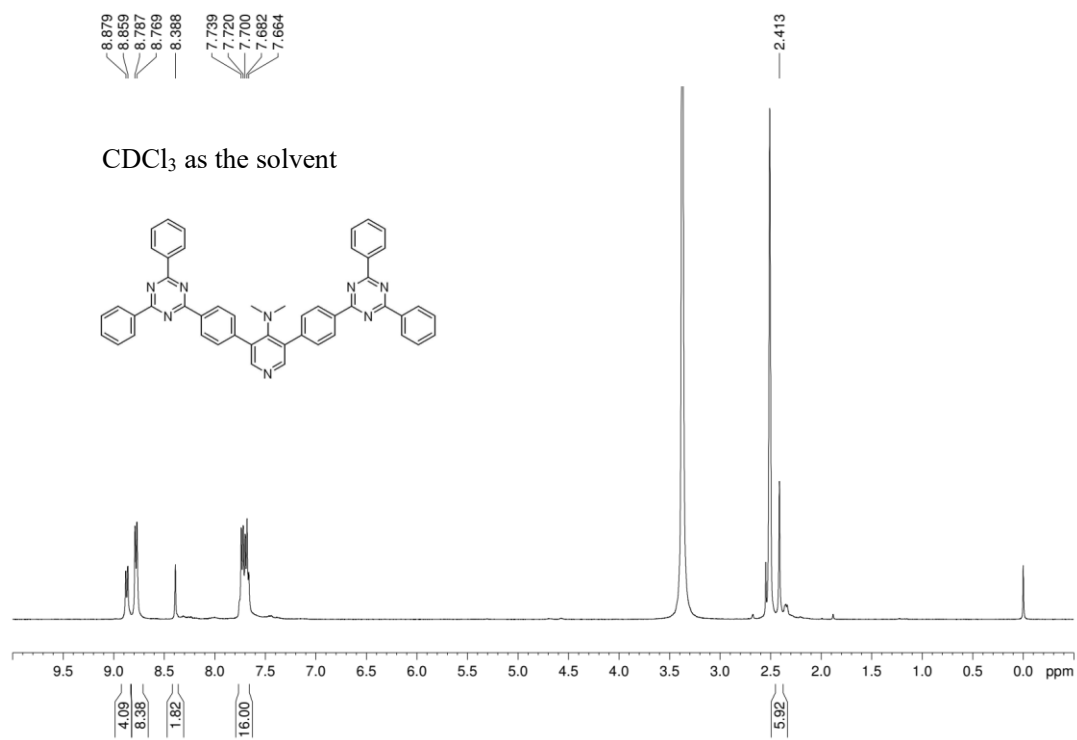
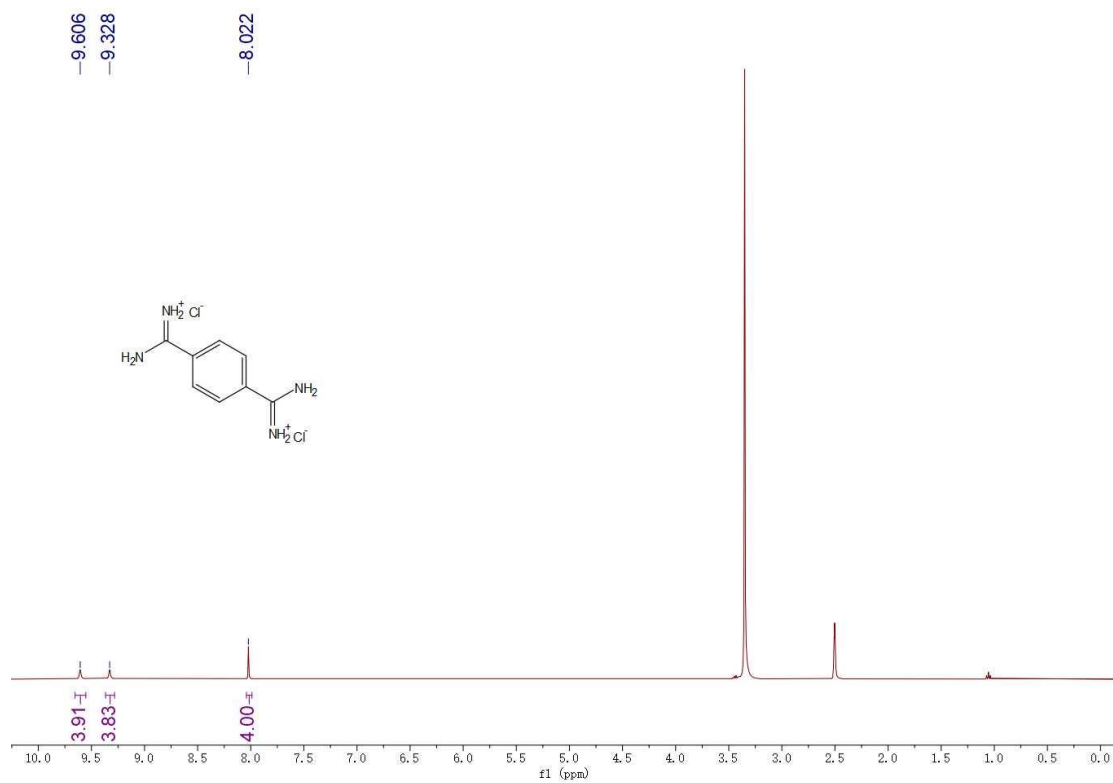
- [20] A. Dutta, R. Abha Saikia, A. Jyoti Thakur, *Eur. J. Org. Chem.* **2022**, 2022, e202101472.
- [21] P. Teli, S. Soni, S. Teli, S. Agarwal, *Nanoscale Adv.* **2024**, 6, 5568-5578.
- [22] L. B. Masram, S. S. Salim, A. B. Barkule, Y. U. Gadkari, V. N. Telvekar, *J. Chem. Sci. (Bangalore, India)* **2022**, 134, 94.
- [23] J. S. Schulze, R. D. Brand, J. G. C. Hering, L. M. Riegger, P. R. Schreiner, B. M. Smarsly, *ChemCatChem* **2022**, 14, e202101845.
- [24] S. Xu, I. Held, B. Kempf, H. Mayr, W. Steglich, H. Zipse, *Chem. Eur. J.* **2005**, 11, 4751-4757.
- [25] P. H.-Y. Cheong, C. Y. Legault, J. M. Um, N. Çelebi-Ölçüm, K. N. Houk, *Chem. Rev.* **2011**, 111, 5042-5137.

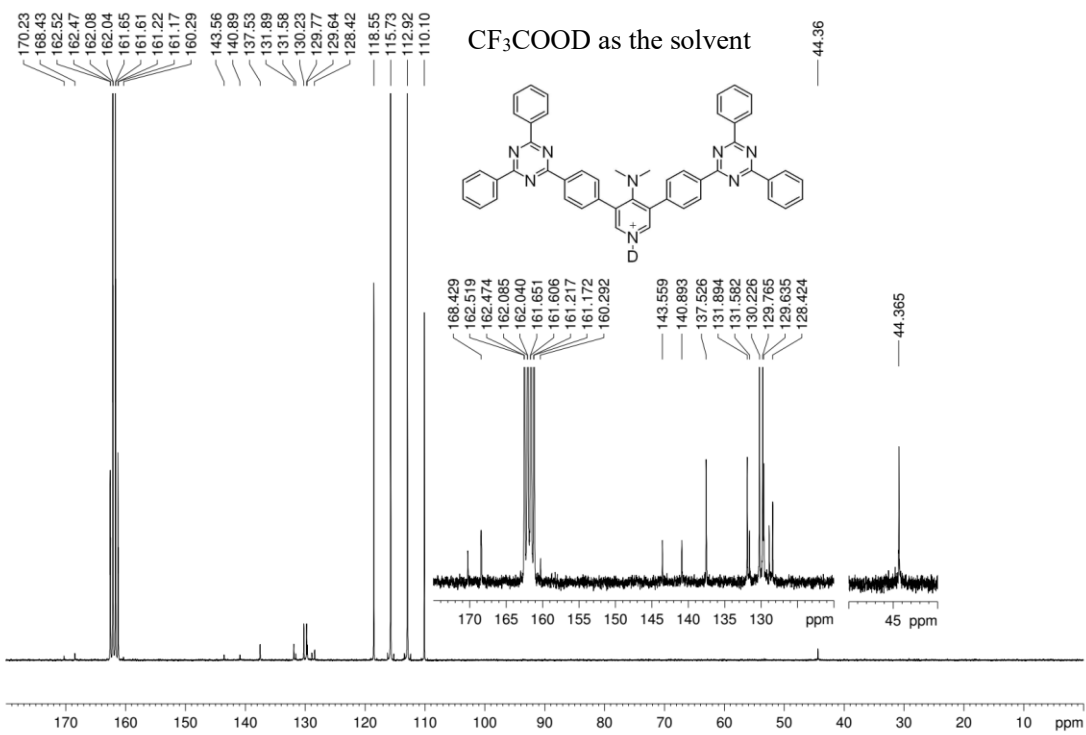
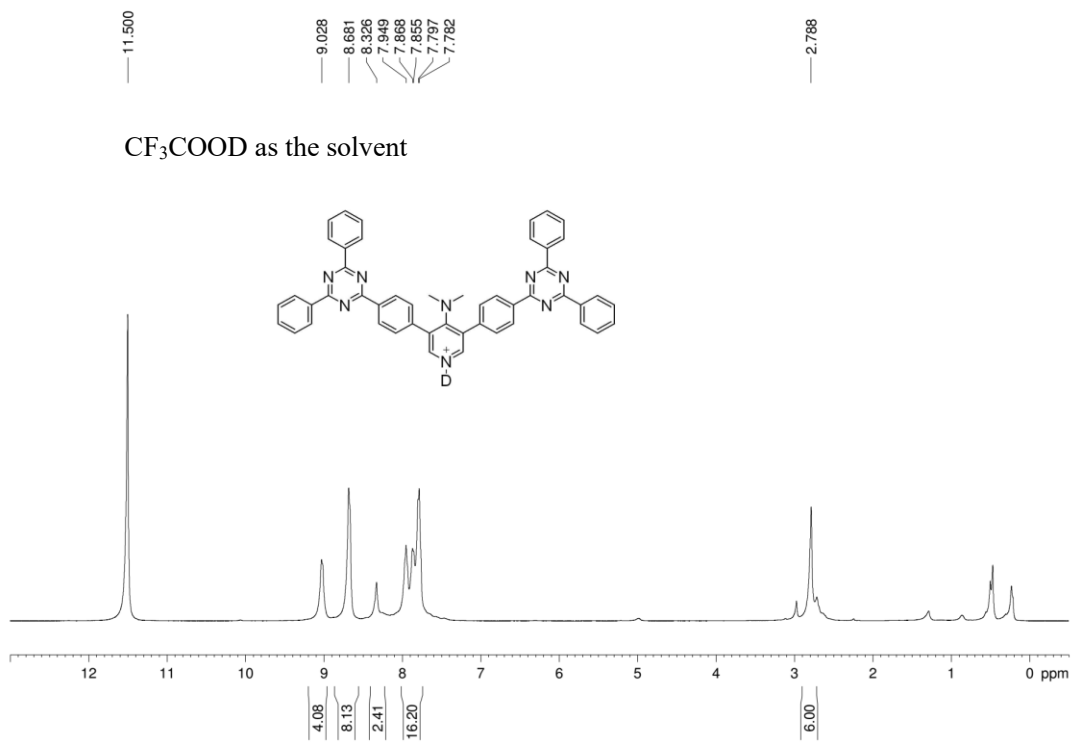
H. Liquid NMR spectra of some compounds

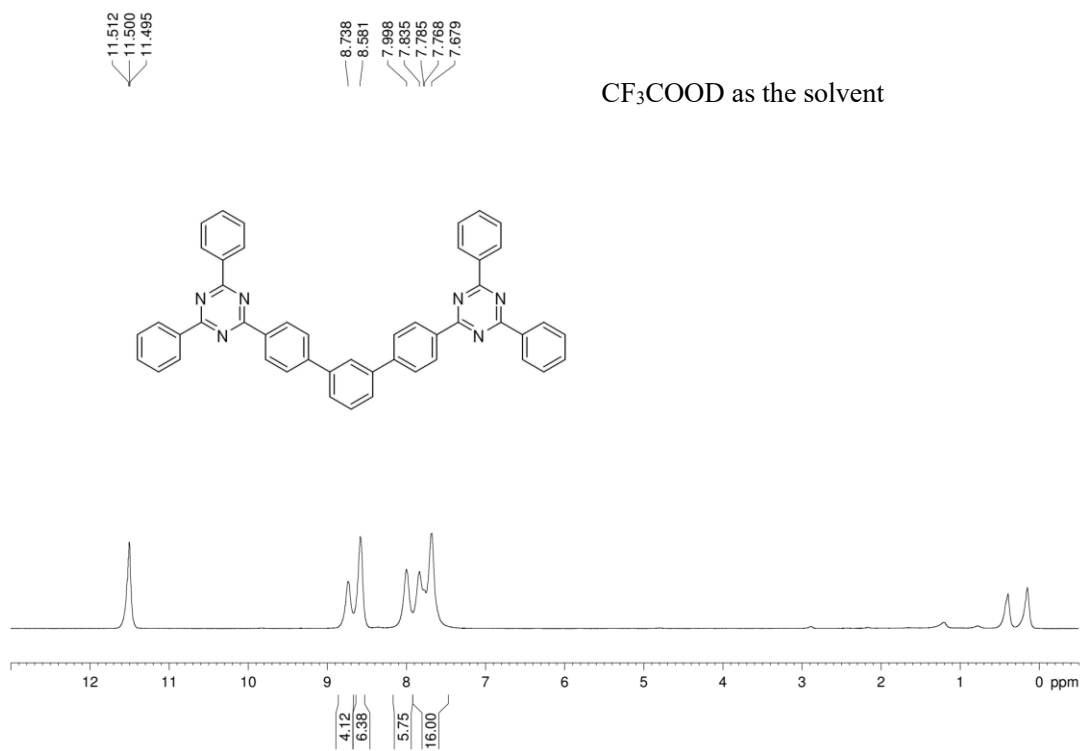
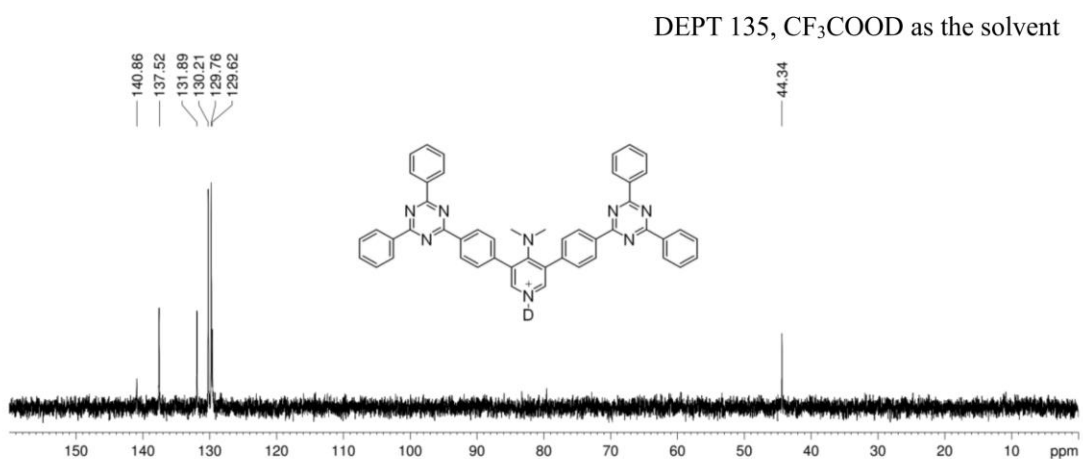
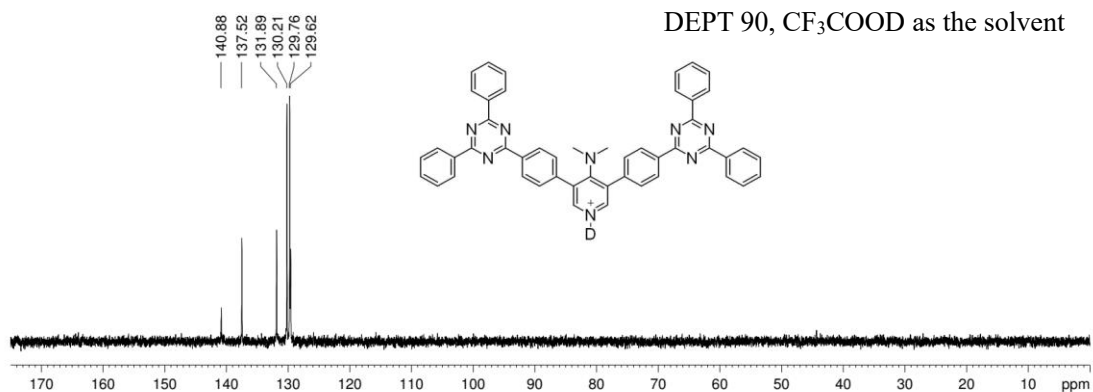


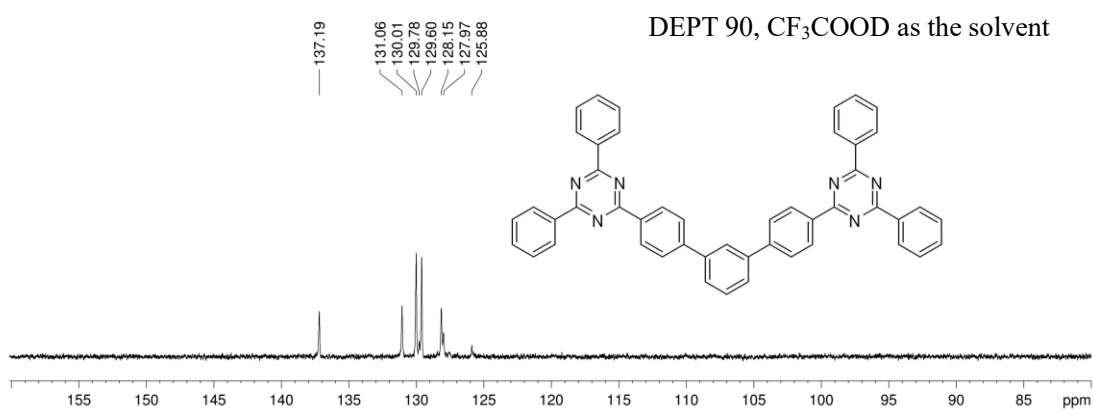
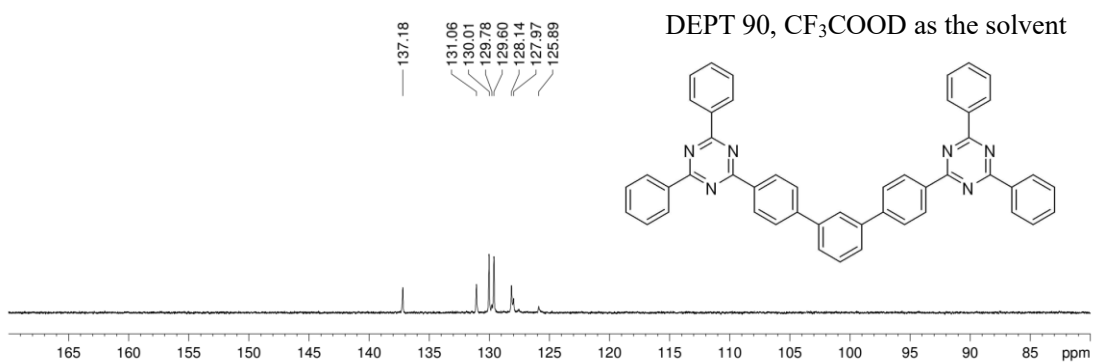
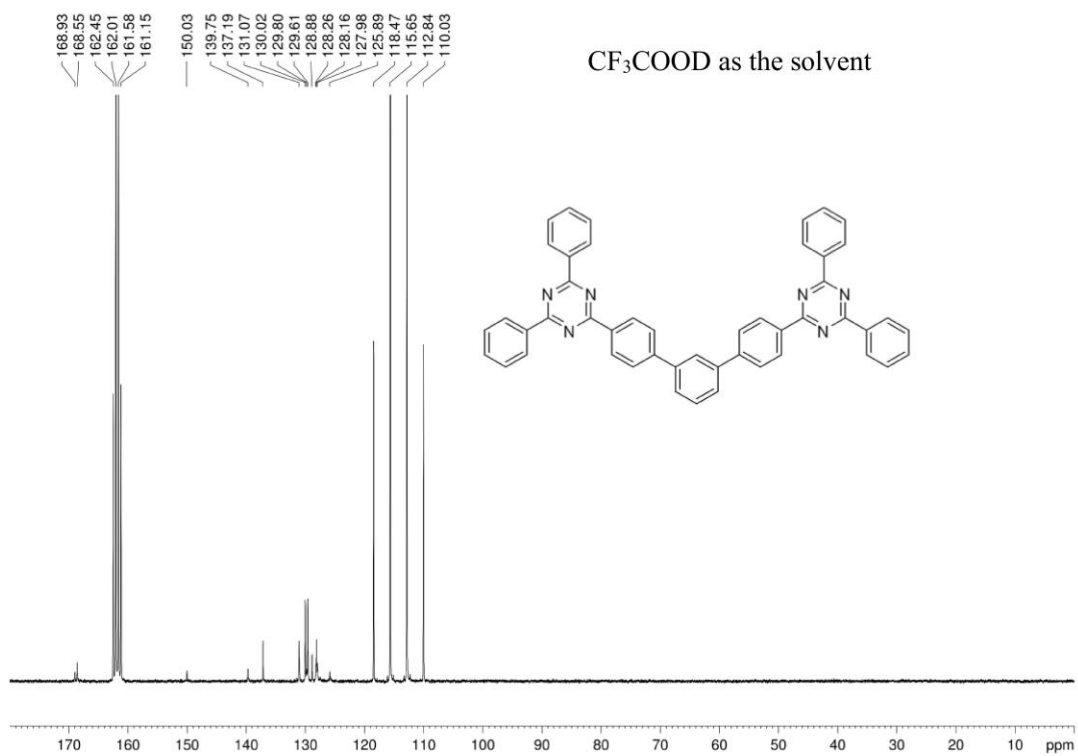


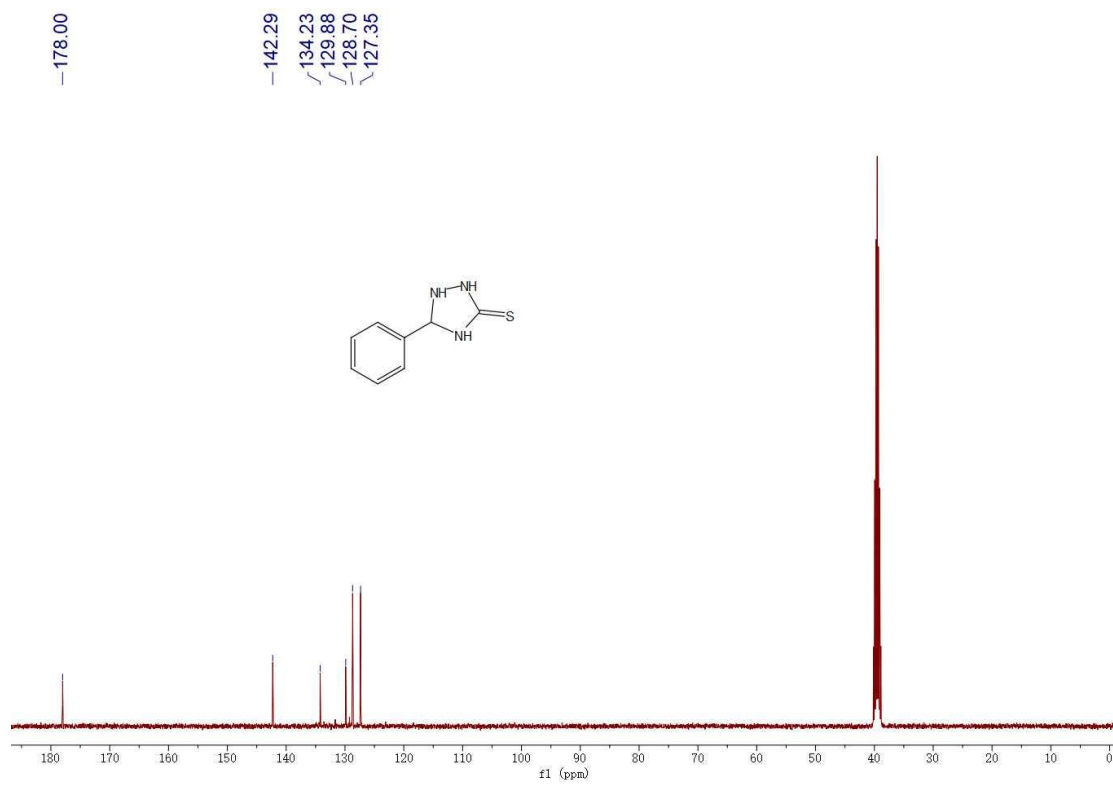
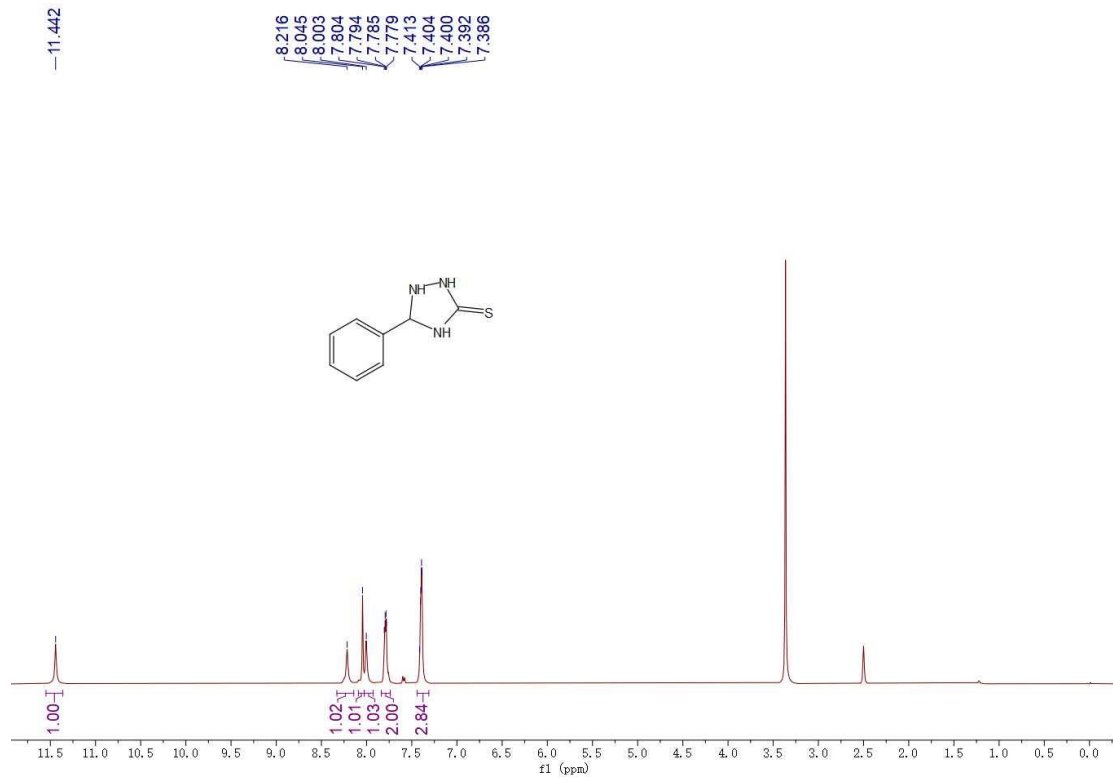


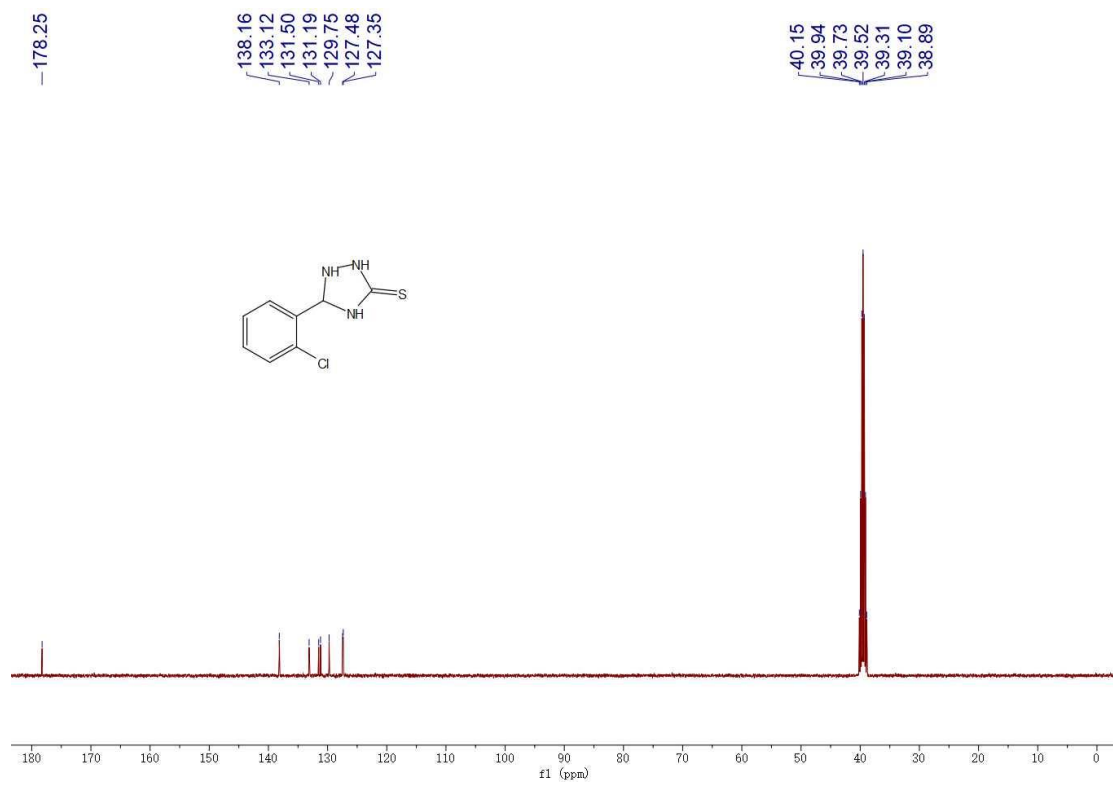
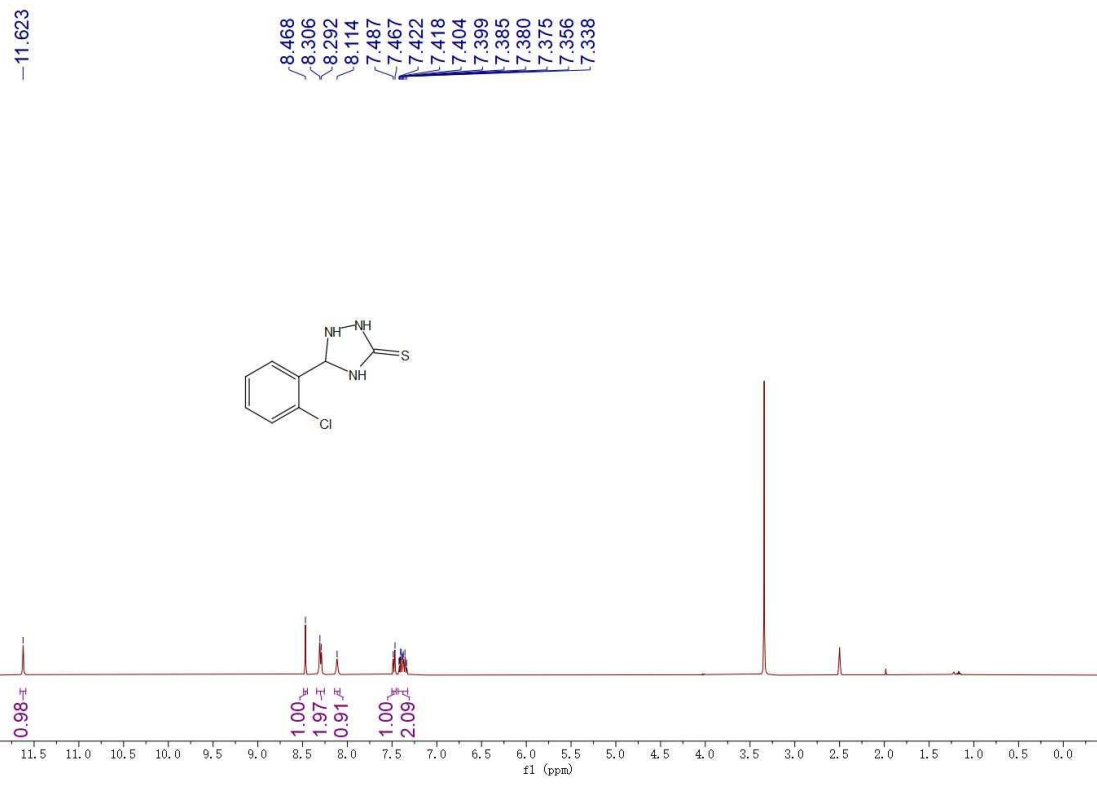


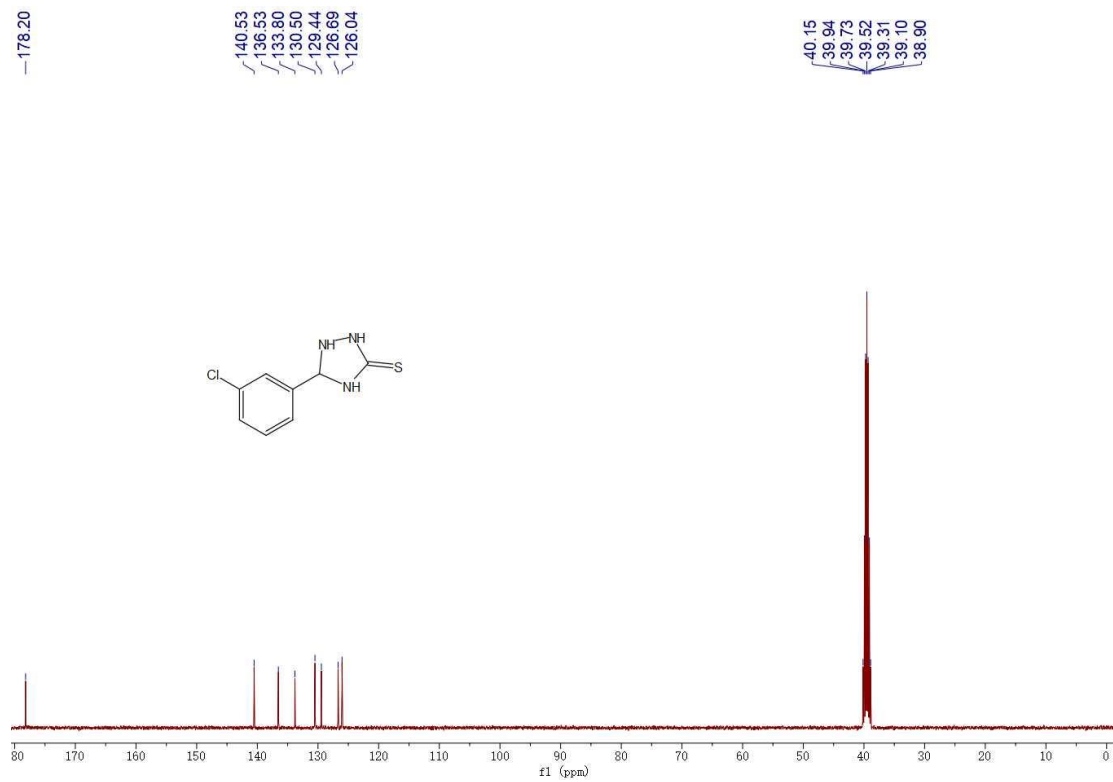
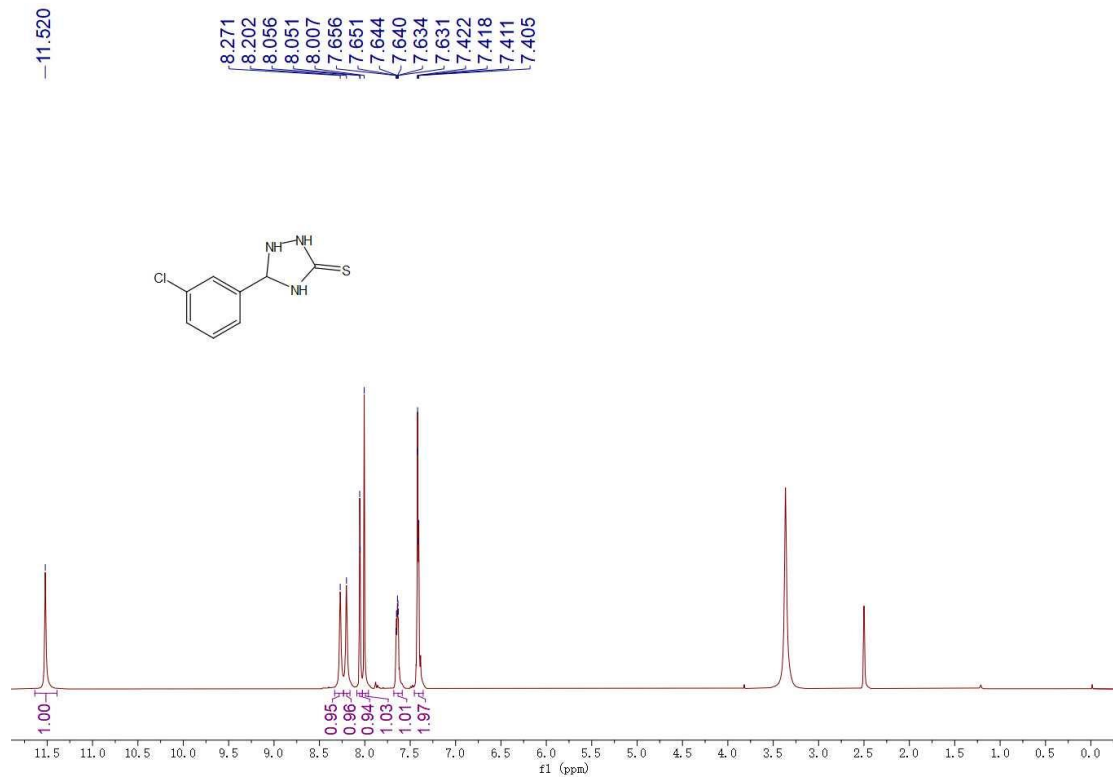


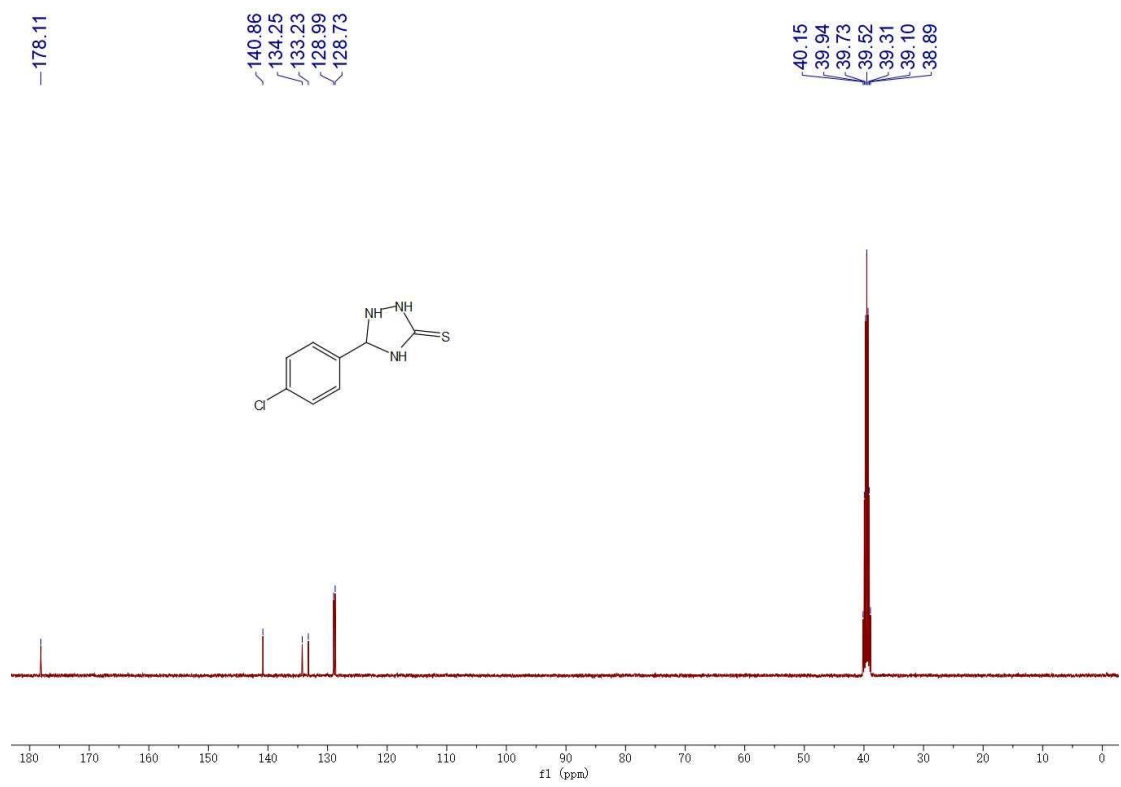
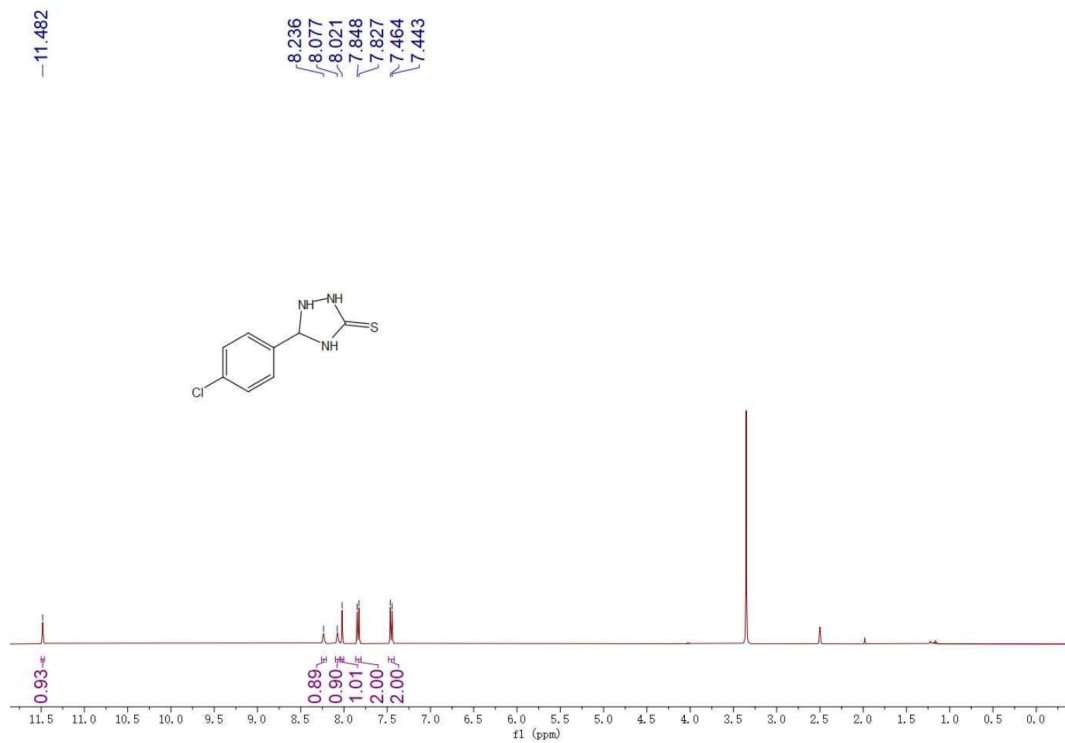


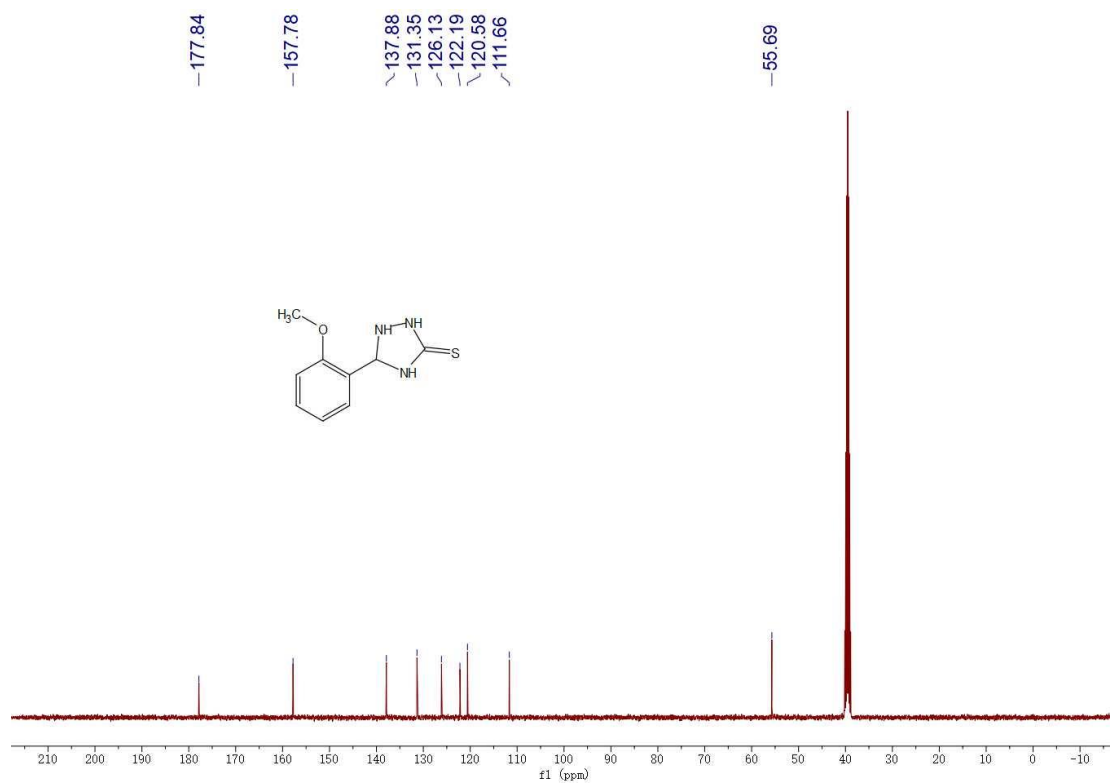
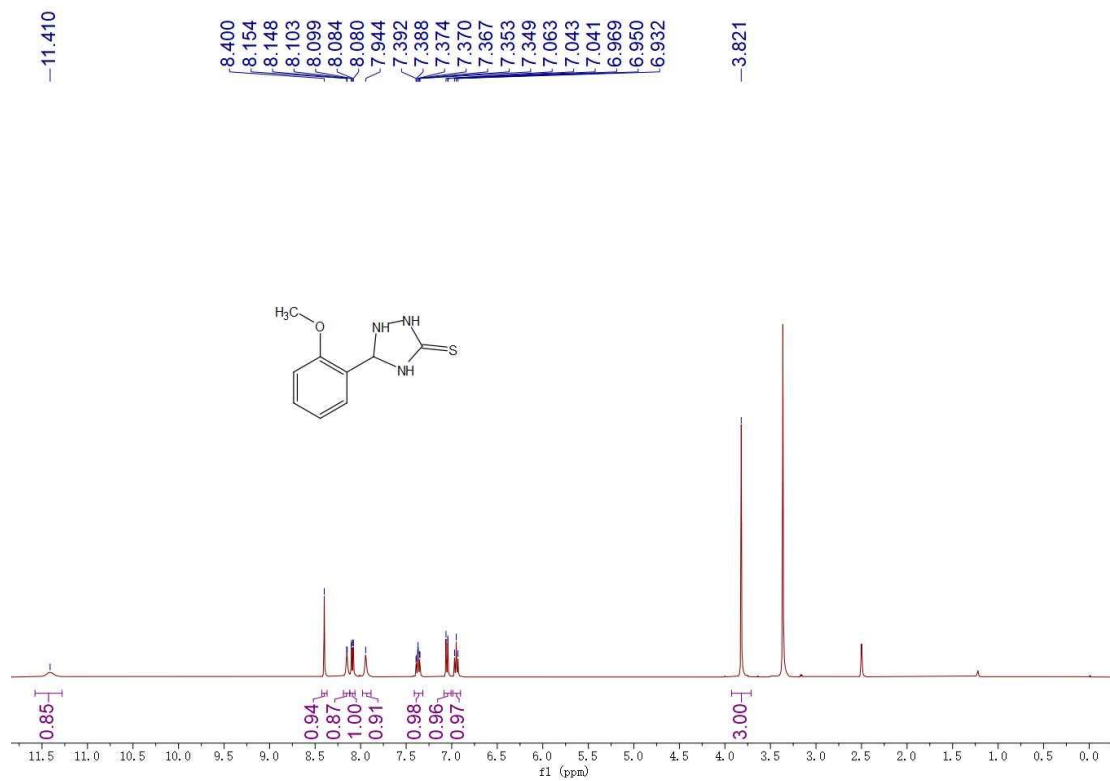


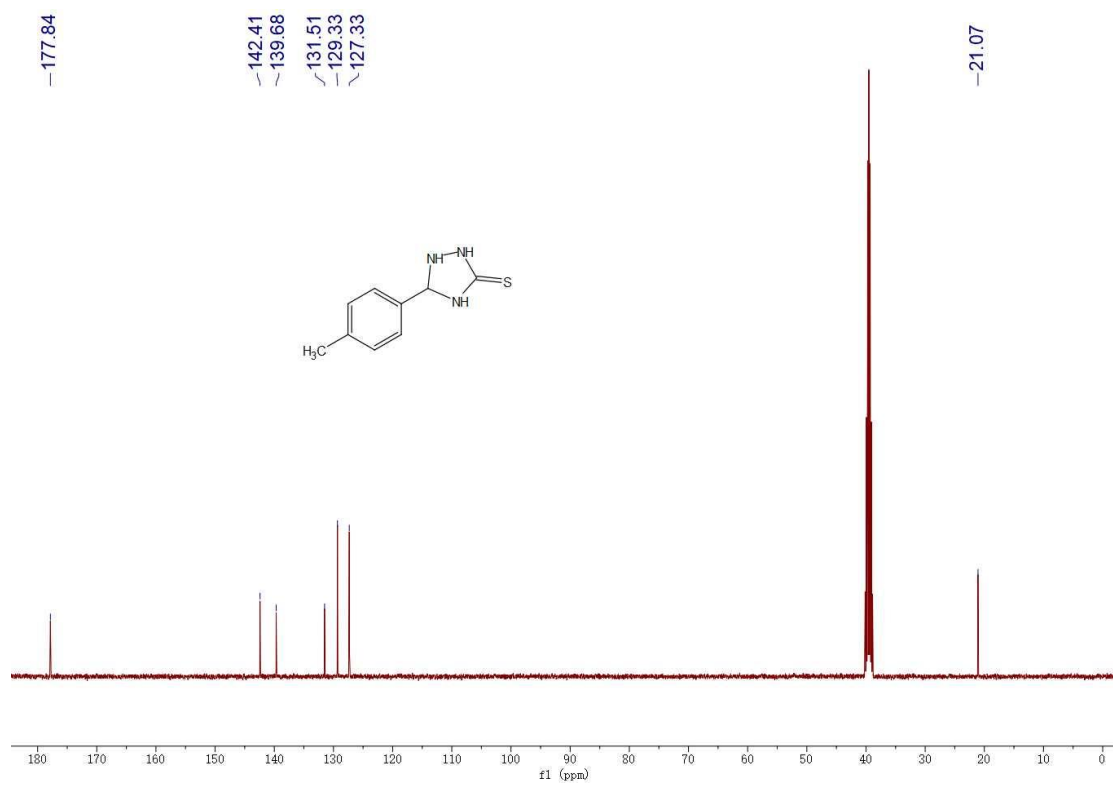
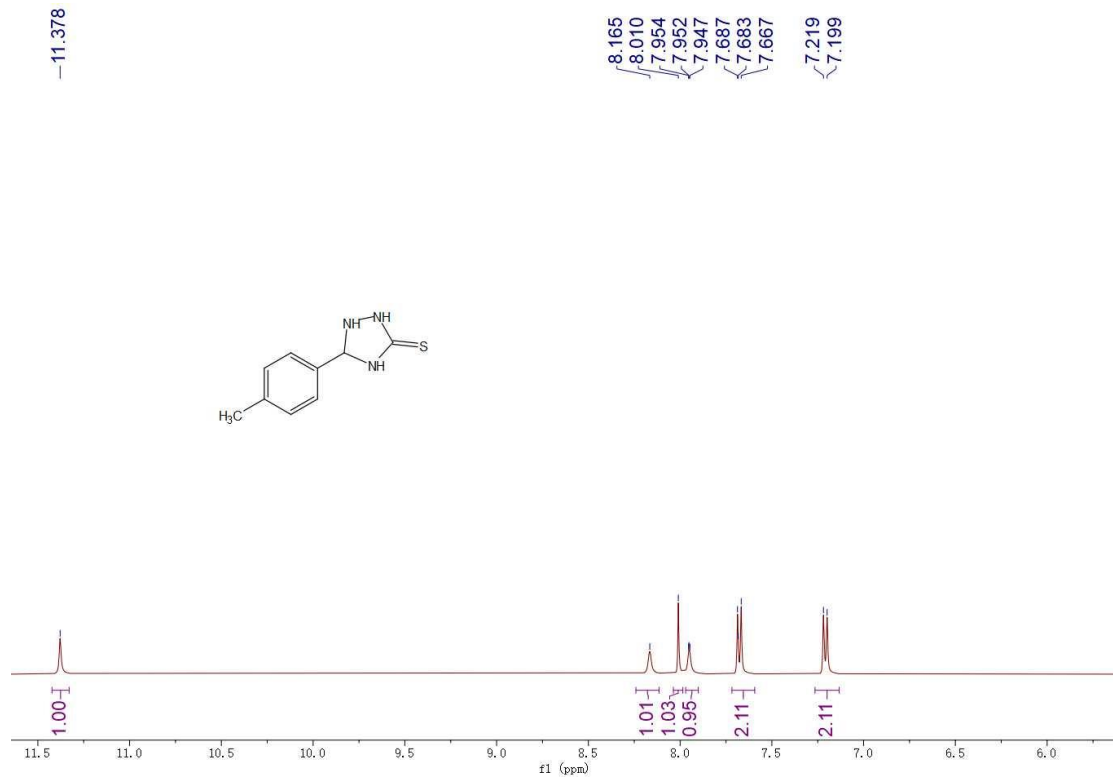


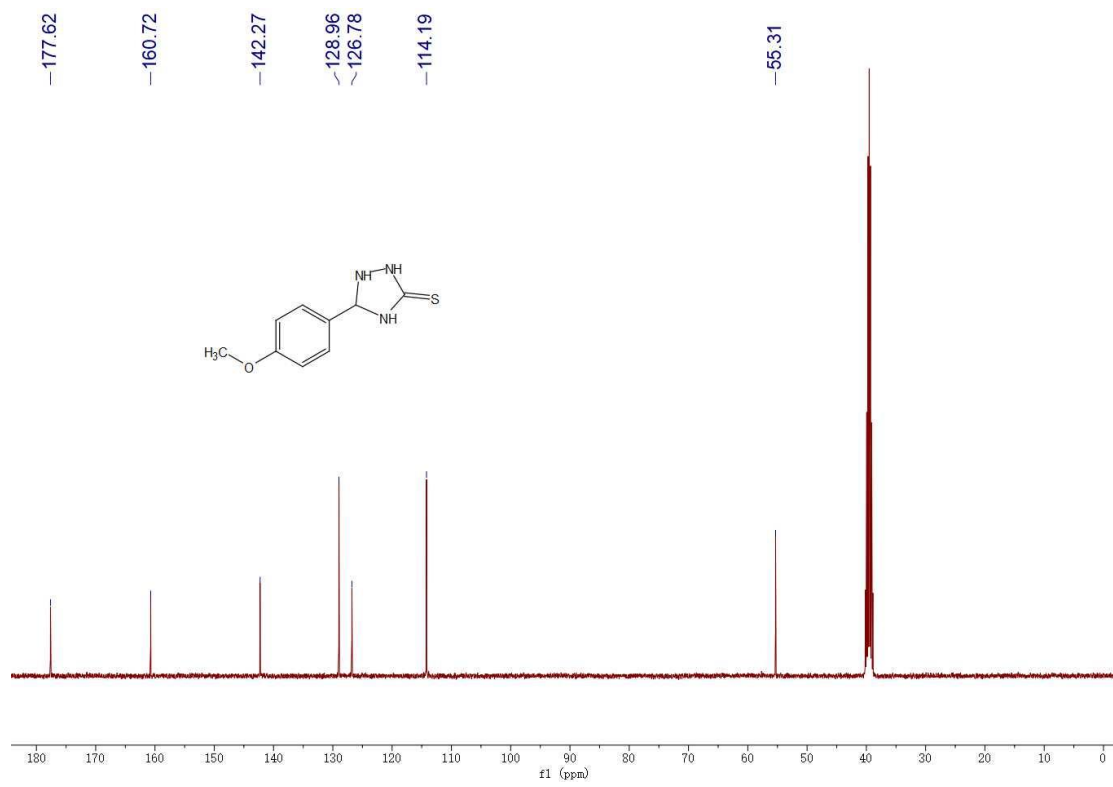
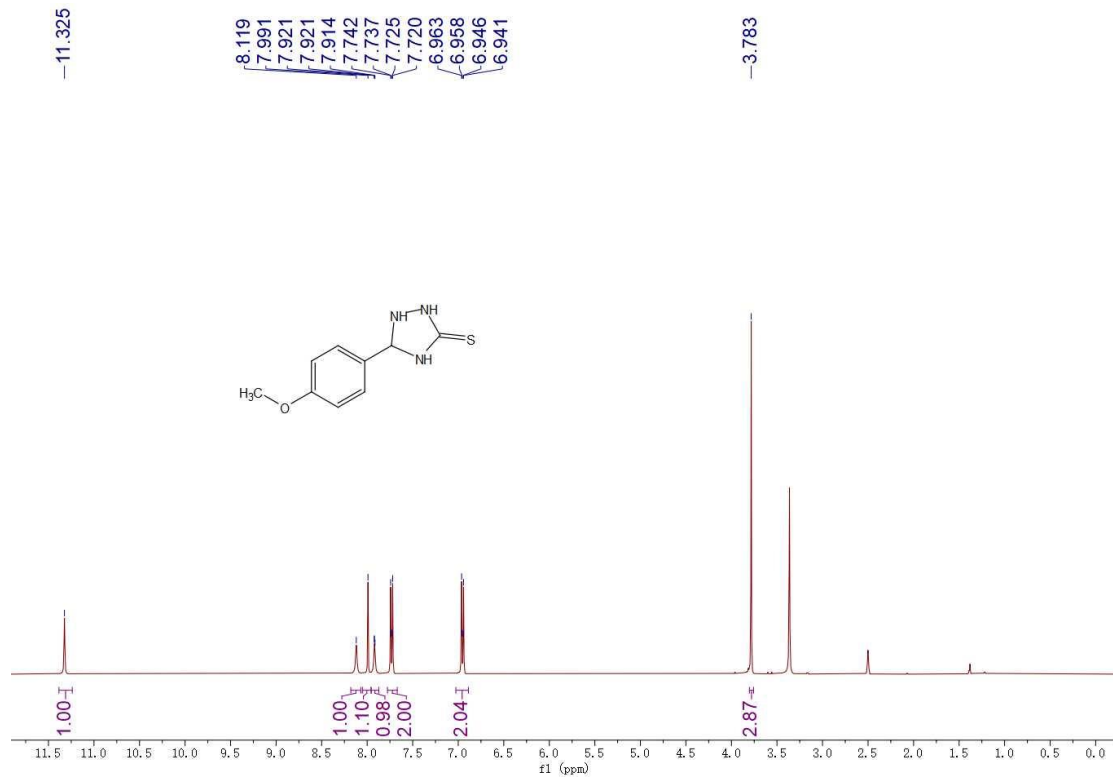


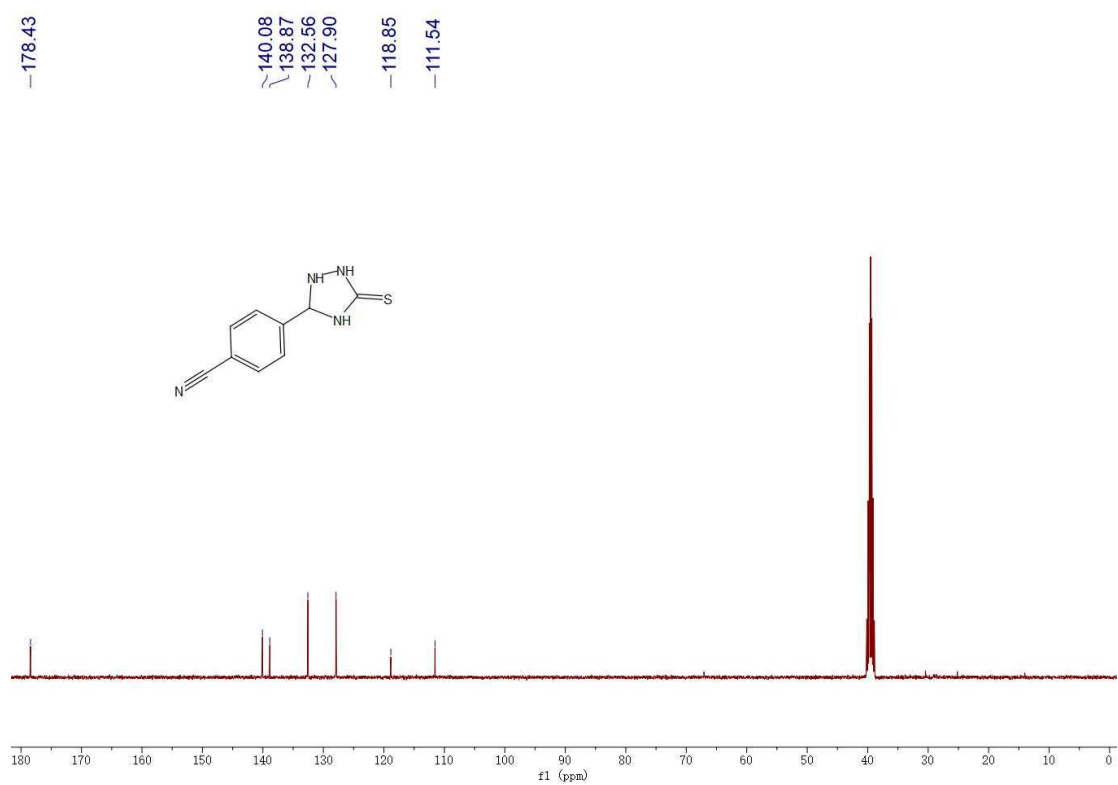
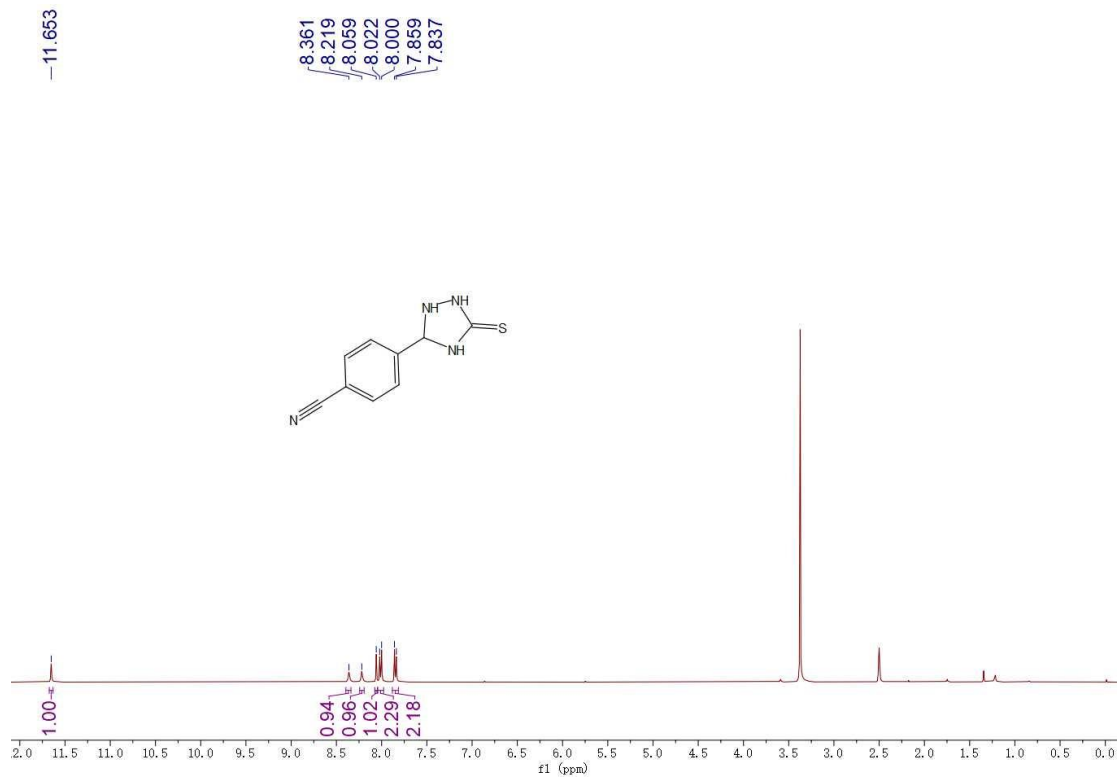


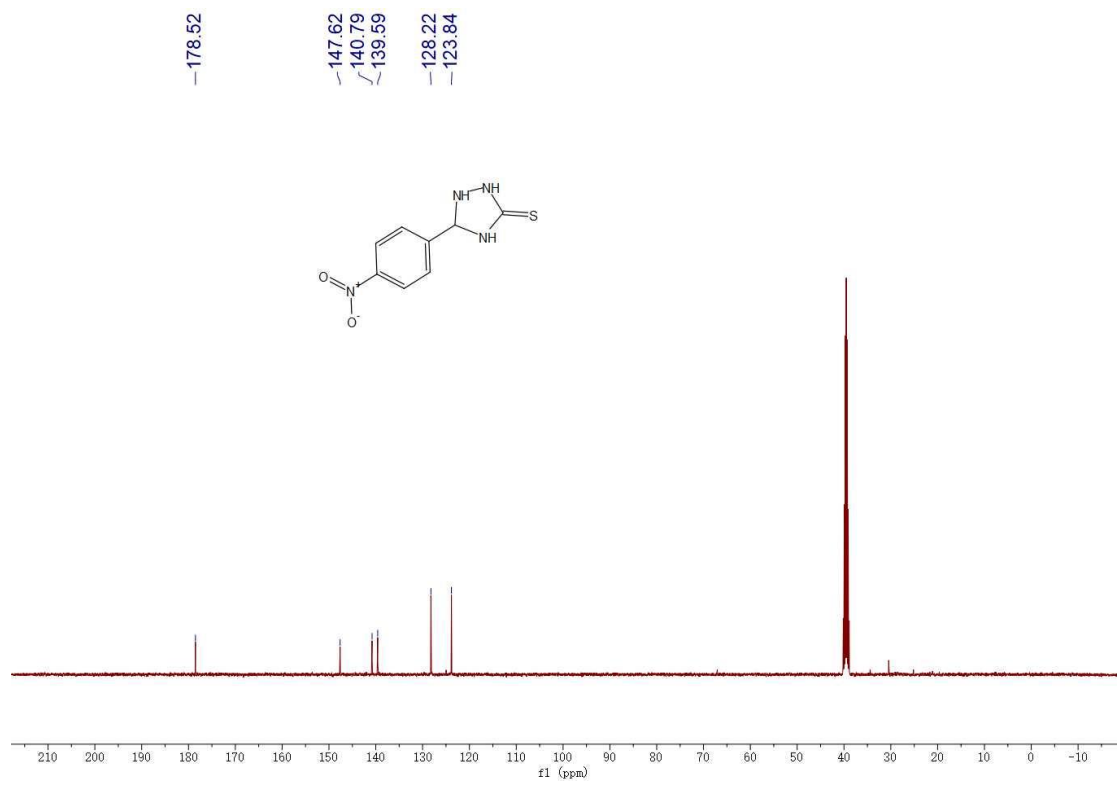
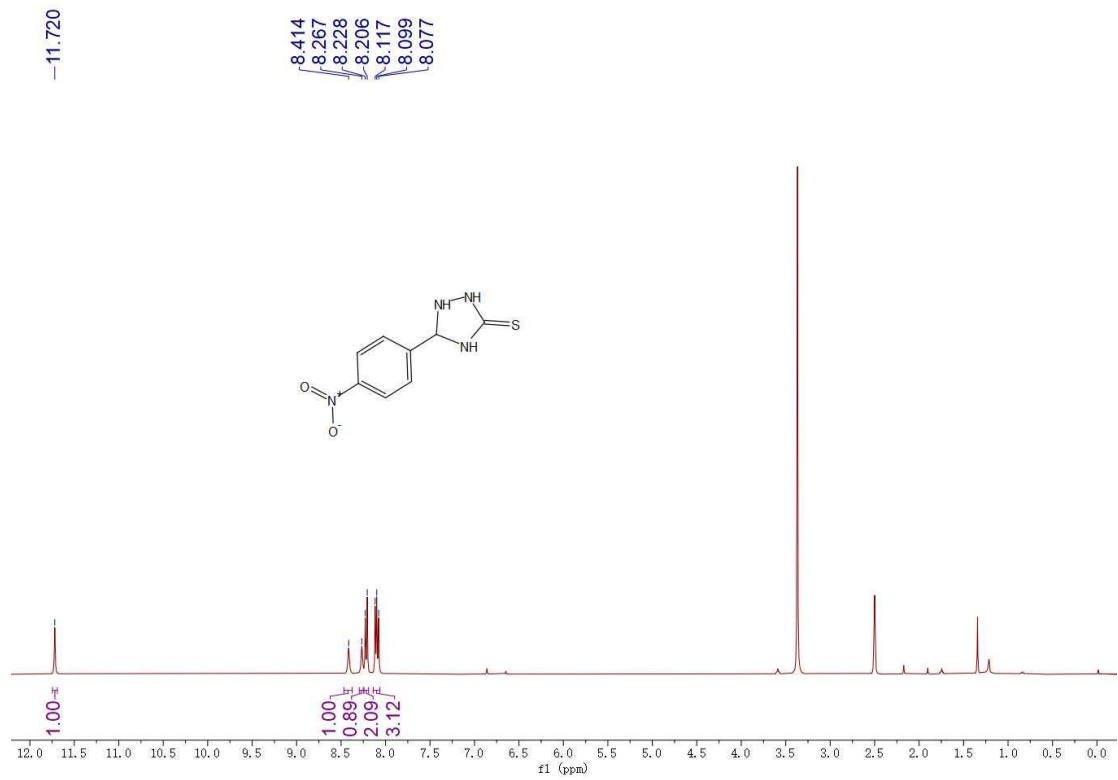


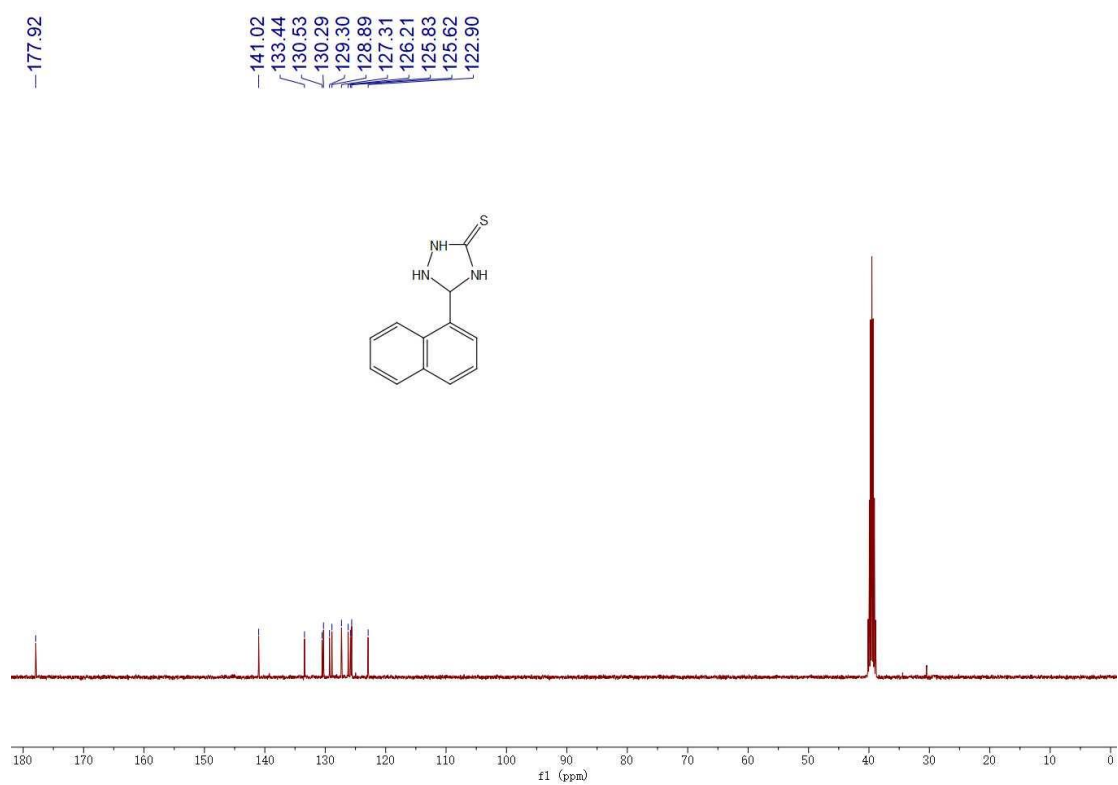
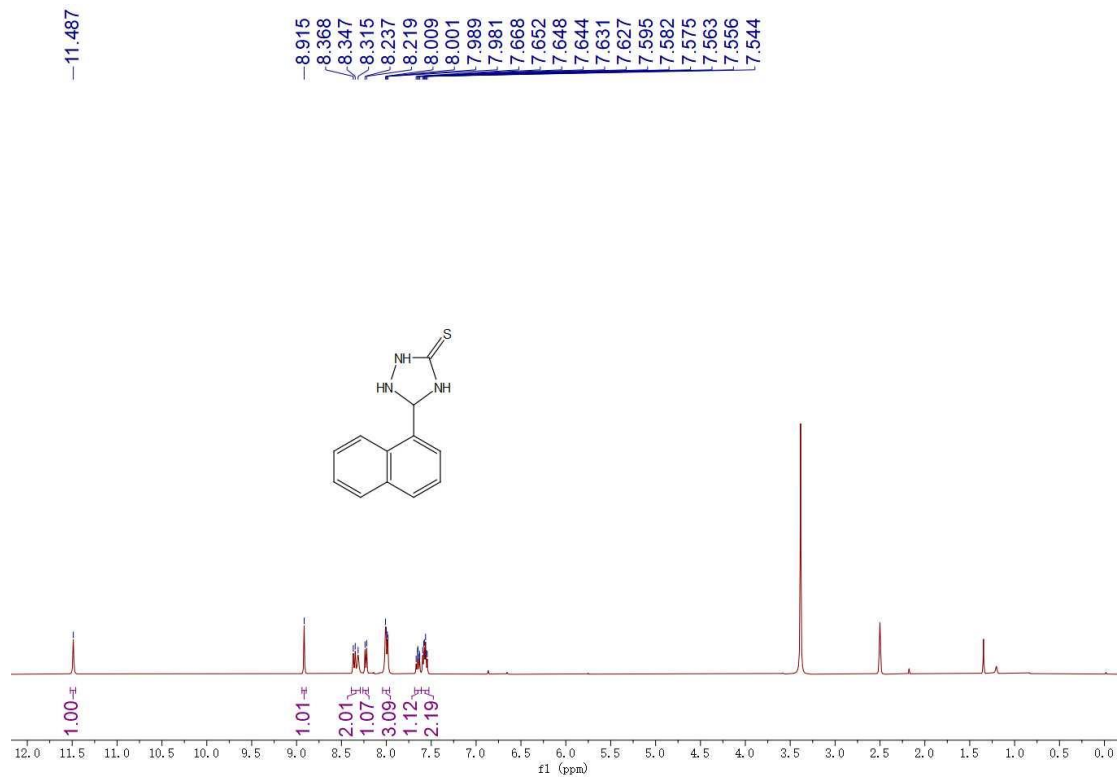


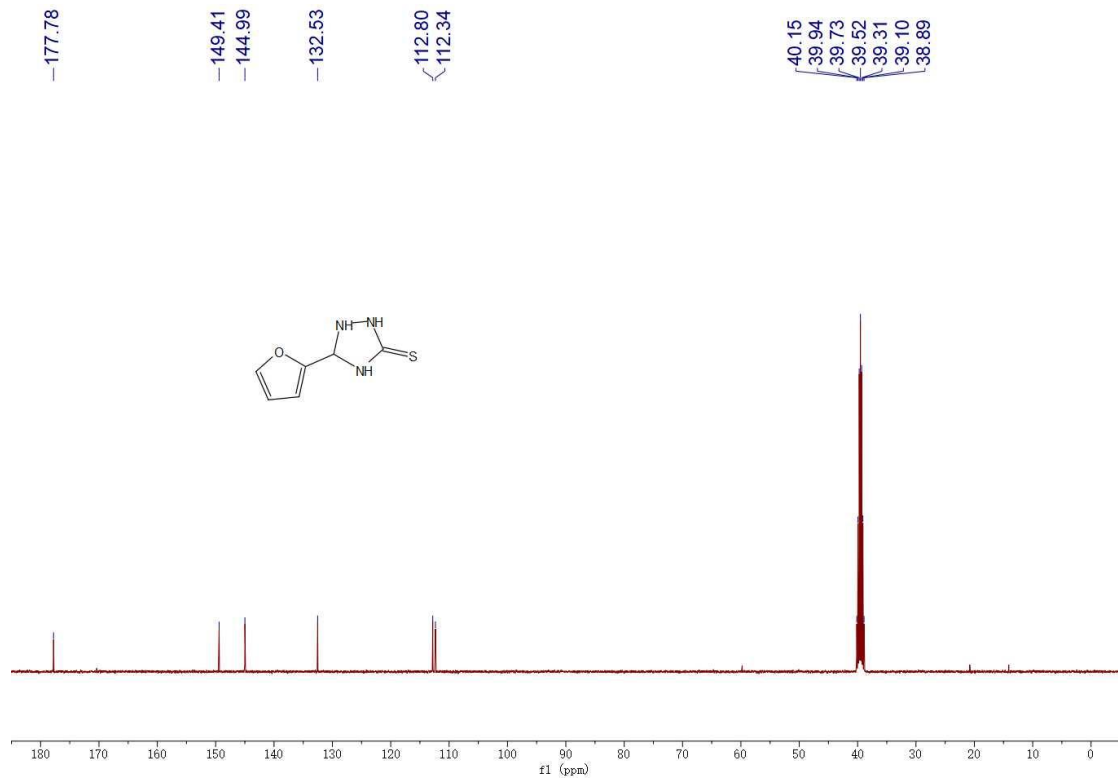
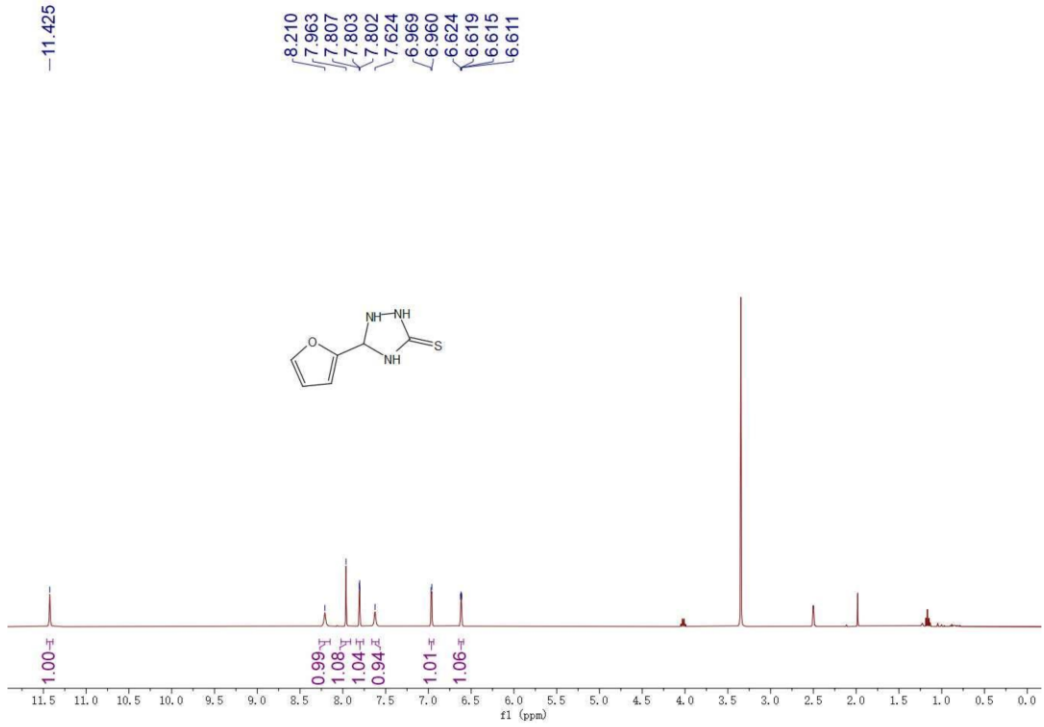


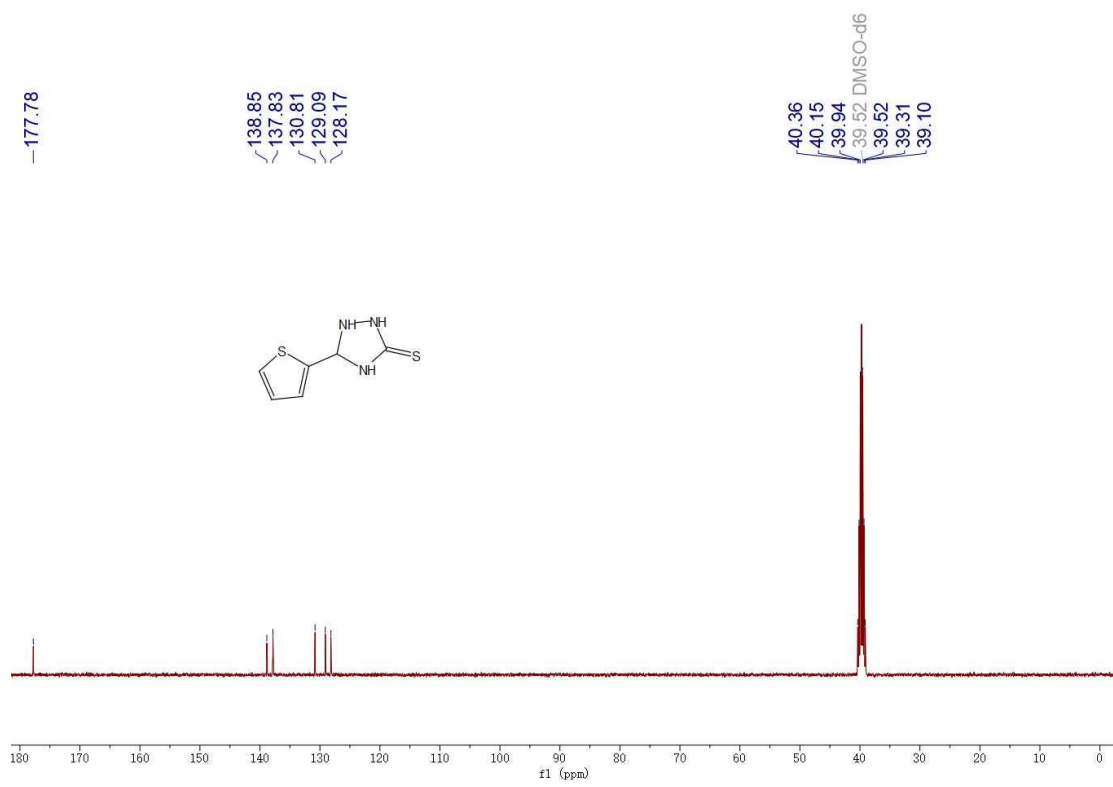
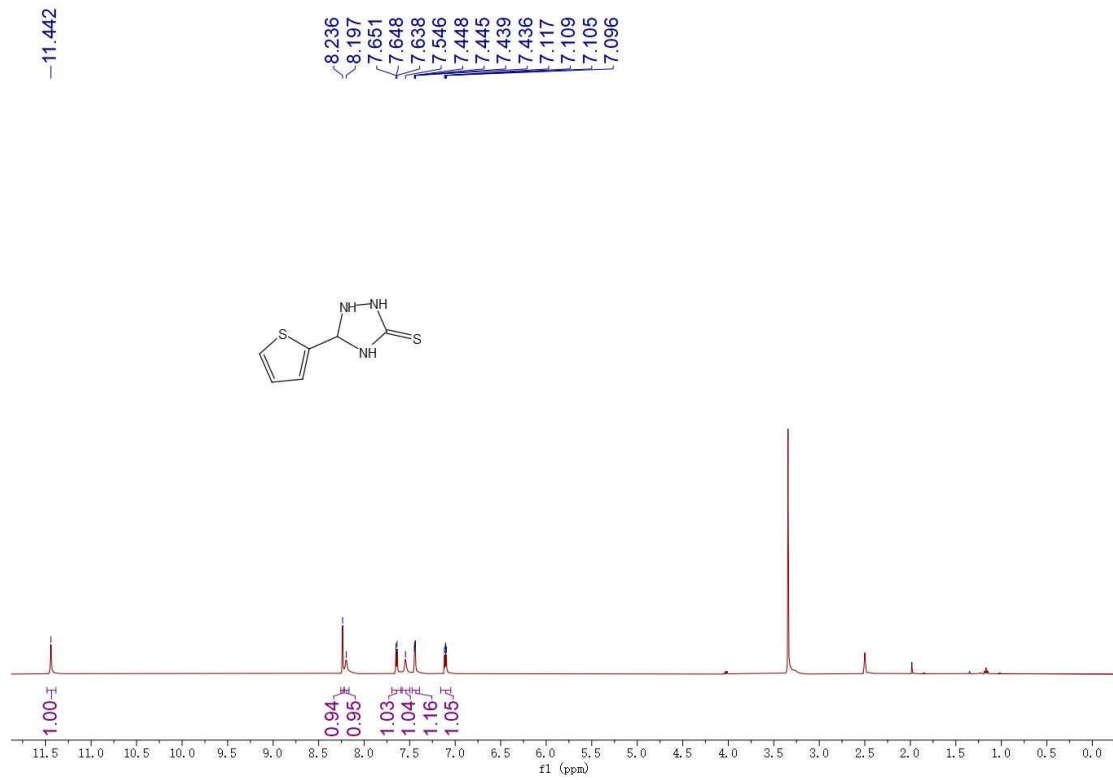


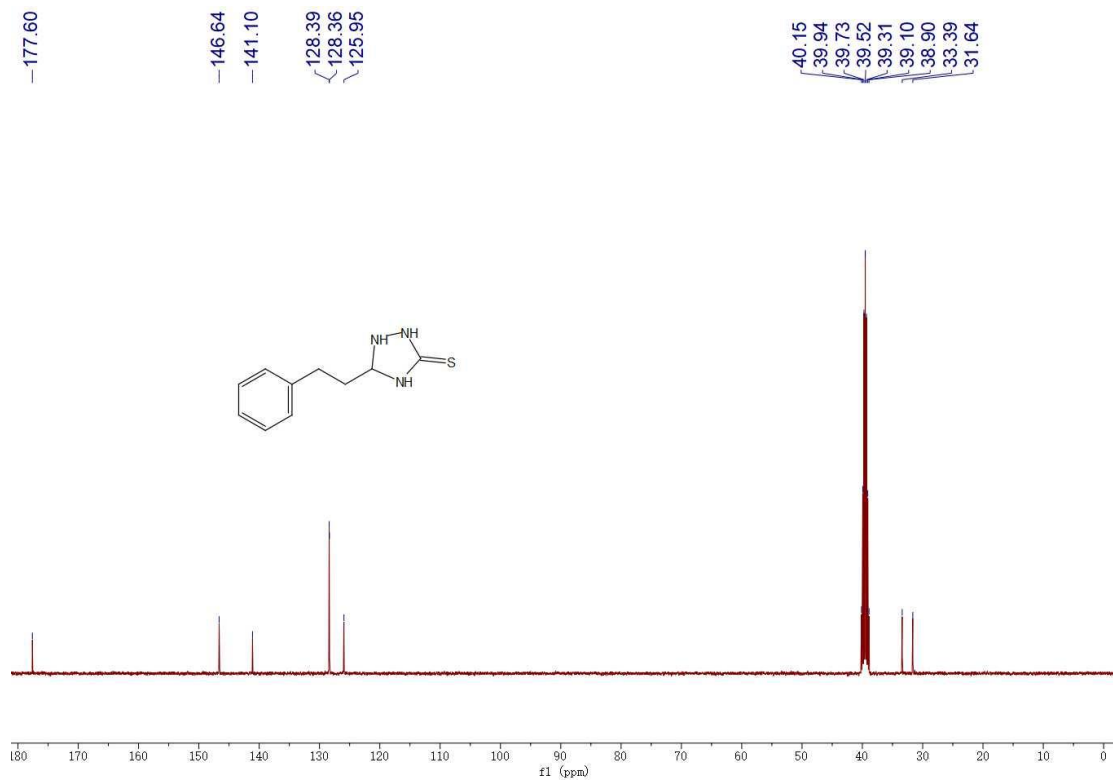
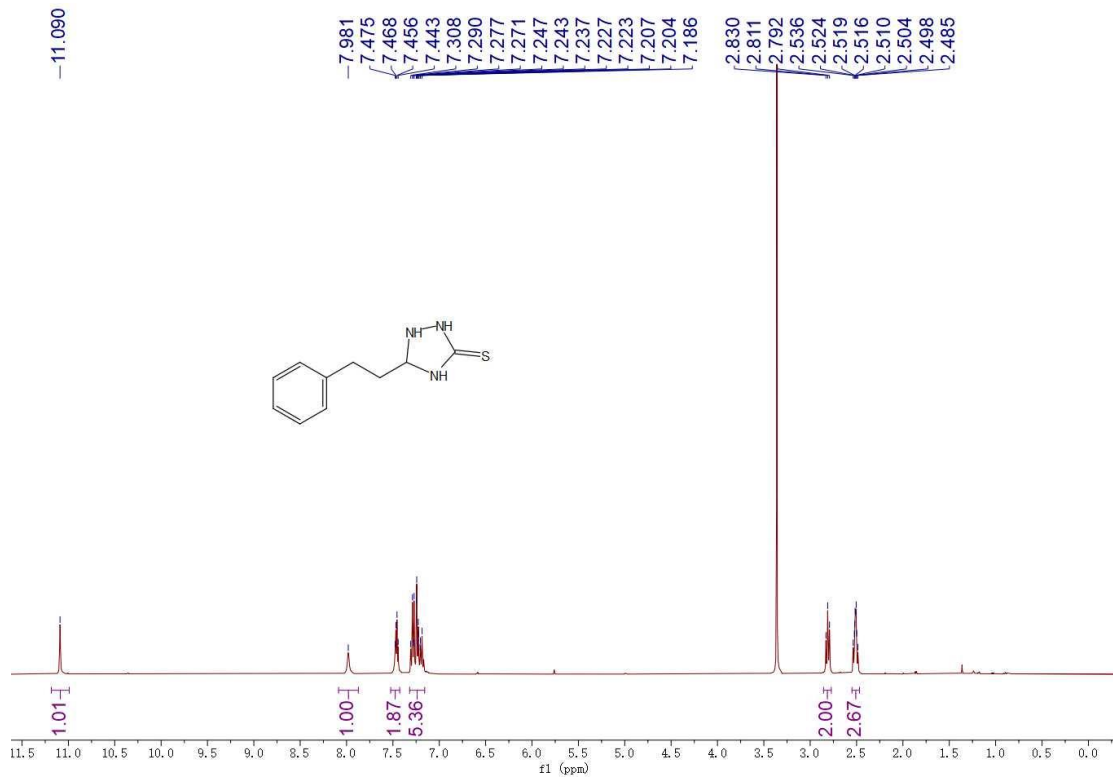


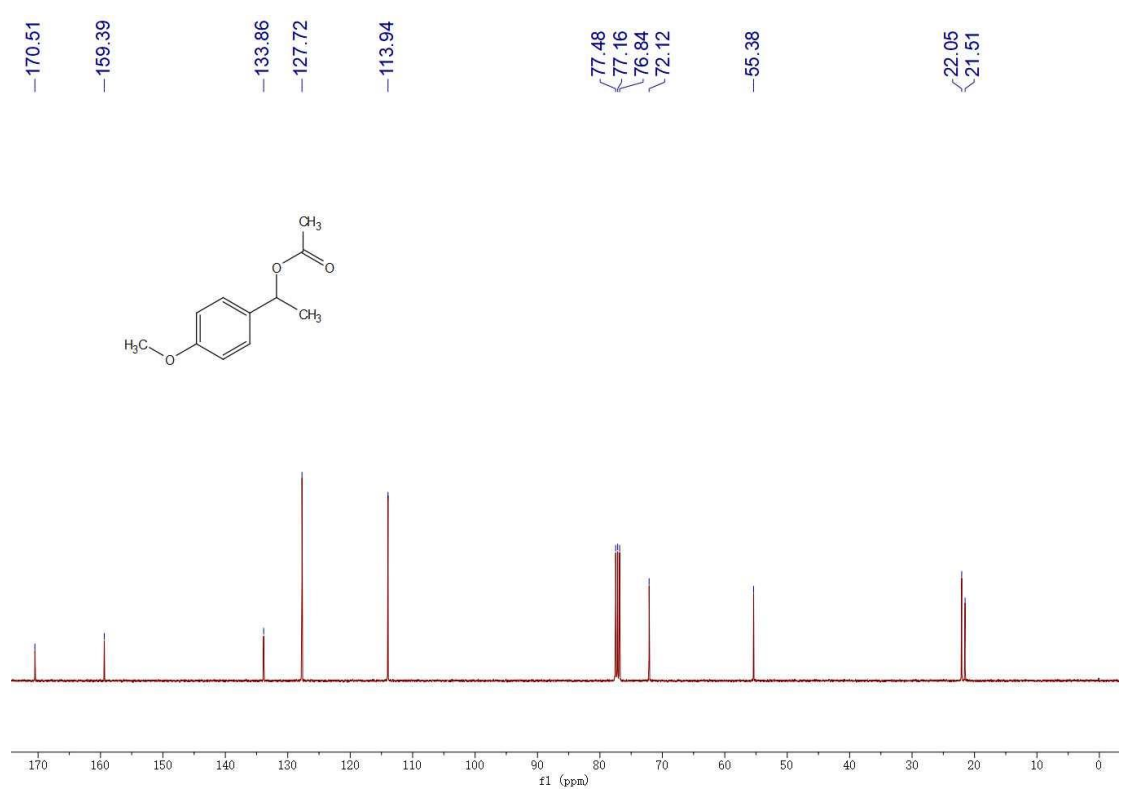
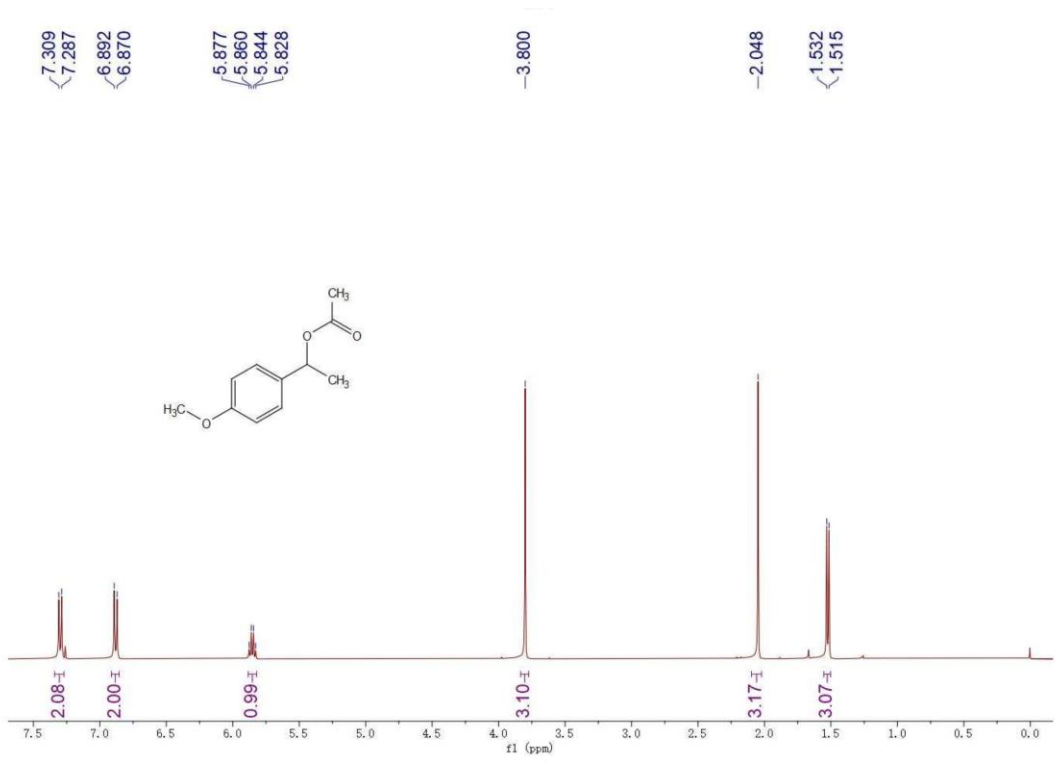


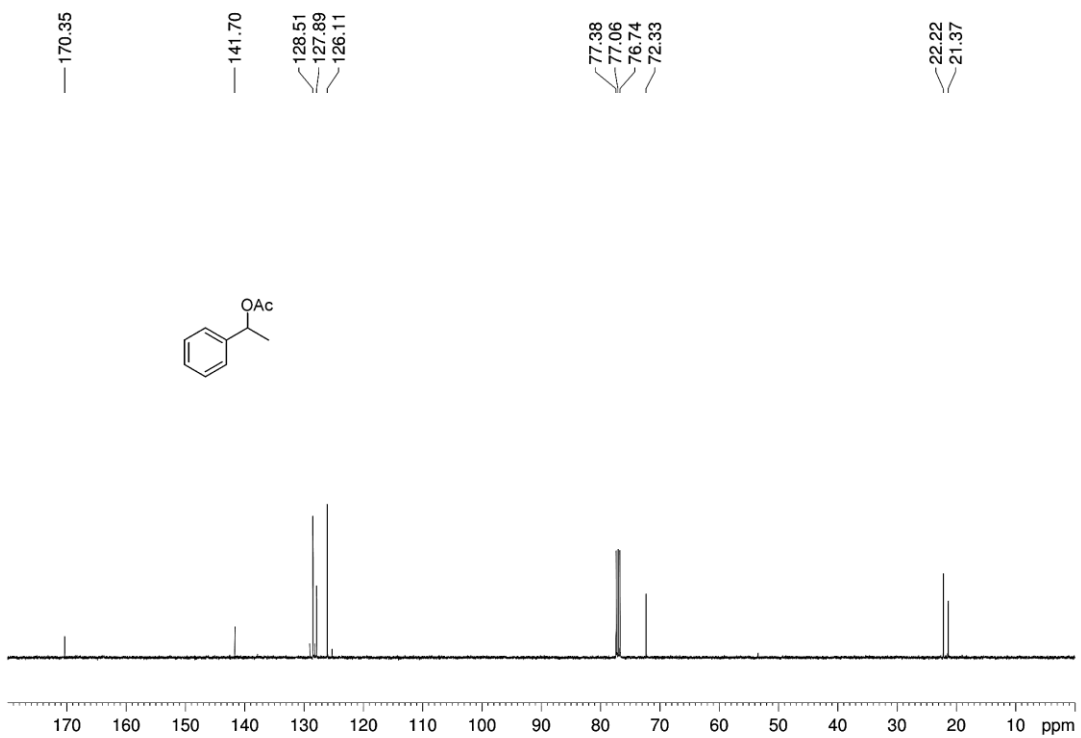
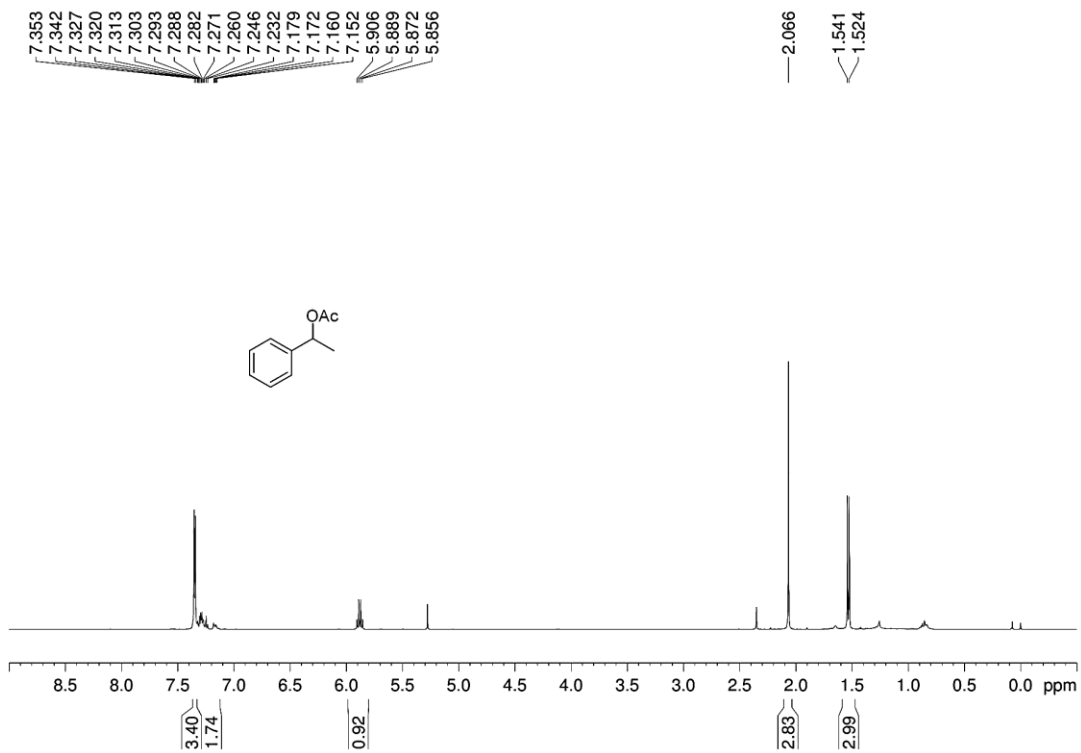


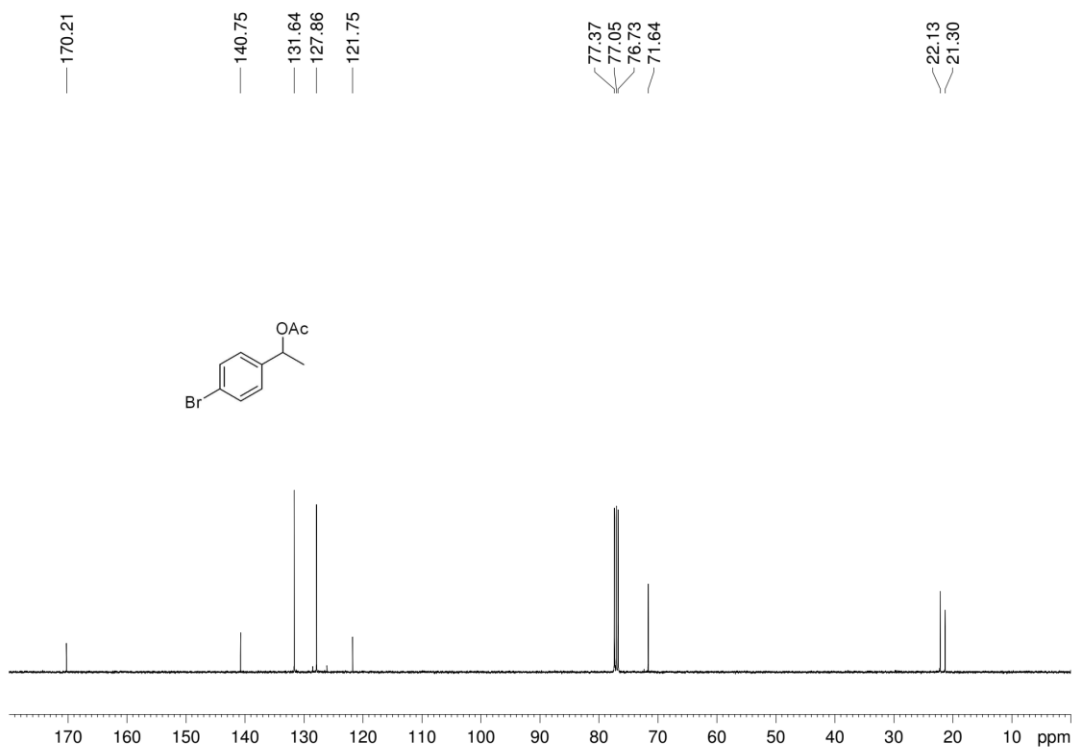
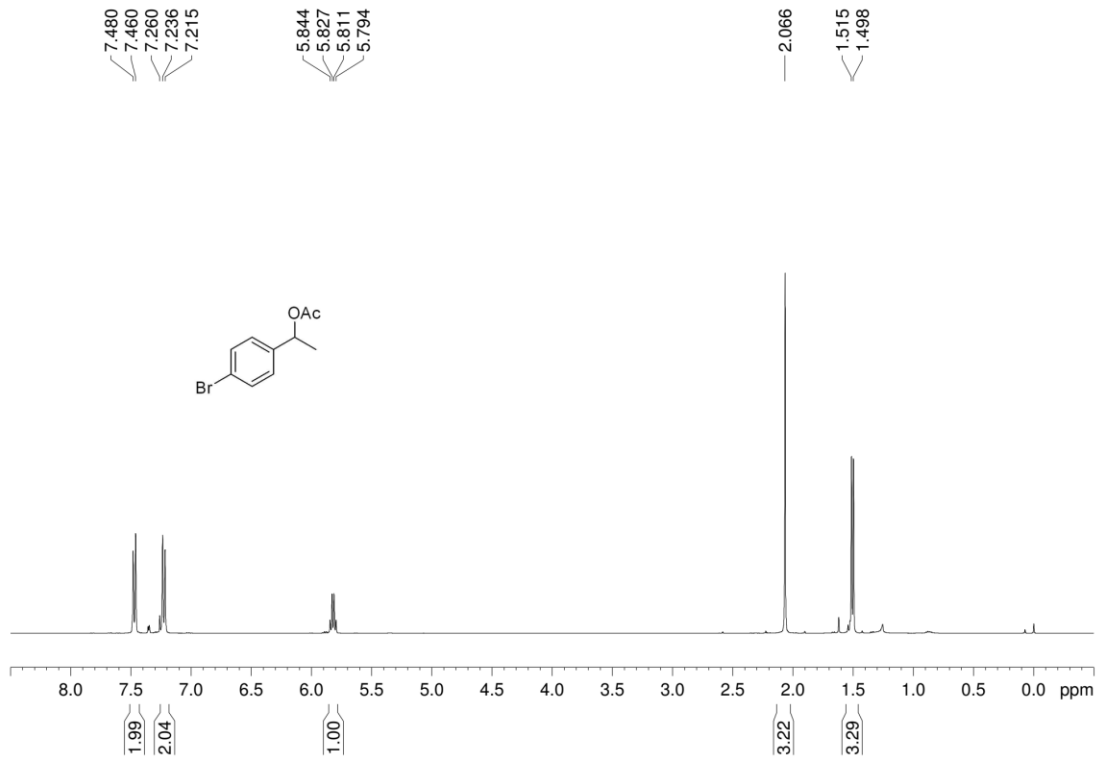


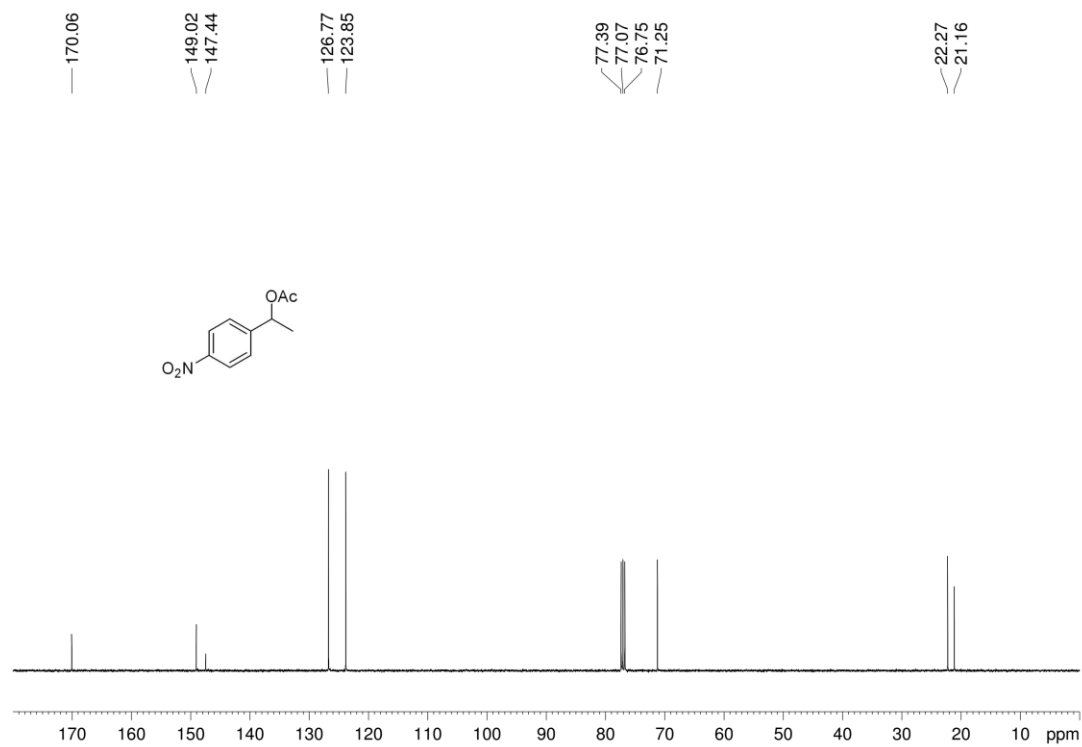
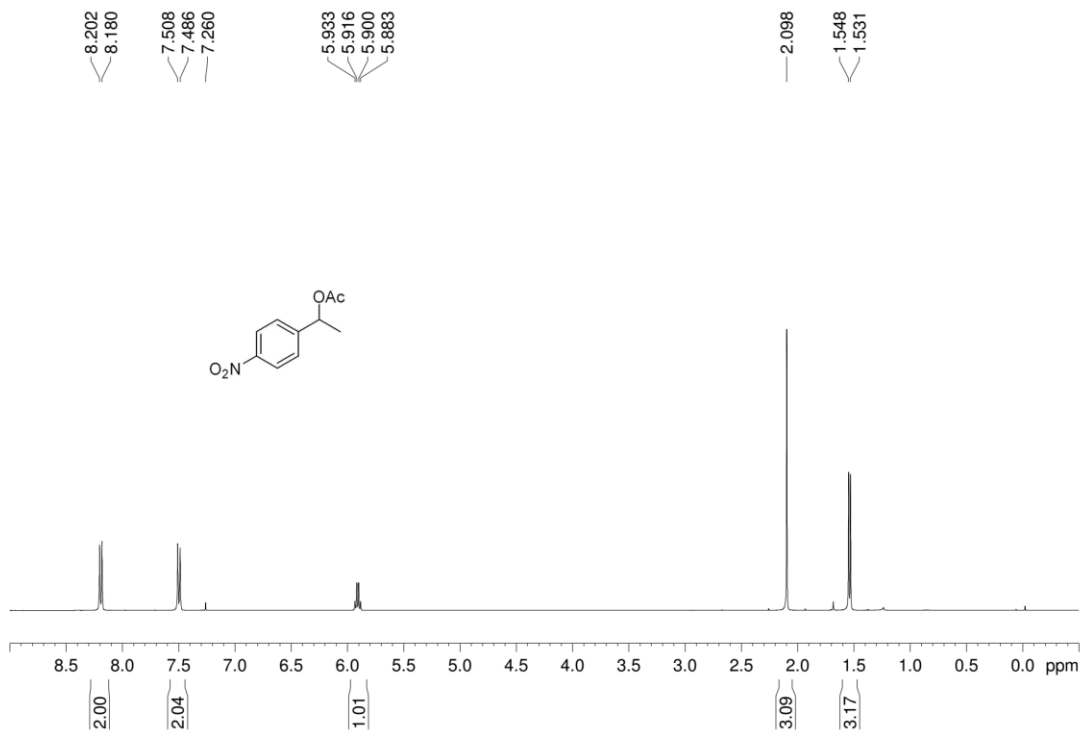


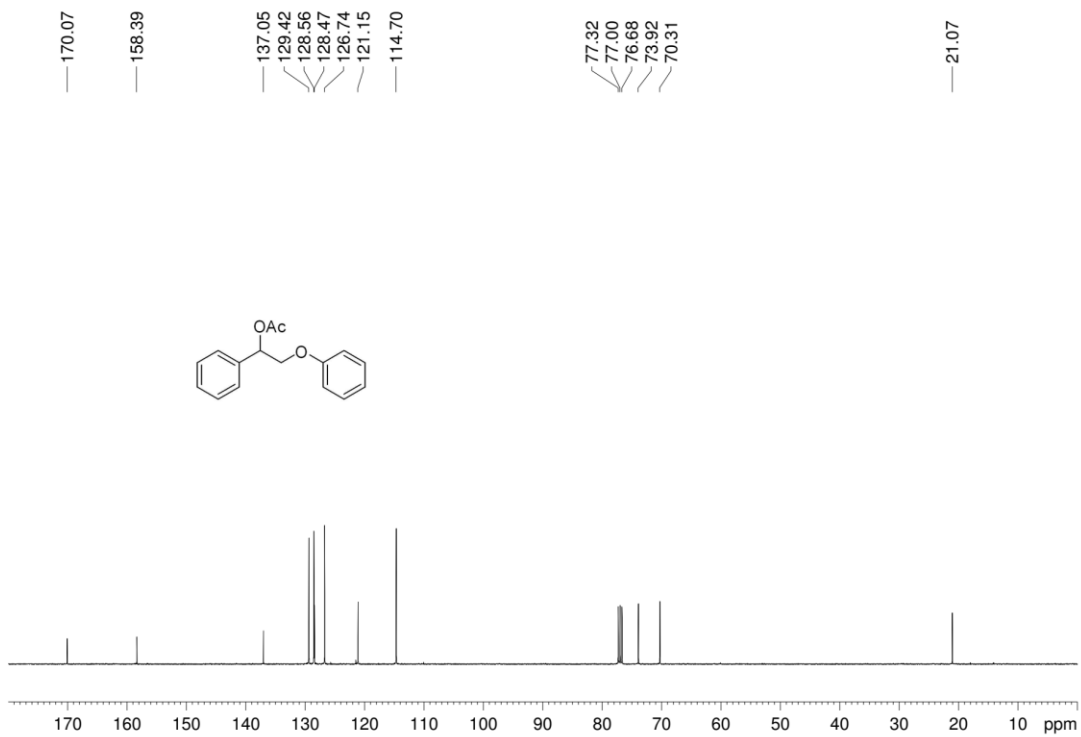
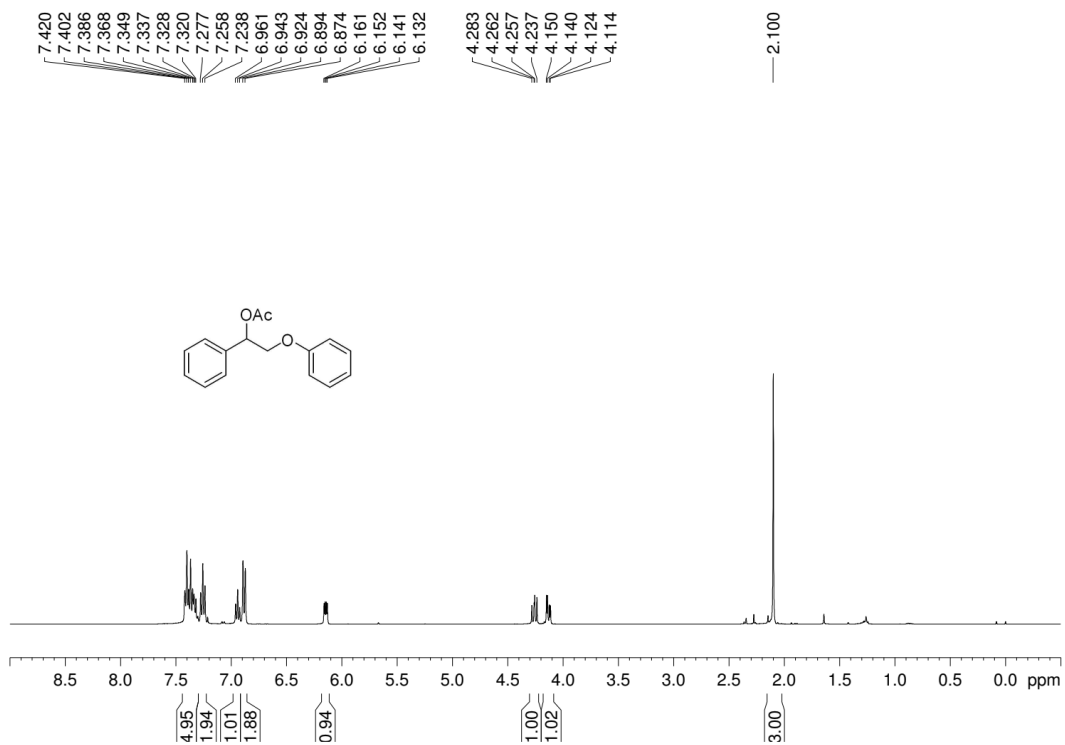


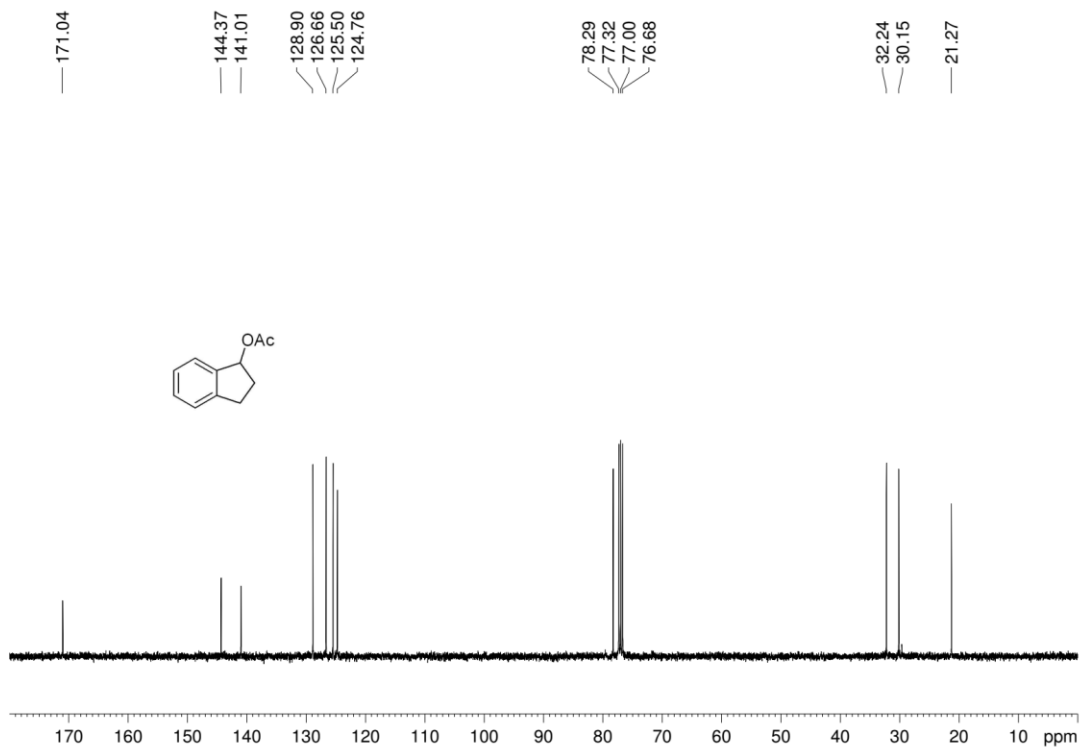
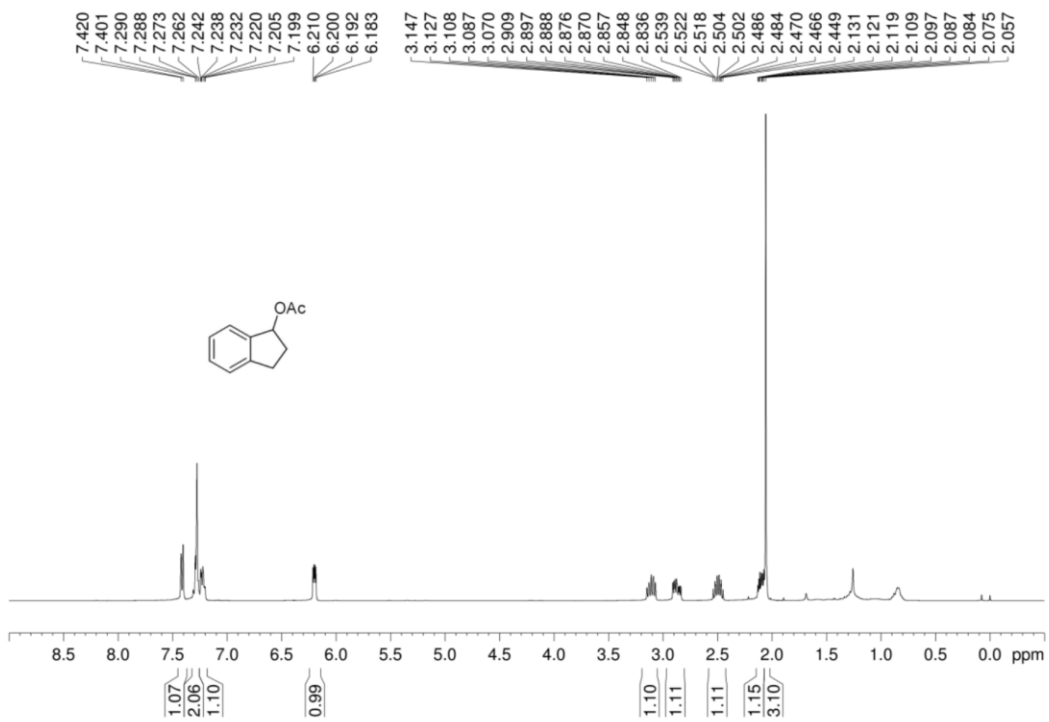


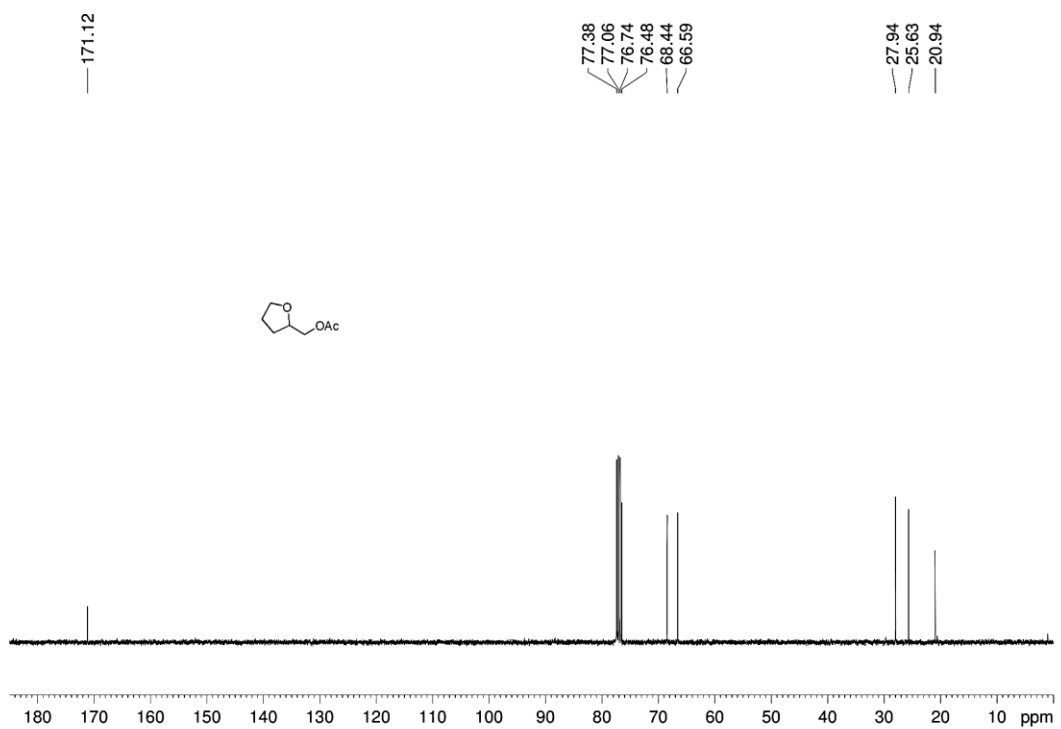
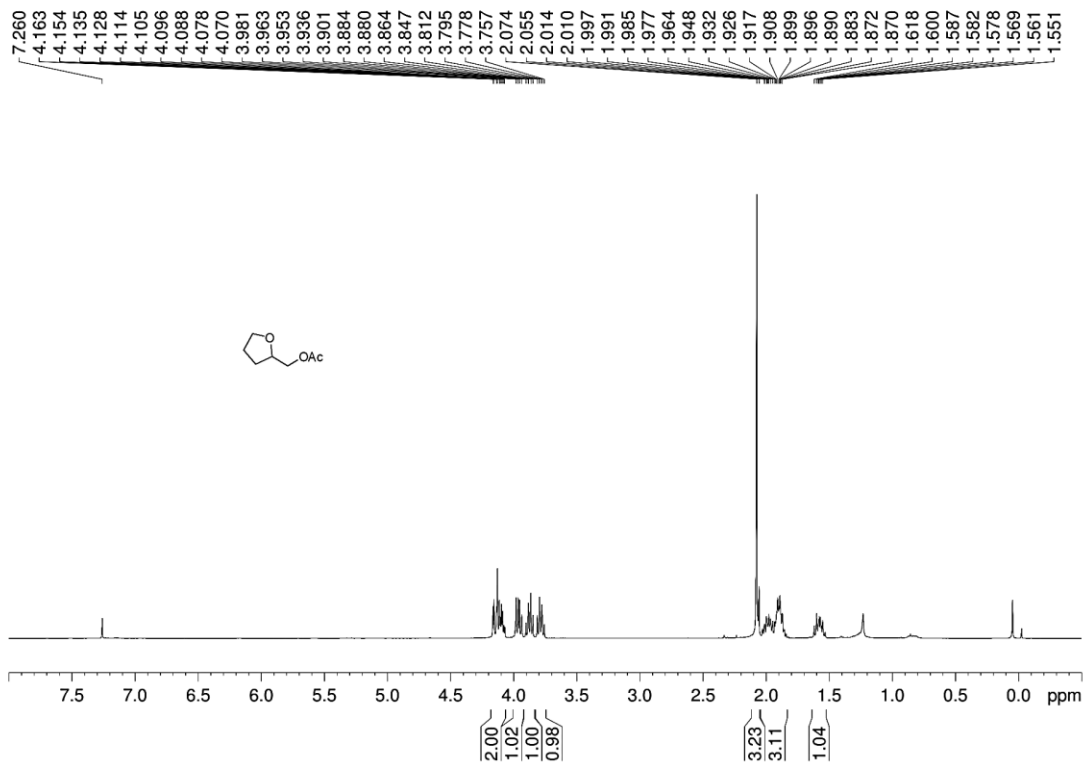


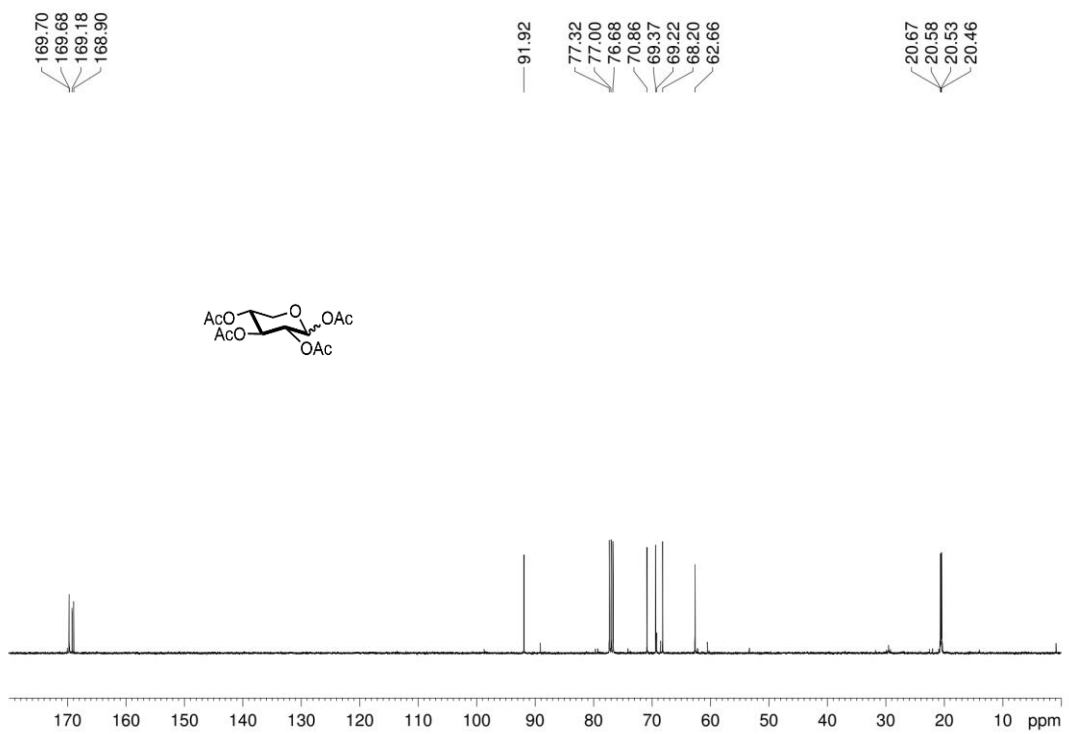
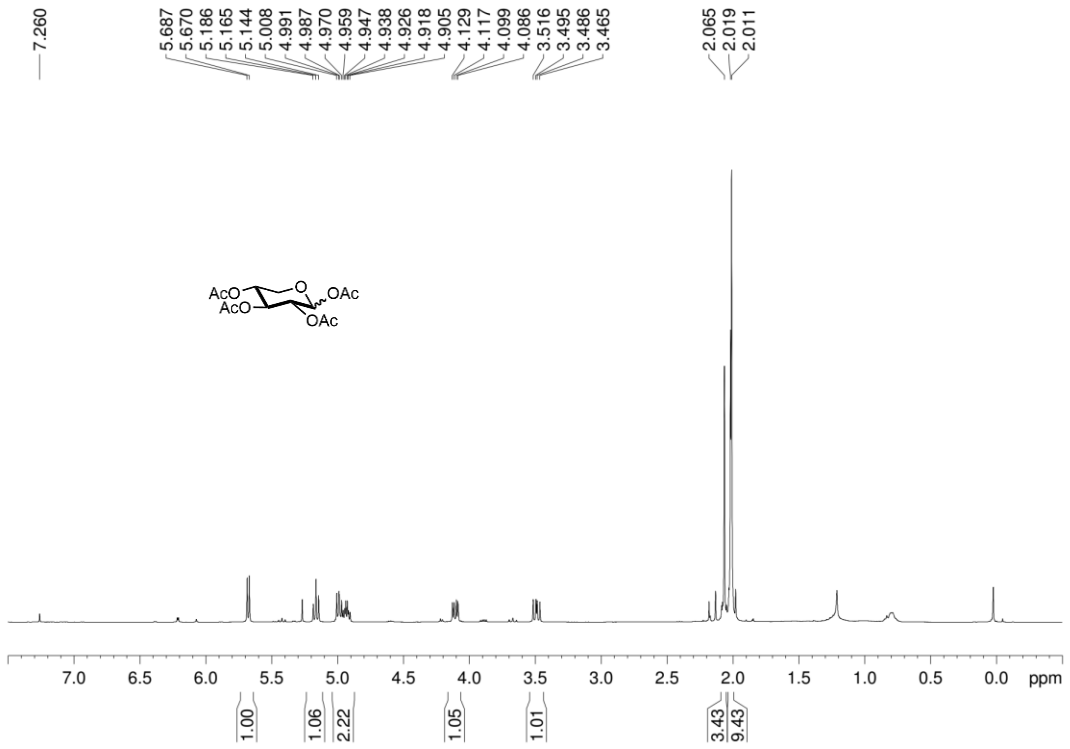


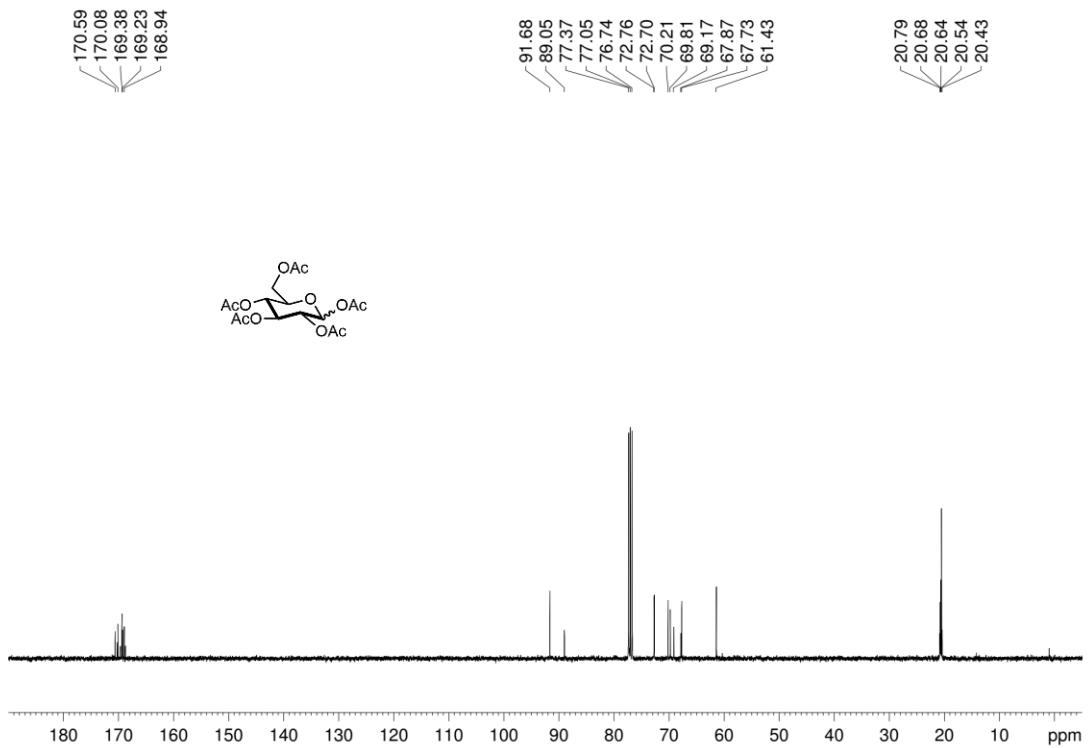
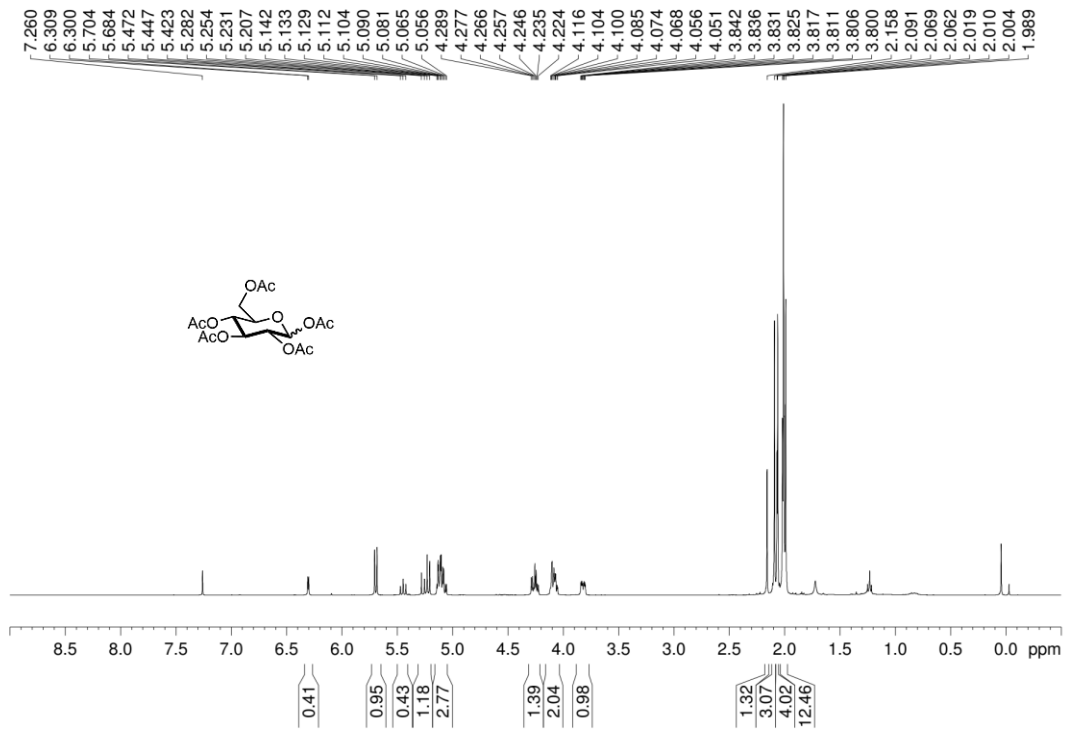


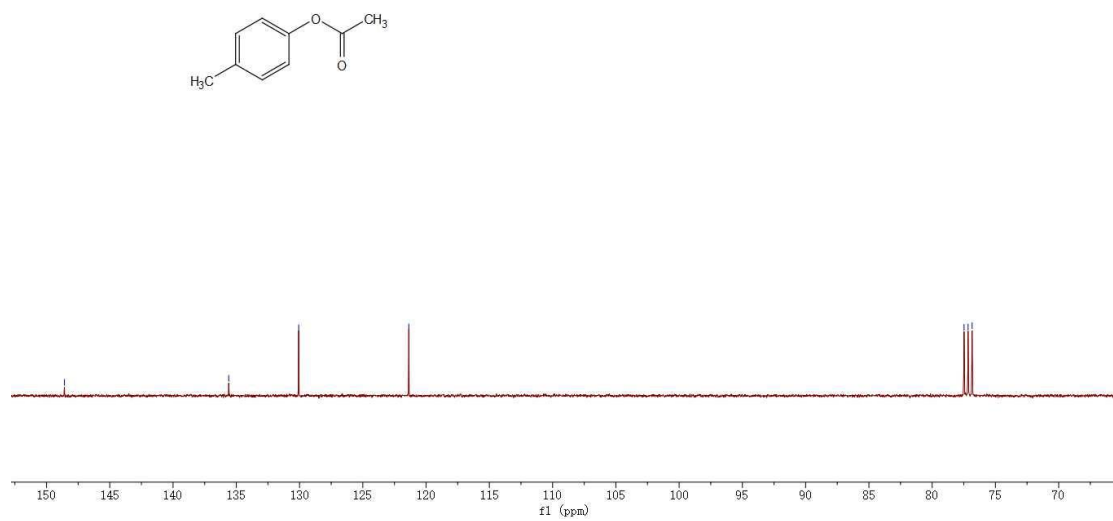
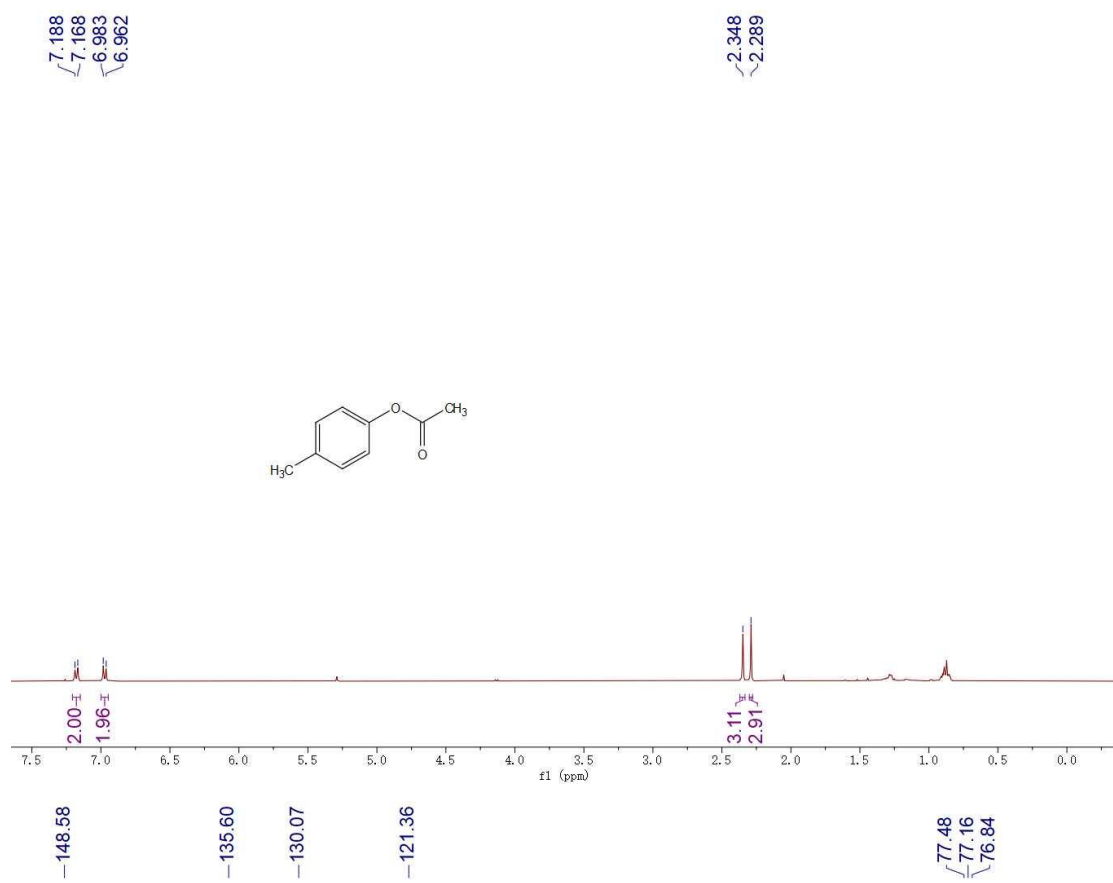


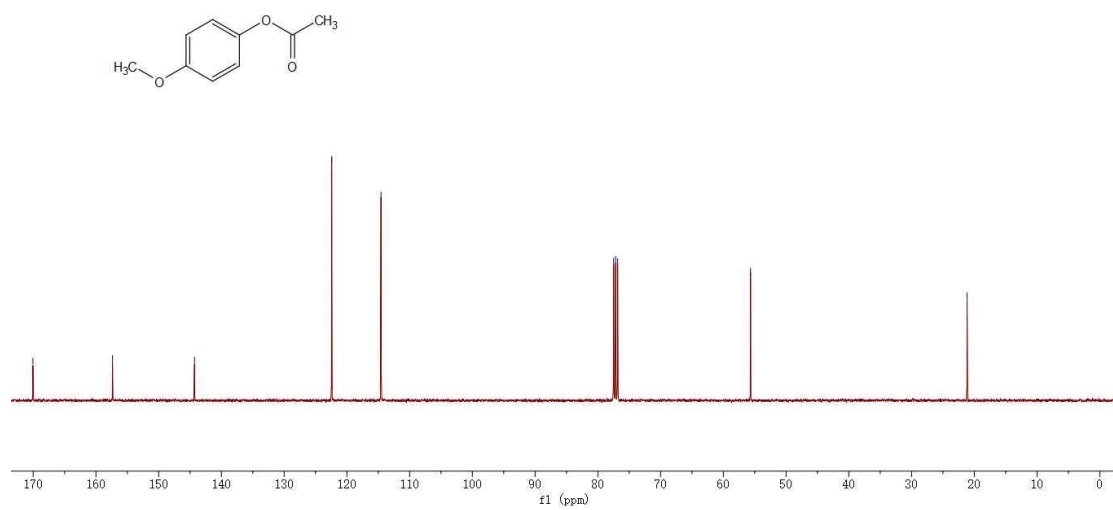
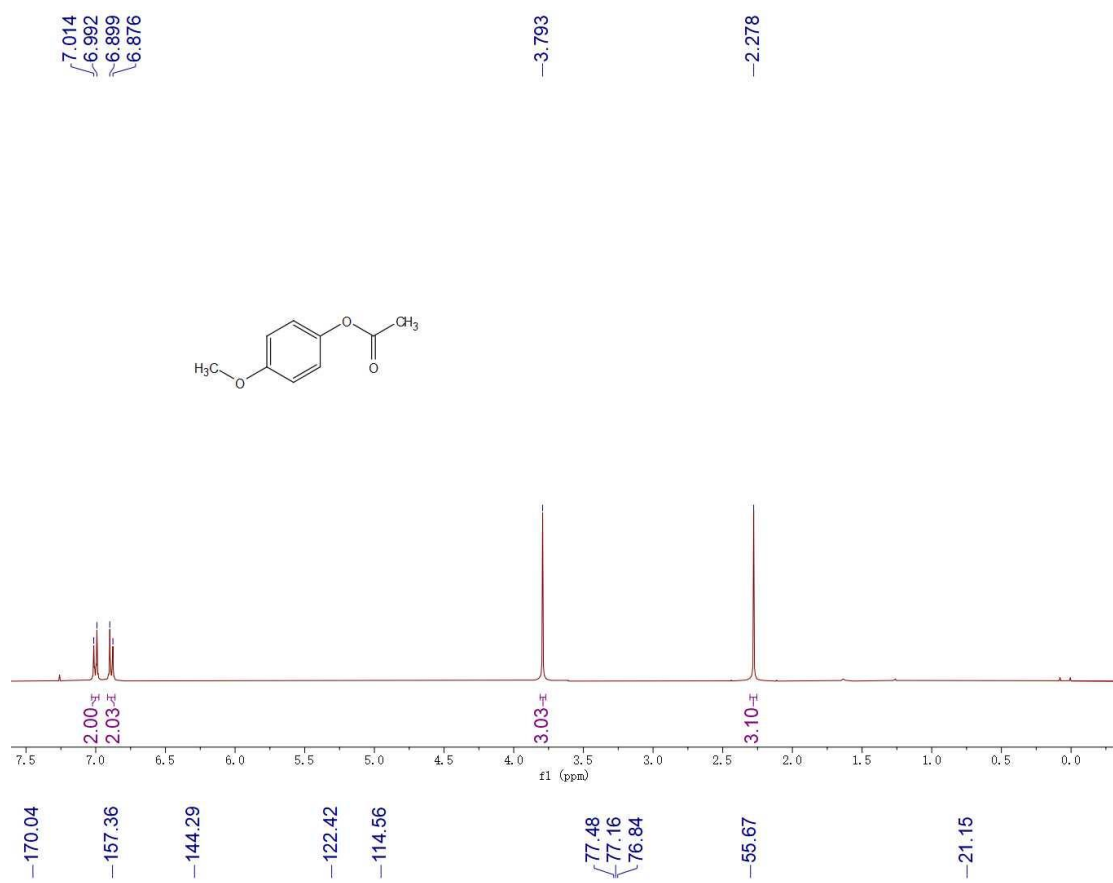


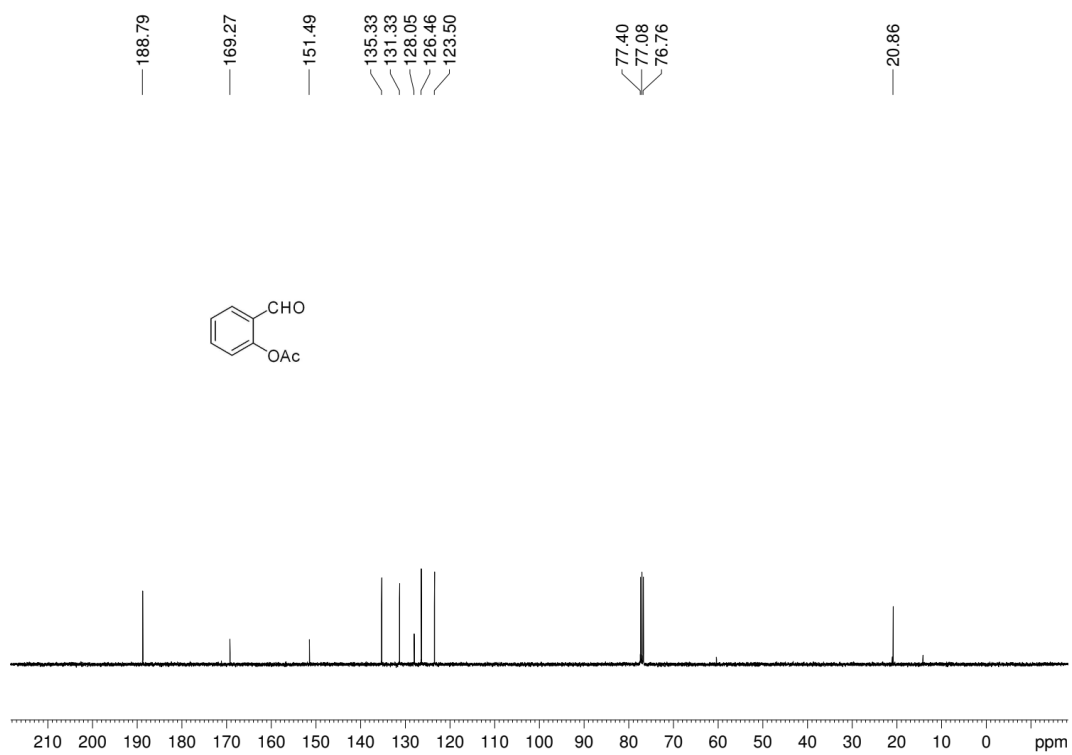
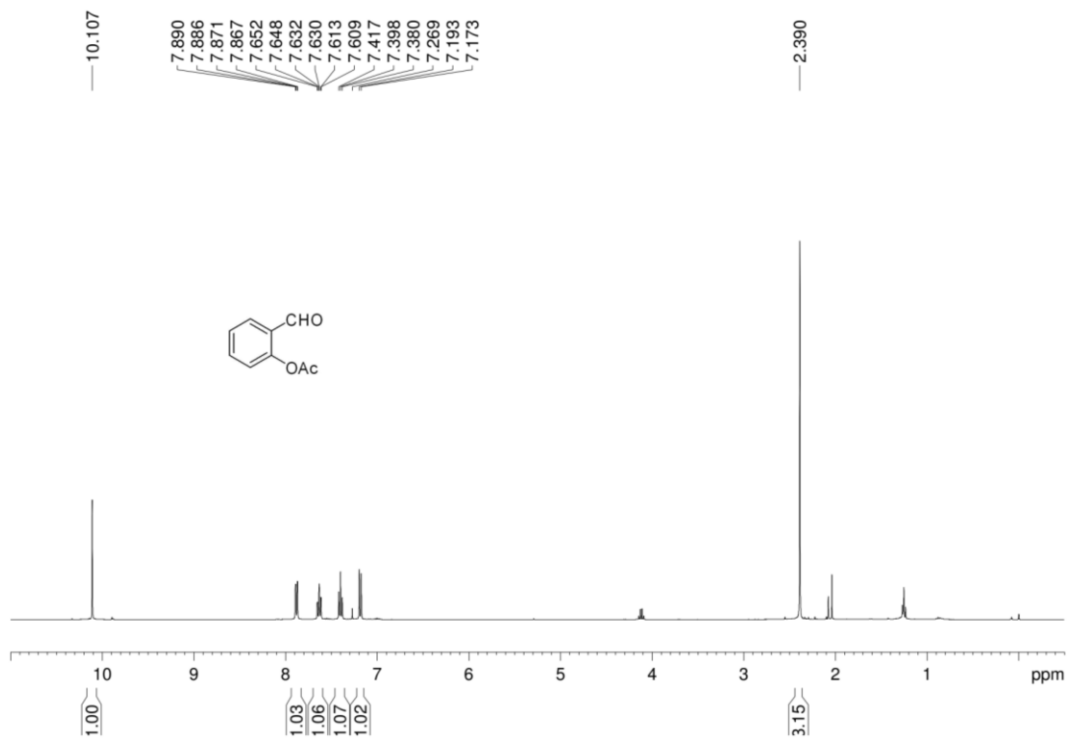


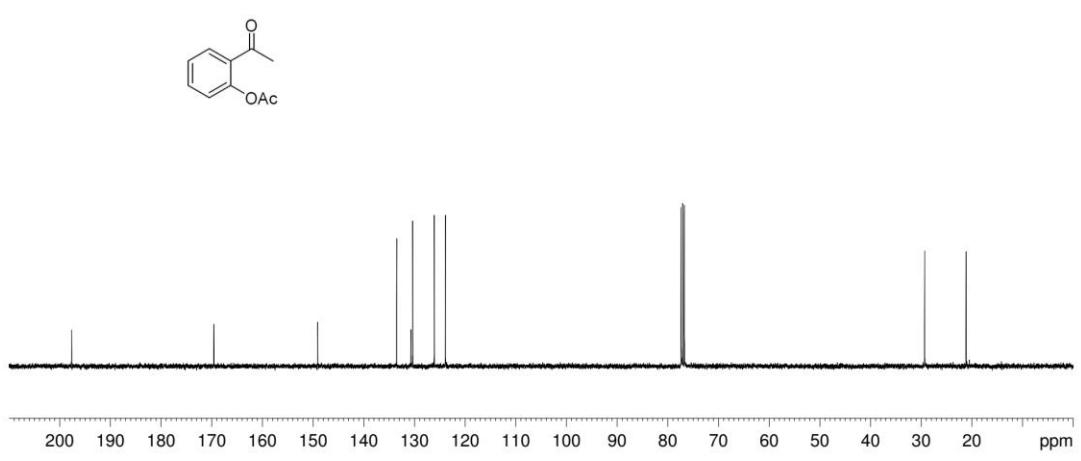
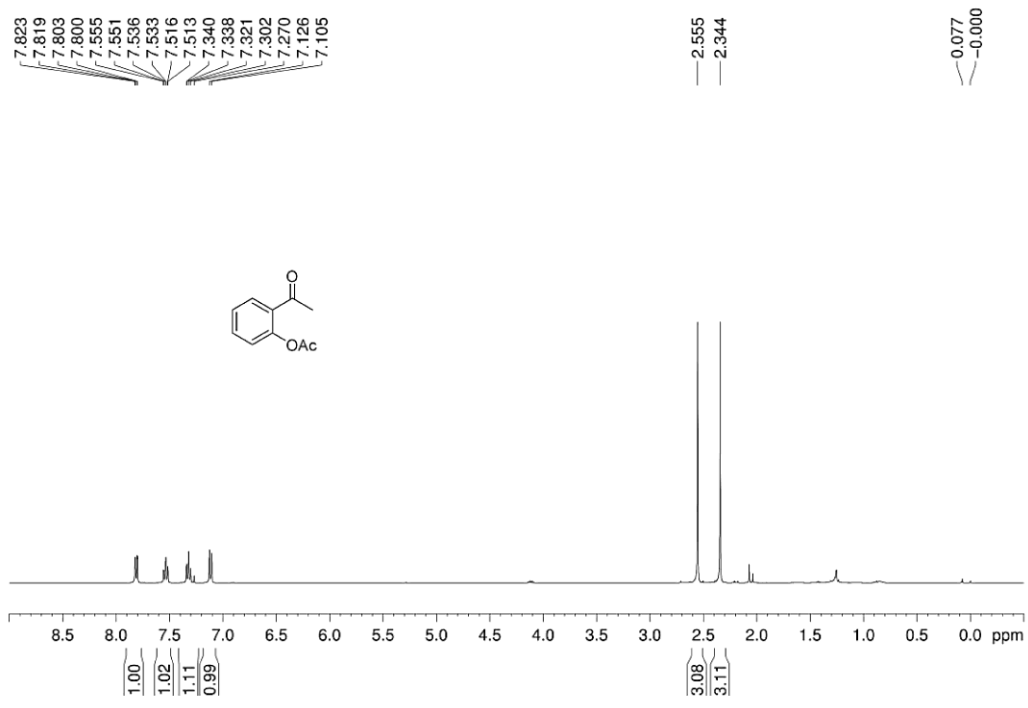


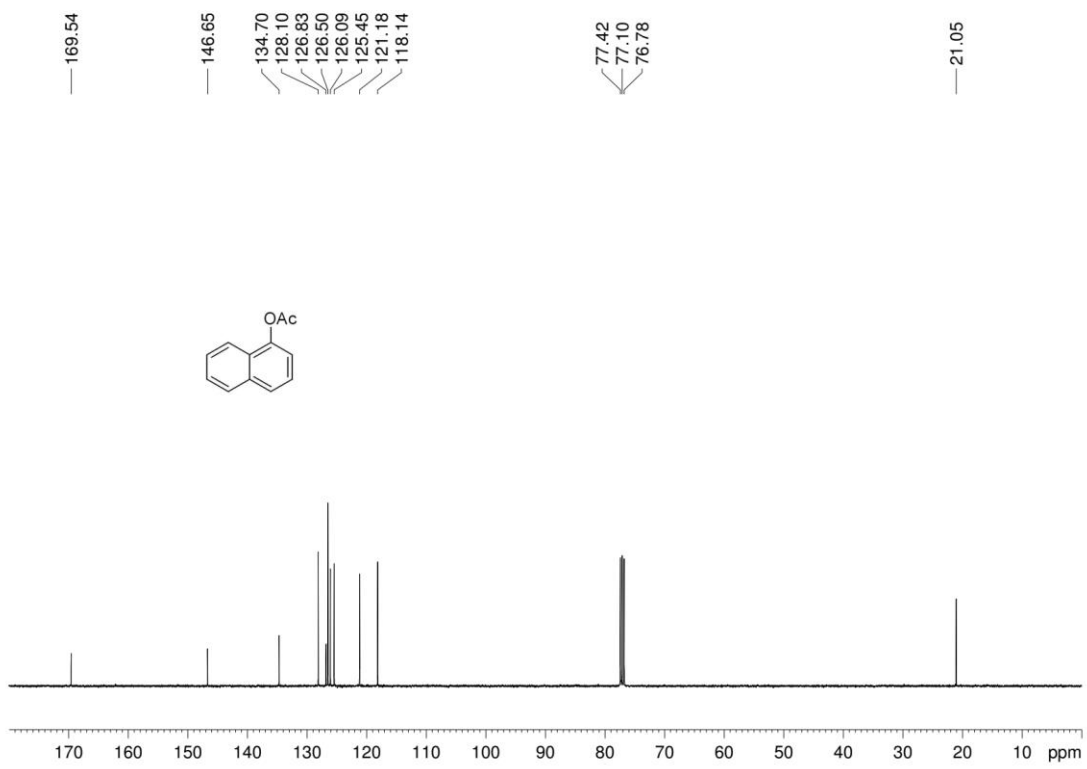
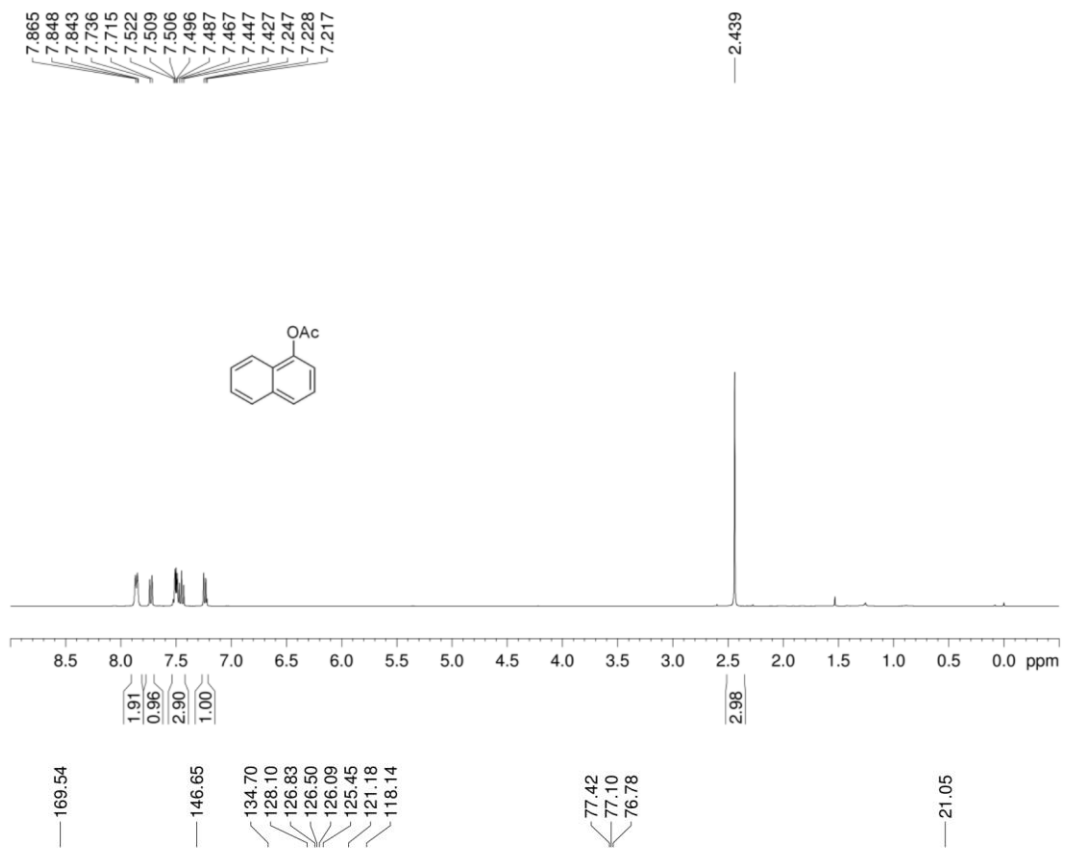


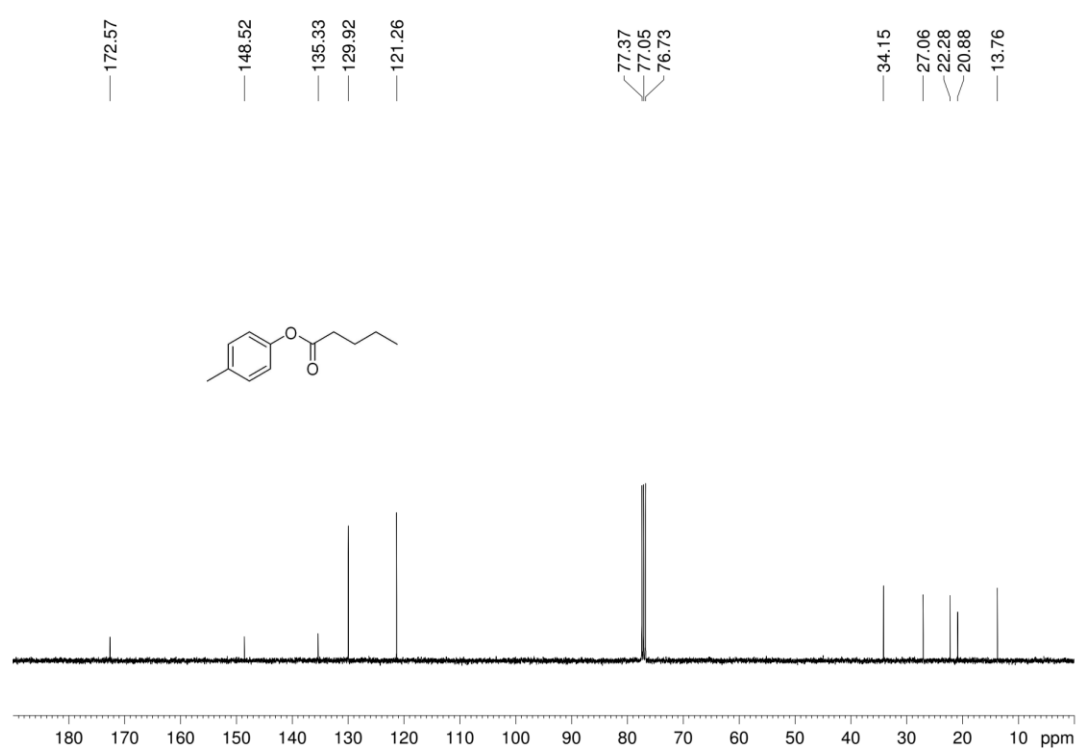
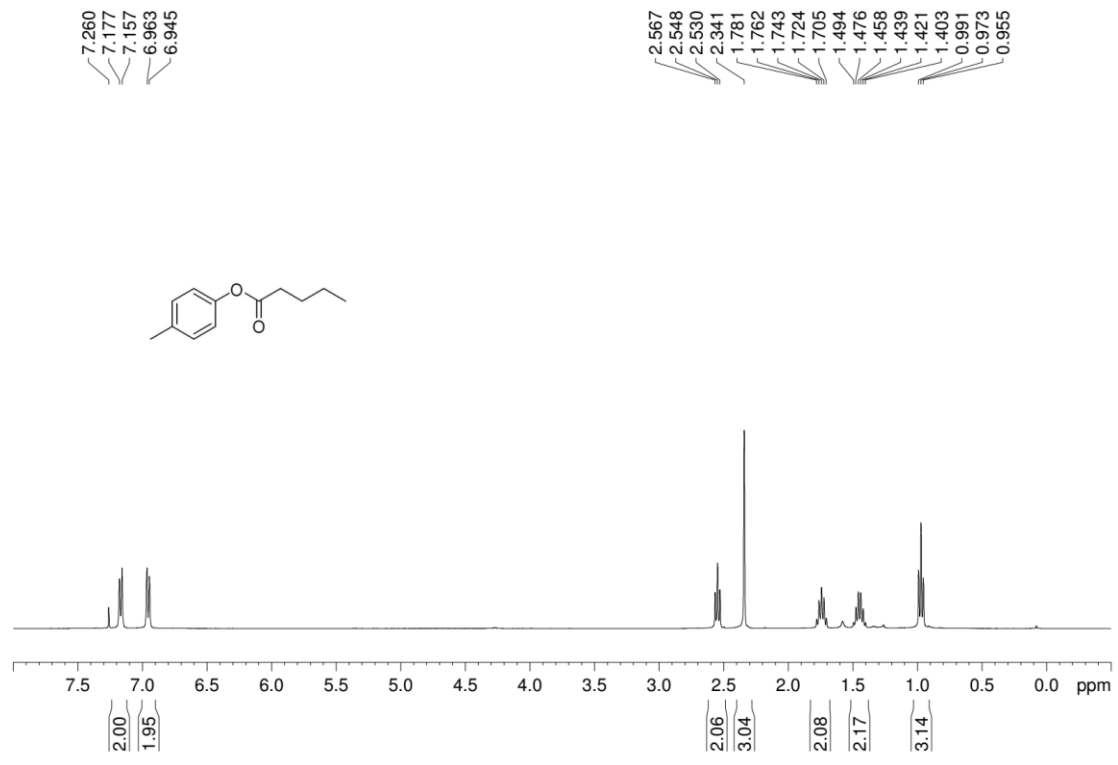


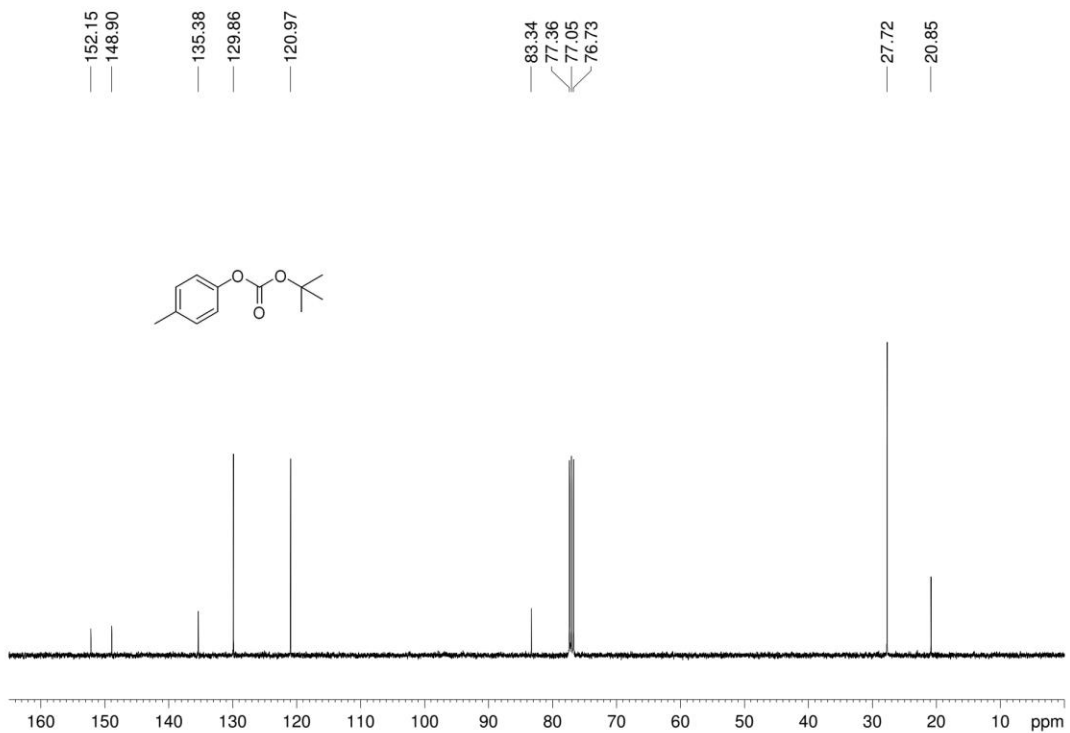
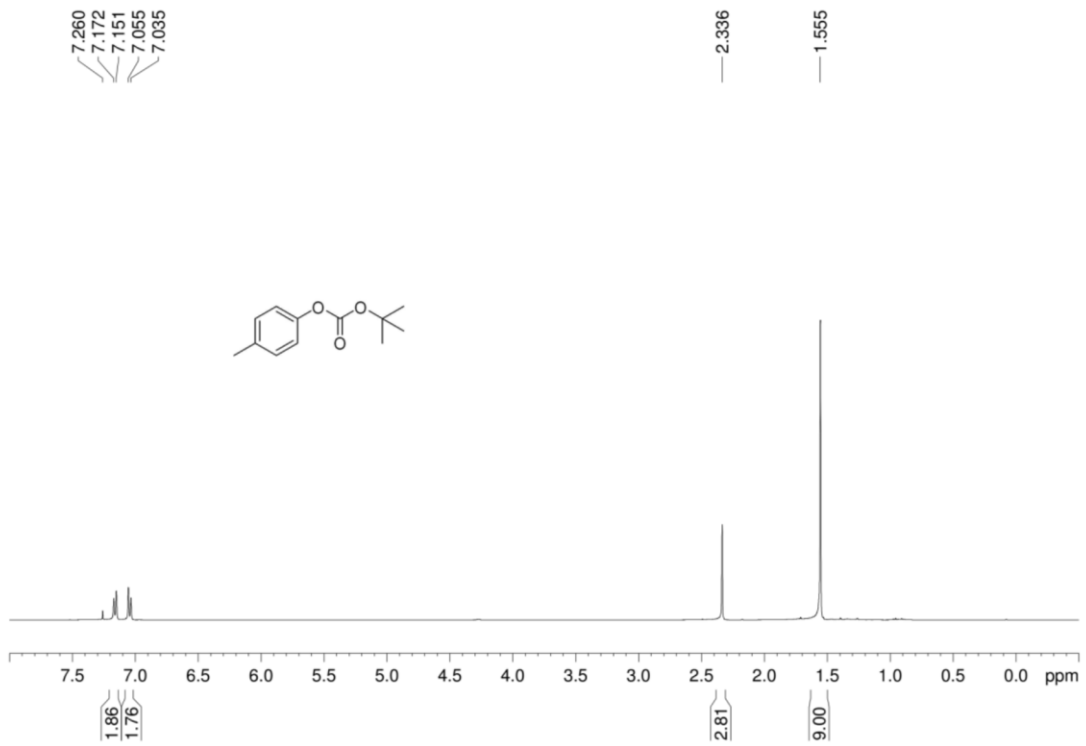


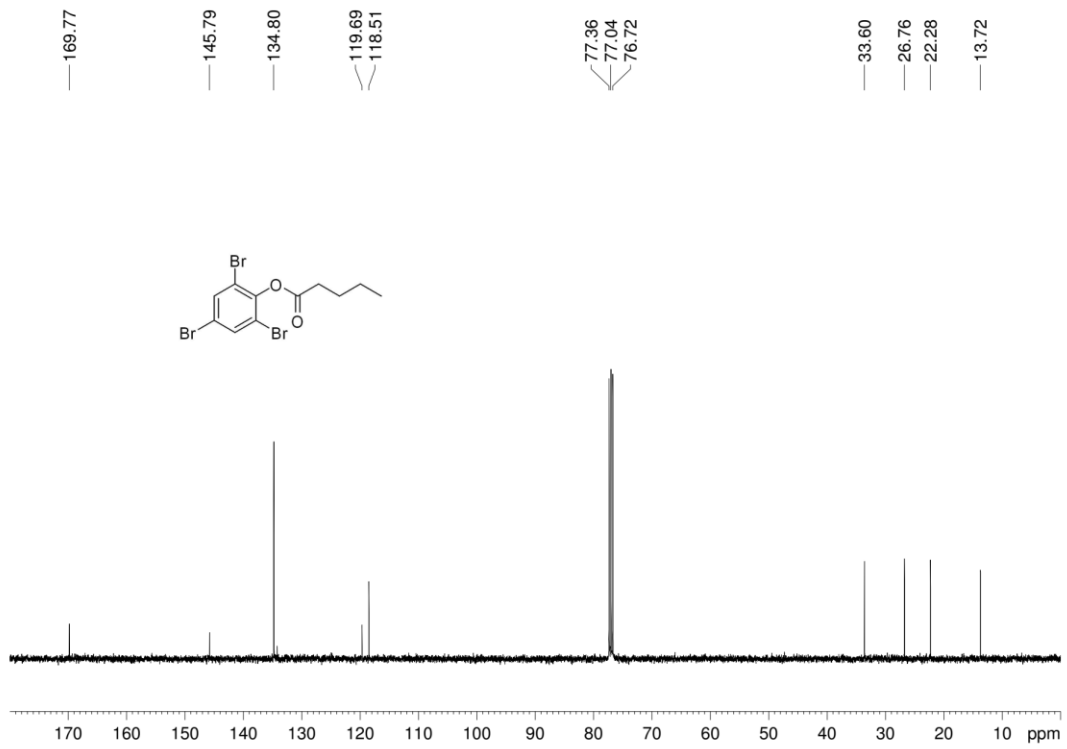
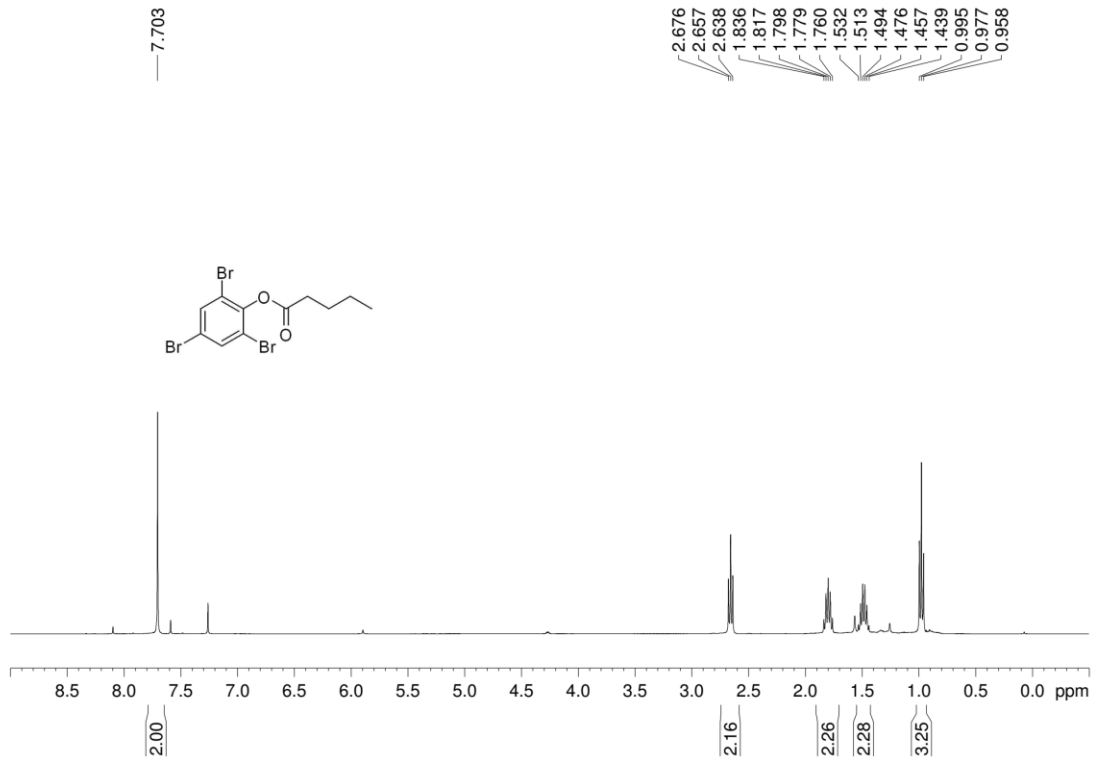


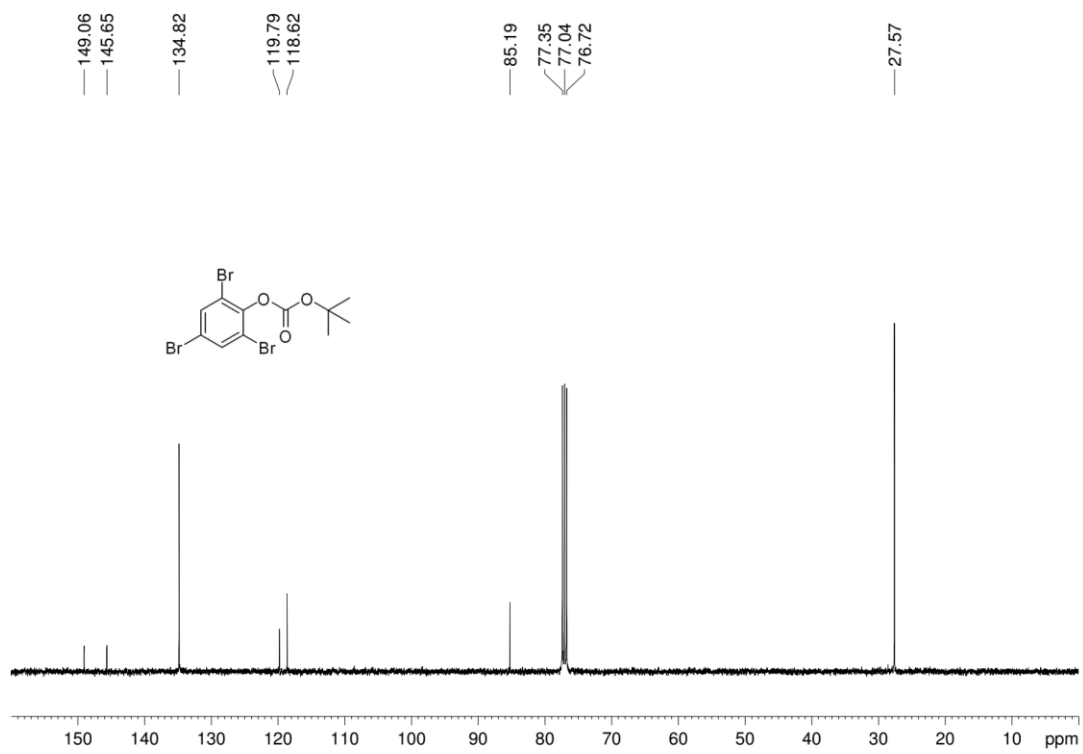
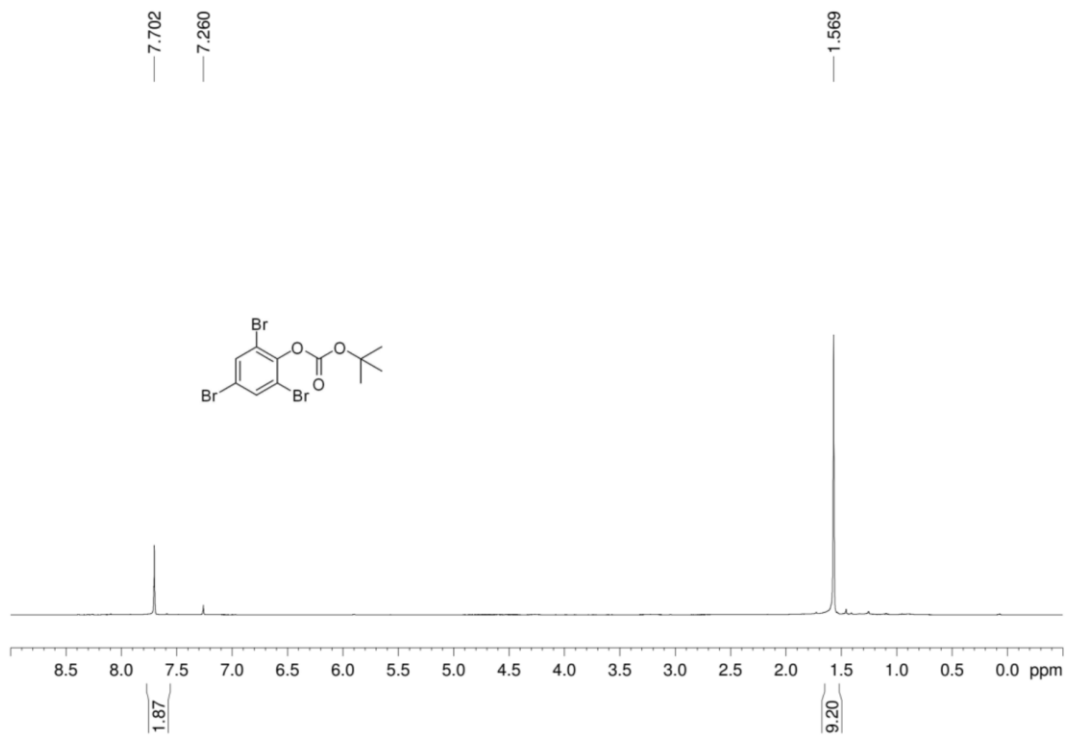




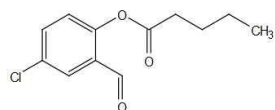






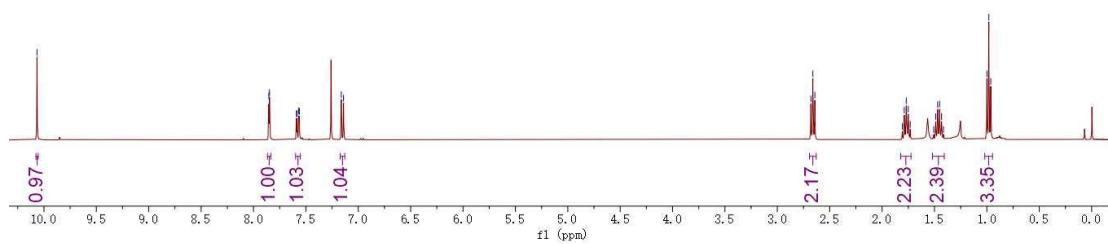


-10.066



7.854
7.847
7.590
7.584
7.569
7.562
7.162
7.141

2.680
2.661
2.642
1.807
1.789
1.770
1.751
1.731
1.507
1.489
1.470
1.451
1.433
1.414
1.000
0.981
0.963



-187.34

-171.96

-150.52

135.18

132.34

130.11

129.21

125.18

77.48

77.16

76.84

33.96

26.87

22.40

-13.84

